DESIGN IMPROVEMENT FOR REAR AXLE COVER

by

Özgür Bank

B.S., Aerospace Engineering, Middle East Technical University, 2005

Submitted to the Institute for Graduate Studies in
Science and Engineering in partial fulfillment of
the requirements for the degree of
Master of Science

Graduate Program in Mechanical Engineering
Boğaziçi University

2009

This work is dedicated to my mother and my father

ACKNOWLEDGEMENTS

This study has been supported Ford Otosan A.Ş. I am indebted to Ford Otosan A.Ş. for the numerical analysis and to Ford of Europe and Dana Corporation for the experimental work.

I would like to express my gratitude to my thesis advisor, Assoc. Prof. Fazıl Önder Sönmez and co-adviser Professor Günay Anlaş for their advice, support, encouragement, and enthusiasm during this study. It was a pleasure to know them and to work with them.

I would like to thank Mr. Ersin Kartal, Rear Axle System supervisor for granting me the chance to engage in this study. I am thankful to Mr. Selçuk Tabak, Mr. Selçuk Hazar, Mr. Nadir Can Altan for their help and advice for the numerical studies, and further many thanks to those who helped me greatly with utilizing, computer, and software for making them available when required.

I would like to take this opportunity to thank my thesis committee members Assist. Prof. Nuri Ersoy, Assist. Prof. Çetin Yılmaz and Dr. Çağrı Sever for their contributions, kind advices, their helpful comments and review of the thesis.

The technical discussions and invaluable support of David Bray from Dana Corporation and Neriya Santosh from Ford of Europe are gratefully acknowledged.

Finally, I would like to express my deepest gratitude to my family in my homeland for their endless love, trust and motivation.

ABSTRACT

DESIGN IMPROVEMENT FOR REAR AXLE COVER

In this thesis, leakages on the rear axle covers used in Ford vehicles are investigated. Main reasons of leakage are discussed and problem is solved by improving rear axle cover design and by improving cover bolt performance.

To simulate the real road condition of the vehicle, vehicle durability test and comparison oriented beam fatigue tests are performed with the current rear axle cover designs. Modifications on the bolt hole locations in the cover, thickness and cover flange lenght are the proposals for improvement. Several FE analyses were performed for each proposal. The results of the analyses were compared with the vehicle and beam fatigue test results, which were performed during cover improvement studies.

Beside cover design improvement studies, load tests, torque vs. angle test and bolt elongation studies were performed in order to reveal the effects of the parameters on cover bolt performance, such as paint on the surface of the cover in contact with the bolt, sealer, sealer process and torque.

Static analyses with static and equivalent dynamic loads considering the condition of the maximum vehicle gross weight effect on the rear axle and the maximum torque transferred from propeller shaft to the rear axle, were performed using finite element software. The results of the analysis were compared with the results of the tests.

ÖZET

ARKA AKS KAPAĞI TASARIM İYİLEMESİ

Bu çalışmada, Ford araçlarında kullanılan arka akslarda görülen kapak yağ kaçakları incelenmiştir. Sorunun kök sebepleri üzerinde durulmuş, kapak parçasının tasarım iyilemesi ve kapak civatasının performansının iyileştirilmesi ile problemin çözümüne çalışılmıştır.

Mevcut tasarım arka aks kapakları ile, gerçek yol koşulları altında çalışma durumunu simüle eden araç dayanıklılık testleri ve karşılaştırma amaçlı yorulma testleri tamamlanmıştır. Kapaktaki çeşitli delik lokasyonları, kalınlık ve kapak kıvrım yüksekliği iyileştirme için sunulan önerilerdir. Her bir öneri için çeşitli sonlu eleman analizleri yapılmıştır. Araç ve yorulma testlerin sonuçları, tasarım iyileştirme çalışmaları sırasında yapılan analizler ile karşılaştırılmıştır.

Kapak tasarım iyileştirme çalışmalarına ilaveten, kapak civatasının performansında etkili olabilecek civata altı boyası, sıvı conta ve tork faktörlerinin etkisini göstermek amaçlı yük testi, torka bağlı açı testi ve civata uzama çalışmaları yapılmıştır.

Analizler static ve dinamik yükler ile, sonlu elemanlar yöntemi ile aracın kendi ağırlığının maksimum düzeydeki etkisi ve kardan milinden aksa iletilen torkun etkisi dikkate alınmak suretiyle sonlu elemanlar paket programı kullanılarak yapılmıştır. Analiz sonuçları, deneysel sonuçlar ile karşılaştırılmıştır.

TABLE OF CONTENTS

LIST OF FIGURES

LIST OF TABLES

LIST OF SYMBOLS / ABBREVIATIONS

a	Distance between mesh point to pinion head bearing centre
A_{gl}	Axial force on carrier at differential bearing position drive gear side
A_{gr}	Axial force on carrier at differential bearing position button half side
A_{ph}	Axial force on carrier at pinion head bearing position
A_{pt}	Axial force on carrier at pinion tail bearing position
b	Distance between mesh point to pinion tail bearing centre
E	Pinion offset distance
F_{ag}	Axial force exerted on gear
F_{ap}	Axial force exerted on pinion
F_{rg}	Seperating force exerted on gear
F_{rp}	Seperating force exerted on pinion
F_{sg}	Seperating force exerted on gear
F_{sp}	Seperating force exerted on pinion
F_{tg}	Tangential force exerted on gear
F_{tp}	Tangential force exerted on pinion
F_A	Resultant force on carrier at pinion head bearing position
F_{AX}	X - force on carrier at pinion head bearing position
F_{AZ}	Z - force on carrier at pinion head bearing position
F_B	Resultant force on carrier at pinion tail bearing position
F_{BX}	X - force on carrier at pinion tail bearing position
F_{BZ}	Z - force on carrier at pinion tail bearing position
F_C	Resultant force on carrier at diff. bearing position button half side
F_{CY}	Y - force on carrier at diff. bearing position button half side
F_{CZ}	Z - force on carrier at diff. bearing position button half side
F_D	Resultant force on carrier at diff. bearing position drive gear side
F_{DY}	Y - force on carrier at diff. bearing position drive gear side
F_{DZ}	Z - force on carrier at diff. bearing position drive gear side
F_{Xp}	The resultant force on pinion at global coordinate system – X dir.
F_{Xg}	The resultant force on ring gear at global coordinate system – X dir.
F_{Yp}	The resultant force on pinion at global coordinate system – Y dir.

F_{Yg}	The resultant force on ring gear at global coordinate system – Y dir.
F_{Zp}	The resultant force on pinion at global coordinate system – Z dir.
F_{Zg}	The resultant force on ring gear at global coordinate system – Z dir.
l_{gl}	Distance differential bearing drive gear side effective load centre to pinion centre line
l_{gr}	Distance differential bearing button side effective load centre to pinion centre line
l_{ph}	Distance pinion head load centre to gear centre line
l_{pt}	Distance pinion tail bearing load centre to gear centre line
R_g	Gear mean radius
R_{gl}	Resultant force on carrier at diff. bearing position drive gear side
Rgl_y	Y - force on carrier at diff. bearing position drive gear side
Rgl_z	Z - force on carrier at diff. bearing position drive gear side
R_{gr}	Resultant force on carrier at diff. bearing position button half side
Rgr_y	Y - force on carrier at diff. bearing position button half side
Rgr_z	Z - force on carrier at diff. bearing position button half side
R_p	Pinion mean radius
Rph	Resultant force on carrier at pinion head bearing position
Rph_x	X - force on carrier at pinion head bearing position
Rph_z	Z - force on carrier at pinion head bearing position
R_{pt}	Resultant force on carrier at pinion tail bearing position
Rpt_x	X - force on carrier at pinion tail bearing position
Rpt_z	Z - force on carrier at pinion tail bearing position
T_g	Crown wheel torque
T_p	Pinion torque
X	Distance pinion centre line to plane of gear mean radius
X_g	Gear axis of rotation
X_p	Pinion axis of rotation
IyI	Distance gear centre line to plane of pinion mean radius
Z	Distance between pinion centre line to mesh point
Z_g	Distance gear centre line to plane of pinion mean radius
Z_p	Distance pinion centre line to plane of gear mean radius

$\cos\alpha_1$	Direction cosines
$\cos\alpha_2$	Direction cosines
$\cos\beta_1$	Direction cosines
$\cos\beta_2$	Direction cosines
γ_g	Ring gear root angle
γ_p	Pinion face angle
ϕ	Pressure angle
θ_{gl}	Direction of force at differential bearing position drive gear side
θ_{gr}	Direction of force at differential bearing position button half side
θ_{ph}	Direction of force at pinion head bearing position
θ_{pt}	Direction of force at pinion tail bearing position
ψ_g	Ring gear spiral angle
ψ_p	Pinion spiral angle

1. INTRODUCTION

A differential box is used to decrease the speed and to increase torque output while transmitting the movement coming from the engine to the wheels and to provide a difference in speeds of inner and outer wheels in turns. Power is supplied from the engine, via gearbox, to driveshaft (British term: propeller shaft), which runs rear axle. A pinion gear at the end of propeller shaft is encased within differential itself, and it engages the large ring gear (British term: crownwheel). The ring gear is attached to a carrier, which holds a set of small planetary gears. The three planetary gears are set up in such a way that the two outer gears (the side gears) can rotate in opposite directions relative to each other. The pair of side gears drive the axle shafts to each of the wheels. The entire carrier rotates in the same direction as the ring gear, but within that motion, the side gears can counter-rotate relative to each other. Thus, for example, if the car is making a turn to the right, the main ring gear may make 10 full revolutions, and during that time, the left wheel will travel more revolutions because it has further to travel, and the right wheel will travel fewer revolutions correspondingly, as it has less distance to travel. The side gears will turn in opposite directions relative to each other by, say, 2 full turns each (4 full turns with regard to each other), resulting in the left wheel making 12 revolutions, and the right wheel making 8 revolutions Schematic of differential is shown in Figure 1.1.

When the vehicle is traveling in a straight line, there will be almost no movement of the planetary system of gears. On the other hand, when the vehicle turns, planetary gear system starts to move.

Rear axle is a system which includes differential system. Rear axle has several components as showed in Figures 1.2 and 1.3. Rear axle cover which is one of the components of this system, is used to prevent axle oil leakage. But, leakage is seen due to poor sealing performance of the cover, gap between cover flange and carrier due to overloading and insufficient stiffness. Oil leakage is crucial since oil defficiency in rear axle leads locking of gears and tires which may lead to heavy accidents.

Improvement of rear axle cover design and improvement on cover bolt performance are the interests of this study. This study is organized as follows;

First of all, a proposed new cover with improved sealing performance and increased flange stiffness will be designed, modeled and produced. Then, vertical beam fatigue and

vehicle tests will be performed to get test results of the current and proposed cover designs to compare design efficiency.(Currently, 2 different types of cover is used for rear axle applications.) Vehicle tests are performed at Ford vehicle test center which is Lommel Proving Ground and beam fatigue tests are performed at DANA UK test center. After that, rear axle system will be modeled and FEA will be performed. The aim is to correlate the FEA model according to exact test results and prove accuracy of the model. Finally, rear axle cover design improvement should be completed by FEA analysis, without performing any further rig and vehicle tests. This will provide Ford Motor Company significant cost saving by eliminating costs. Further studies and tests are performed to obtain effective parameters on bolt performance. Sealer, sealer process and bolt toque affect bolt performance. Load test, torque to angle test and bolt elongation studies are performed to reveal each parameters effect on performance. Finally, the most appropriate process which improves cover and system performance is presented.

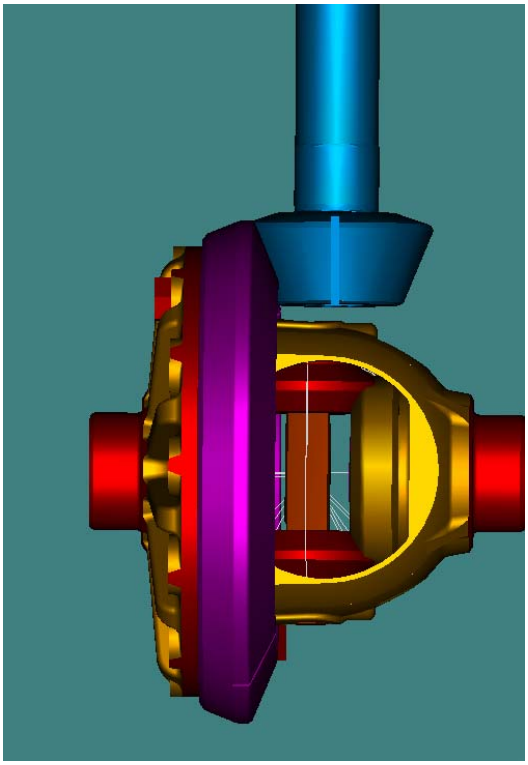

Figure 1.1. Schematic of differential

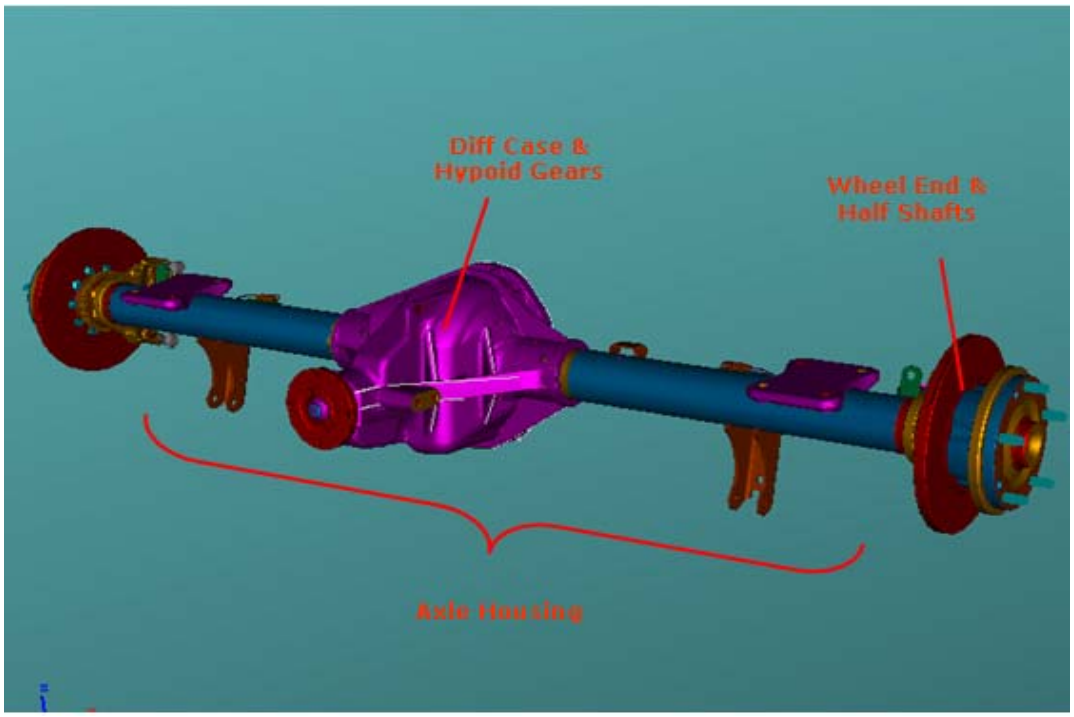

Figure 1.2. Schematic of rear axle

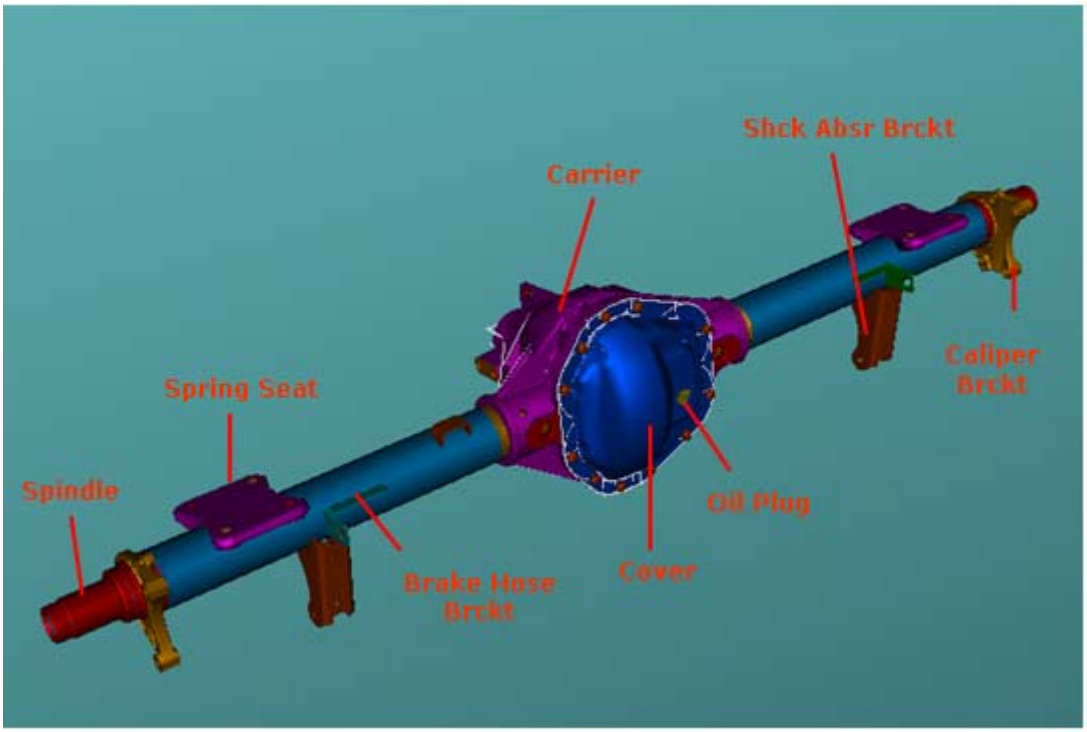

Figure 1.3. Schematic of rear axle housing

1.1. Literature Review

There are a number of studies on differentials and rear axle. But, there is no similar study on rear axle cover in literature. Studies on differential systems are generally about the gear sets, failure modes and fatigue. Bayrakçeken [1] carried out a failure analysis of a differential pinion shaft. Mechanical characteristics of the material were obtained. Then, its microstructure and chemical composition were determined. Das et al. [2] performed a failure analysis of the pinion. Stevenson et al. [3] studied on the failure of a high speed pinion shaft. Examination of the shaft revealed cyclic fatigue as the failure mechanism with a substantial distribution of nonmetallic inclusions near the fracture initiation site. Wang et al. [4] described a research work on modeling and numerical analysis of torsional vibration in automotive manual transmissions. The focus of that study was on a decoupling procedure for the numerical analysis of gear rattle. Asi [5] performed a failure analysis of a rear axle shaft used in an automobile which had been involved in an accident. The investigation was carried out in order to establish whether the failure was the cause or a consequence of the accident. Vogwell [6] described an investigation which was carried out on a failed drive shaft component used on an unmanned remotely operated vehicle. A study of the broken shaft showed how vulnerable such a rotating component could be to fail by fatigue even when operating under steady conditions, if basic preventative design actions are not taken. Bensely [7] performed the failure investigation of crown wheel and pinion. The study concludes that the failure was due to a compromise made in raw material composition by the manufacturer. Sabnavis et al. [8] performed on the cracks of the shafts and diagnostics. Types and causes of the shaft cracks are explained. Clegg [9] studied on the failure of planetary pinions. A failure analysis approached is described in this study. Sinou et al. [10] investigated the influence of cracks on the failure of shafts. Dumitru et al. [11] performed an experimental study of torsional impact fatigue of shafts - presented a methodology to study the fatigue strength of shafts under repeated impacts. Alvarez et al. [12] presented a computer application to dimension shafts. Safety factors according to several classic theories can be obtained by indicating shaft dimensions and particular discontinuities, as grooves or holes. Ranganath et al. [13] described a failure of a swing pinion shaft of a dragline. The causes of failure of a swing pinion shaft of a coal handling dragline have been investigated in this work. Along with the failed shaft, a small piece of material from the tooth of another shaft that rendered design life in service was also

analyzed. Law et al. [14] performed on vehicle axle load identification using finite element method. responses. A new moving load identification method was presented using on finite element method and condensation technique. Lehr [15] applied new generation fiber gasket material to high-stress, dynamic flange environments. These applications include flywheel housing-to-block gaskets, gear case-to-block gaskets, axle covers, cast aluminum oil pan gaskets, rear seal carrier gaskets, heavy duty valve cover gaskets, etc. What these applications have in common is a high degree of torsional or shear stress on the gasket which can lead to failure. Lehr [16] studied on the subject of a new flange sealing technology. A new flange sealing technology is described which meets industry standard durability and seal ability testing. Santosh et al. [17] presents a web-based tool to calculate gear and bearing forces for a front or rear axle. Force equilibrium is ensured in both gear and bearing load calculations for front and rear axles in both drive and coast modes. The gear forces along with the bearing spans are used to calculate bearing loads on the axle carrier at the pinion and differential case locations. James at al. [18] describes a numerical simulation method to predict the system deflections and misalignments in a loaded axle assembly. A fully-coupled, non-linear algorithm has been developed to analyze the cage & shaft & bearing & gear & carrier system. Sun et al. [19] presents the FEA modeling techniques in studying axle system dynamics and the level of accuracy of the model that can be achieved in predicting forced system responses. The use of a driveline system model in the development of a design optimization for total system NVH performance is discussed. Examples are provided to demonstrate the effects of modal alignments and appropriate system tuning. Beutler [20] optimized sealing of an axle cover pan gasket. Axle cover pan bolted joint sealing with a fiber composition gasket material can be challenging to achieve leak-free sealing. A project was conducted to optimize a stamped steel cover pan/fiber composition gasket static sealing ability by utilizing the robust engineering method. An analytical FEA modeling approach in combination with the robust parameter design technique was utilized to evaluate and optimize the stamped cover pan crown embossment geometry shape. Sreedhar et al. [21] worked on the recent trends of increasing driveline torque and use of traction control devices call for increasingly higher durability capacity from driveline components. Traditional finite element analysis (FEA) procedures have been used effectively in the re-design of driveline components to reduce stress, and occasionally, to predict fatigue life. Hussien et al. [22] developed a three dimensional finite element method for the dynamic and vibration analysis of the rear axle

system. The method allows for the dynamic modeling of several components of the axle system including the input shaft, the output shafts, the control arms, track bar, tires, bearings, bushings, and helical springs and dashpots of the suspension system.

1.2. Motivation and Objectives of the Study

In most of the rear axle studies shaft failures are investigated. Failure analysis and metallurgical inspections are performed to reveal the failure mode. The main problem for the axle parts is fatigue or fracture. Further studies on the material of the parts are performed.

Cover leakage issue cannot be evaluated as a fracture or fatigue problem. Leakage from cover may be due to unacceptable bolt elongation, insufficient clamp load, insufficient pressure distribution, assembly bolt torque values, insufficient sealer performance and insufficient stiffness. Therefore in this study, it is aim to reveal the main reasons of the leakage problem and prevent this by taking corrective actions.

Cover leakage issue was not studied before in the literature. Analyses performed for the rear axle parts did not consider torsional effects, also. In this study, torsional effect will be considered in the FE analysis to point out the effectiveness of the torsional effect on the cover analysis.

1.3. Thesis Outline

The thesis consists of three main chapters. In Chapter 2, the subject of rear axle cover leakage is explained. Also, possible root causes and corrective actions which were taken are stated. More, current cover designs and proposed cover design are represented. Vehicle test (General Durability Test) and rig test (Vertical Beam Fatigue Test) results are showed for each cover design. In Chapter 3, FE model and input parameters are explained. Current design and proposed design cover FE analysis results are represented. In Chapter 3, test results presented in are compared to finite element simulation results obtained by using Hyper-mesh program for 3g beam load and forward torque input. Robustness of the FE model for rear axle analysis is showed. New cover designs with changing bolt locations,

curvature dimensions and different thickness are proposed. FE analysis is performed for proposed cover designs, also. Finally, the design which gives the best results in FE analysis is stated. In Chapter 4, cover bolt studies are discussed. Load tests are performed to check the sealer and paint on bolt face effect, angle to torque tests are performed to check torque effect. Moreover, elongation studies are performed to see both sealer process and torque effect on bolt performance. Finally, most convenient sealer process and torque value are presented and implemented to the assembly line.

2. THE REAR AXLE COVER LEAKAGE ISSUE AND THE ASSOCIATED STUDIES

As it is seen, numerous studies were conducted on the behavior of differentials. One of the components of the rear axle, which is the cover should also be investigated due to failures (leakages) in the vehicle durability (TTGD) and beam fatigue (rig) tests. The test procedures are explained in Appendices A & B.

2.1. Cover Leakage Issue (Possible Root Causes and Corrective Actions)

The first objective of this study is to reveal the reasons for the leakage from the rear axle cover, which might be due to unacceptable bolt elongation resulting from paint effect on cover and insufficient clamp load, insufficient pressure distribution, assembly bolt torque values, sealer application process (thickness, width, location, surface cleaning), sealer performance and insufficient stiffness.

Various studies were performed and several actions were taken to improve the deficiencies of the system and prevent from cover leakage such as stated below:

i. Paint was removed from the bolt seat faces on the cover to eliminate unacceptable plastic elongation of bolt due to paint effect. Removal of the paint resulted in an increase in clamp load.

ii. Surface cleaner Loctite 7070 was implemented in the process in order to increase sealing performance

iii. To improve sealer application process, guides were used in the assembly process in order to help having a continuous bead of sealant around the inside wall of the cover

iv. To improve sealer application process, error proofing was implemented to control the time between sealer application and fastening of the cover to the housing.

v. To improve sealer application process, clearing process on carrier mating surface before cover assembly was redefined.

vi. To improve sealer performance, Loctite 5900 was started to be used instead of Loctite 5699.

Although the above precautions were taken to improve the design and the process, still cover leakages were observed during the vehicle durability tests as shown in the next chapters. This meant the precautions were not effective enough. In the present thesis study, the geometry of the cover was redesigned to minimize the deformation at the interface between the cover and the carrier to uniform pressure distribution on the cover flange face, and improve sealer performance.

2.2 Current Cover (Cover 1) vs Proposed Covers (Cover 2 & Cover 3)

Design change 1&2 : In order to increase flange stiffness and sealer performance, the flange of the current rear axle cover (Figure 2.1) is bent with 0.5 mm width stamping as shown in Figure 2.2 and Figure 2.3.

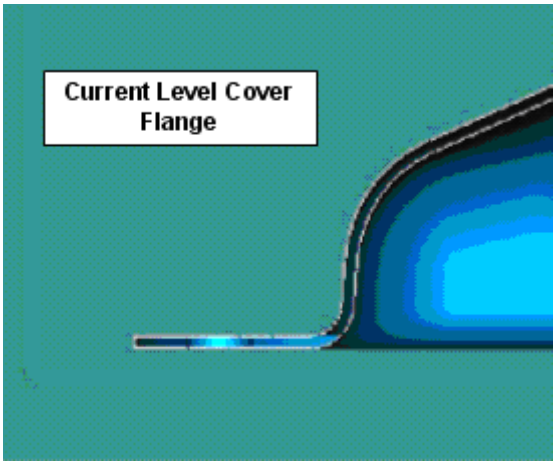

Figure 2.1. Current level cover (Cover 1)

In addition to the aforementioned changes, there are some other dimensional differences between the cover designs. Due to some design requirements, the inner regions of cover 3 are the same as that of cover1. The other dimensional differences are explained in the Figure 2.4. The spherical radius of the cover 1 is 149.3 mm, and cover 2 is 149.23 mm. The distance between spherical center and cover flange for cover 1 is 76.15mm, the same distance for cover design is 69.85mm. So,it can be concluded that cover 2 design is approximately 7mm larger in depth.

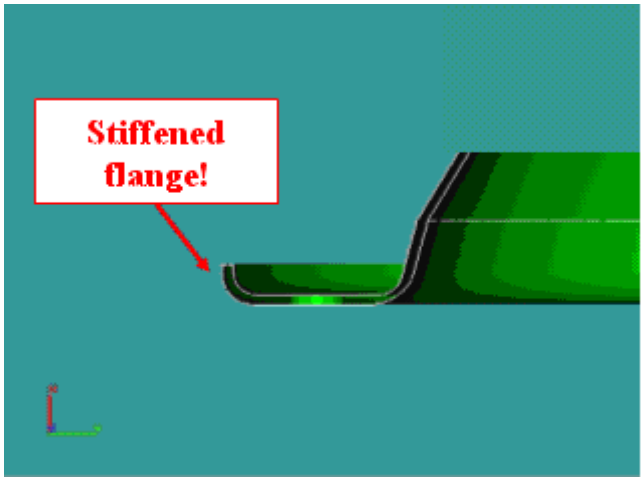

Figure 2.2. Proposed cover (Cover 2&3) flange design

Adding curved form on the outer edge of the flange increases its stiffness.

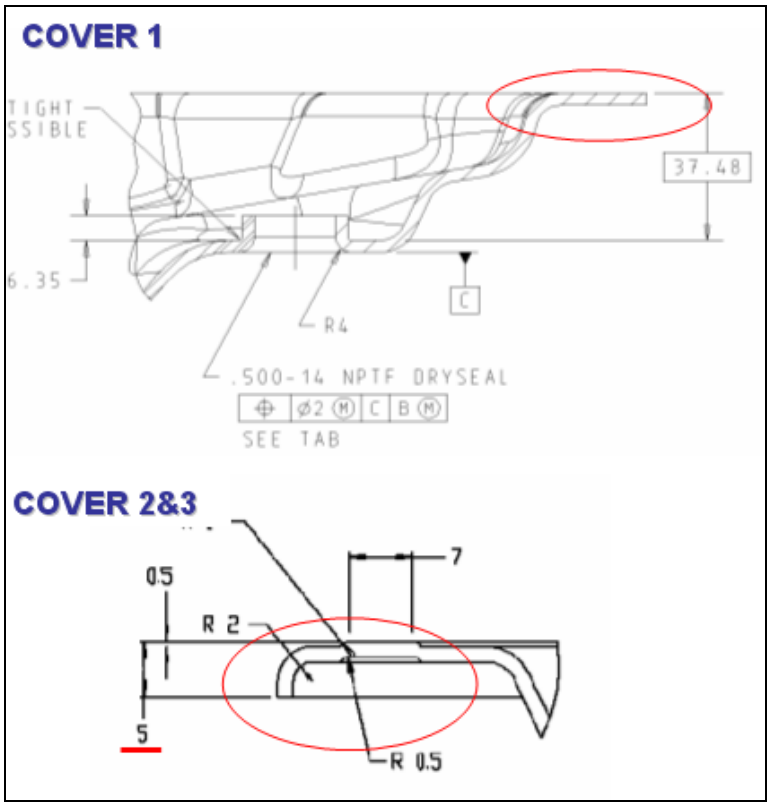

Figure 2.3. Cover 2 &3 design that is added curvature and 0.5 mm stamping

Proposed Stamping/Bead form applies uniform pressure between bolt holes even for increased bolt torques.

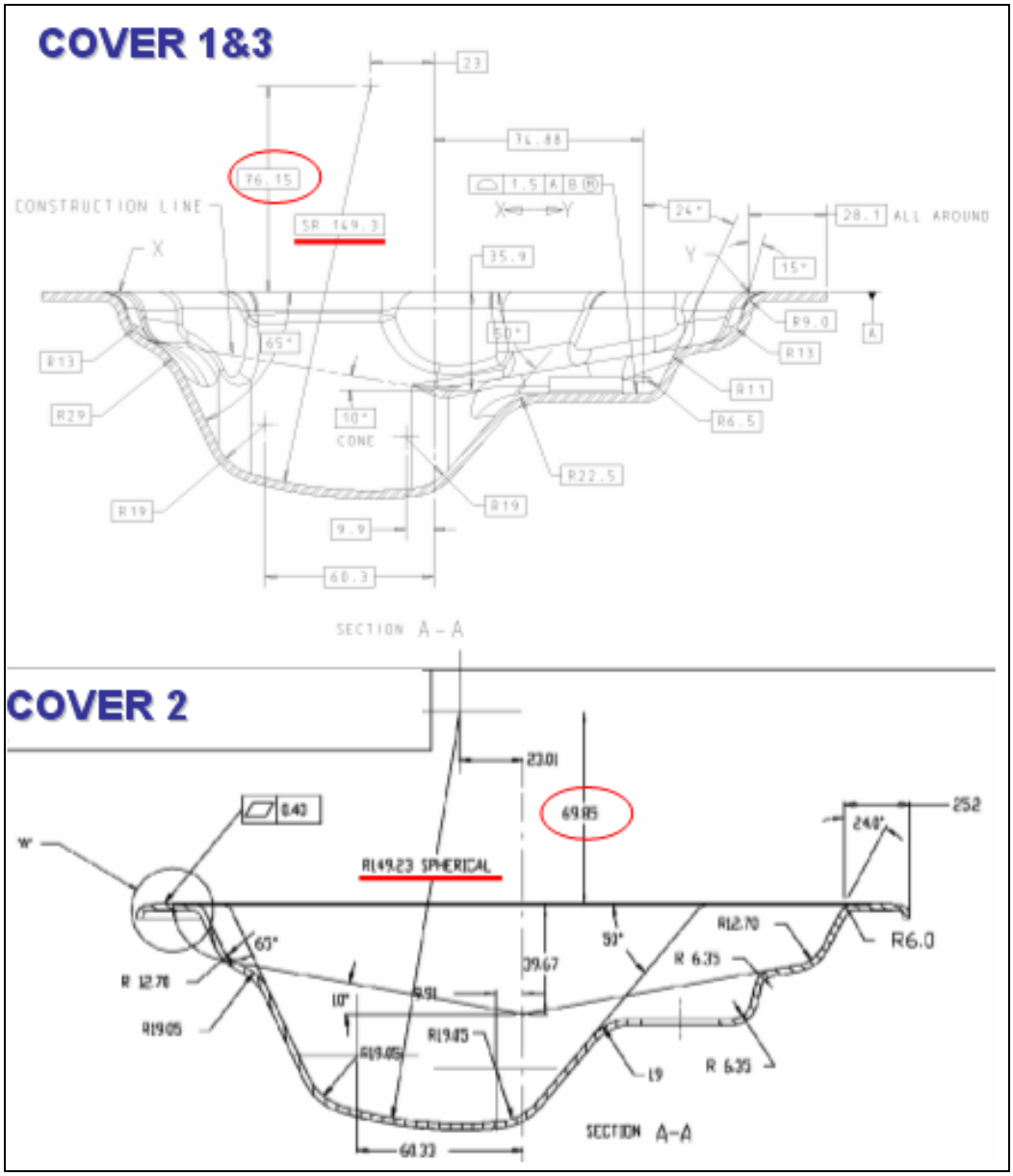

Figure 2.4. Dimensional difference of cover 2 (app. 7 mm larger in depth)

2.3 Vehicle Durability Test Results

The purpose of this test is to validate the strength, durability and functionality of all components of the vehicle over 240,000 km or 1 life - drive train, components of all types of light trucks, including, but not limited to rear axle, drive shaft (prop shaft), gearbox, clutch and engine mounts. All components which complete this test without failure are considered to be durable. For a good evaluation, it is mandatory that this procedure is executed as accurately as possible.

2.3.1 Cover 1 Results

During the durability vehicle test, several cover leakage issues were investigated. For cover 1, the holes where leakage was observed during testing are pointed out in Figure 2.5-2.8.

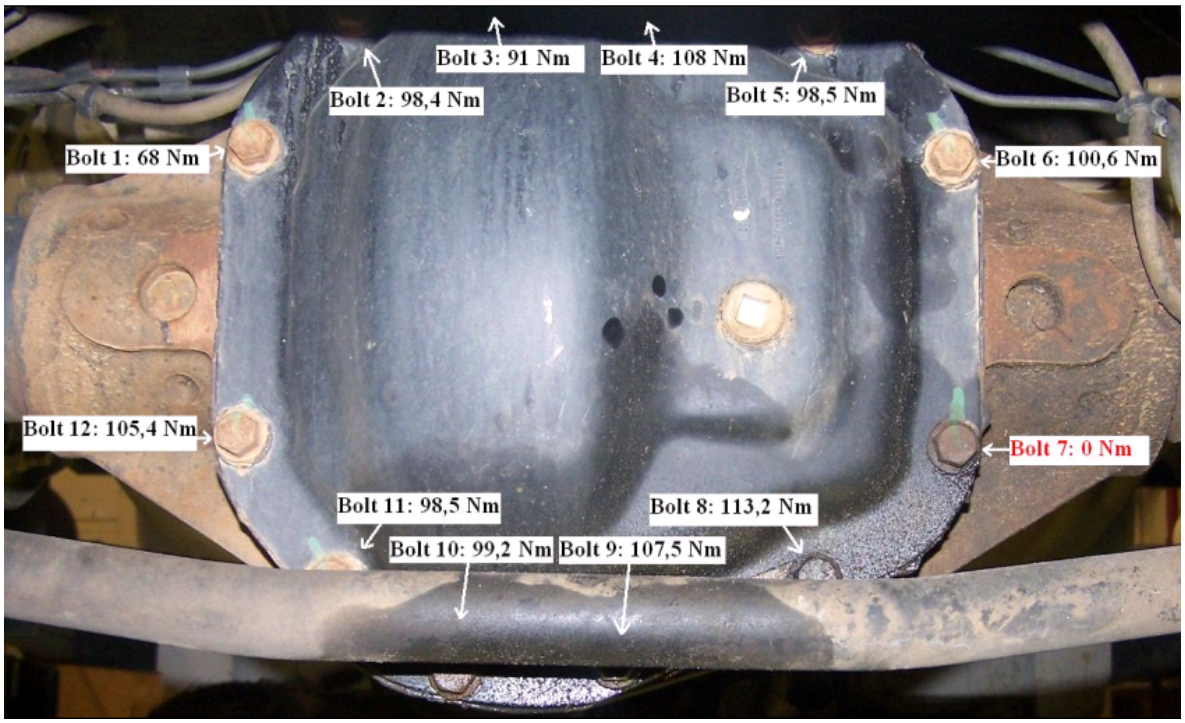

Figure 2.5. Leakage from rear axle cover 1, after TTGD test and bolt torques

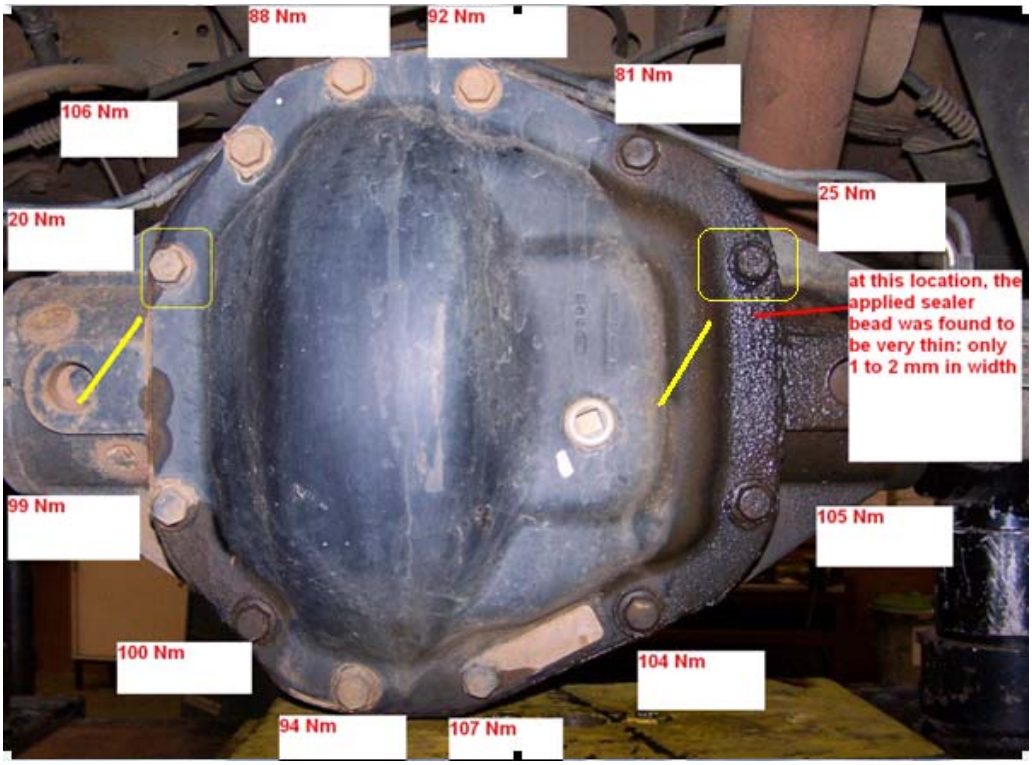

Figure 2.6. Leakage from rear axle cover 1, after TTGD test (including bolt torques)

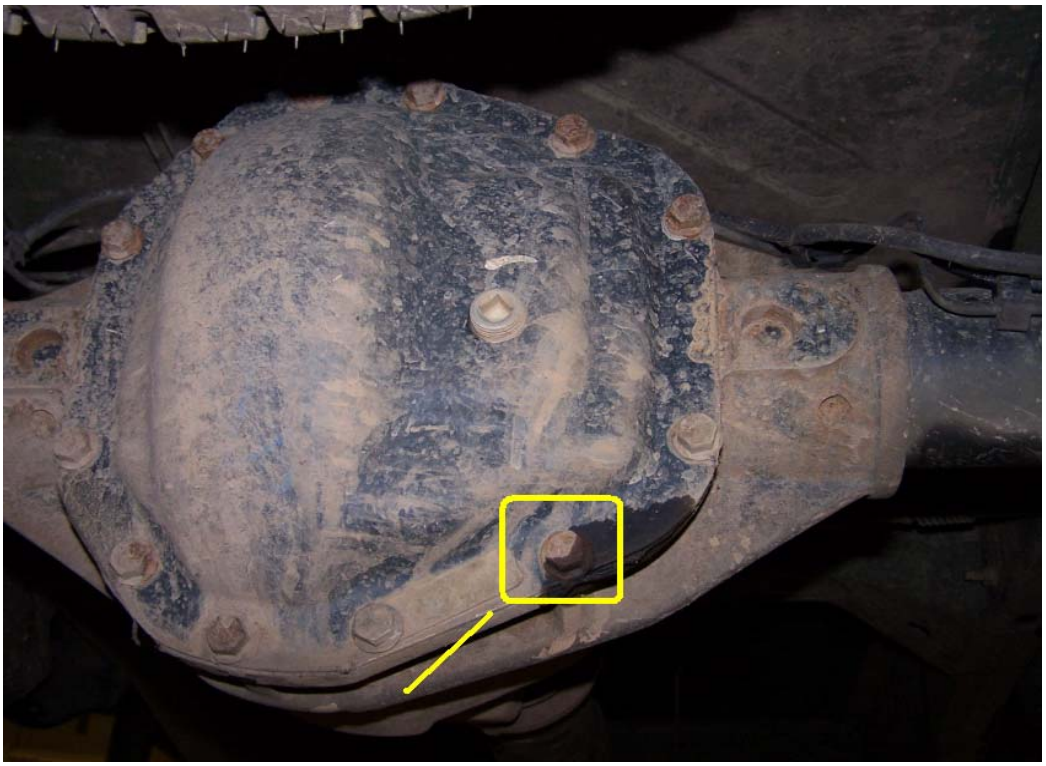

Figure 2.7. Leakage from rear axle cover 1, after TTGD test

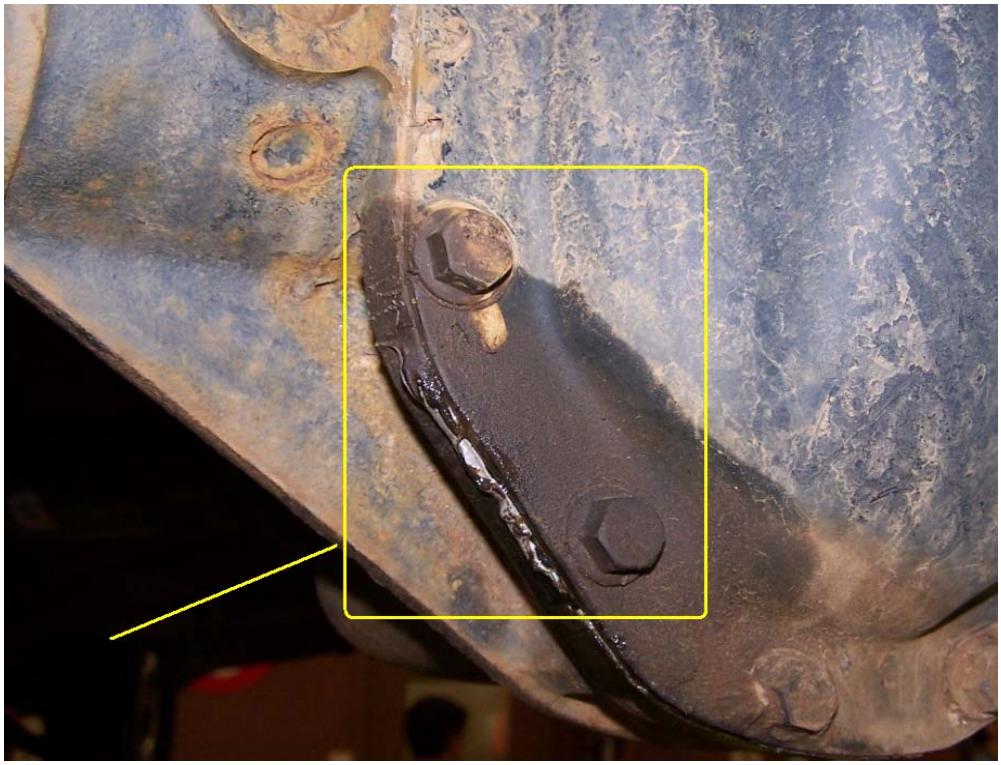

Figure 2.8. Leakage from rear axle cover 1, after TTGD test

2.3.2 Cover 2 Results

For cover 2, the holes where leakage was observed during testing are pointed out in Figure 2.9-2.12.

Figure 2.9. Leakage from rear axle cover 2 after TTGD test

Figure 2.10. Leakage from rear axle cover 2 after TTGD test

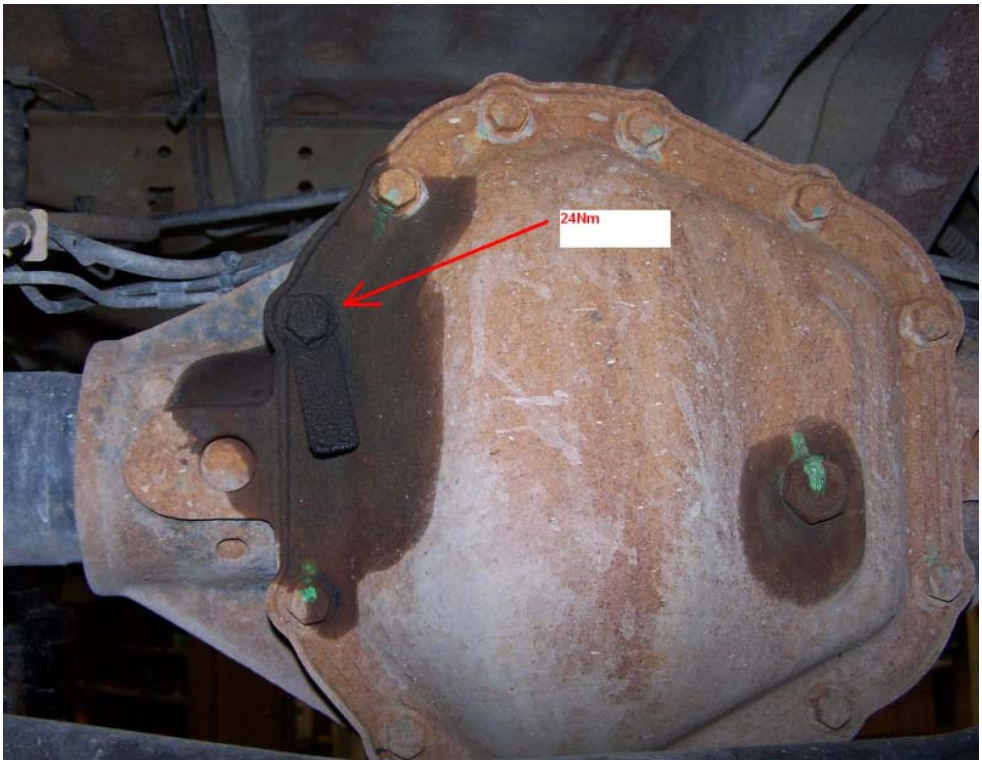

Figure 2.11. Leakage from rear axle cover 2 after TTGD test (including bolt torque)

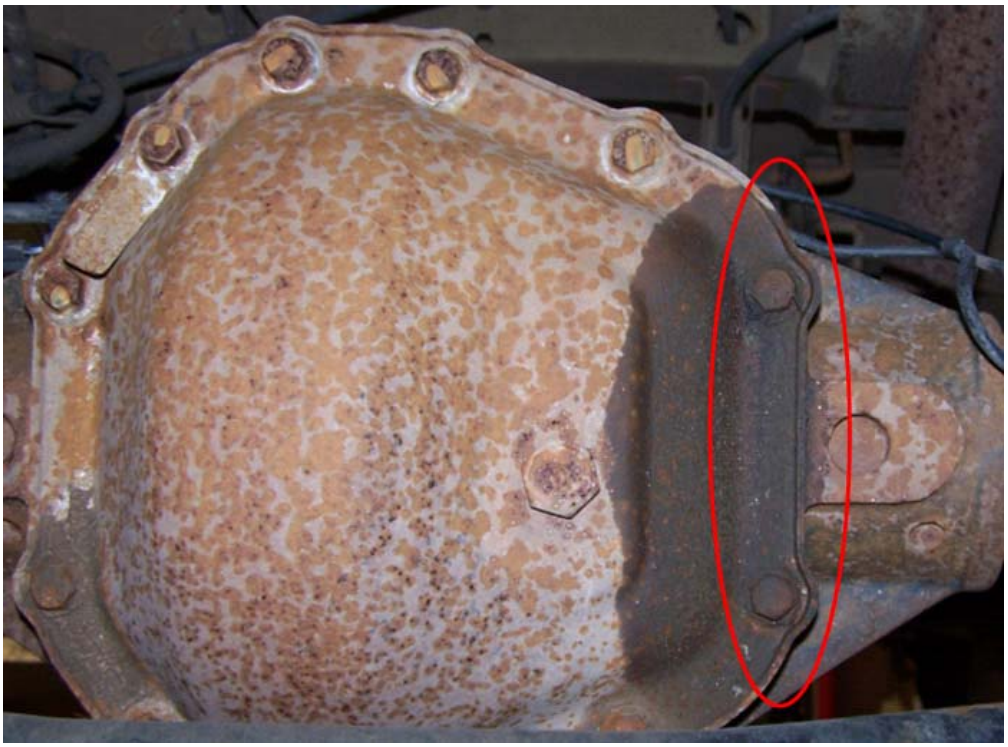

Figure 2.12. Leakage from rear axle cover 2 after TTGD test

From the test results, it can be concluded that leakage is likely to occur at various hole positions for both cover designs. In the Figure 2.13, leakage locations are indicated with red circles and critical regions on the cover are pointed with yellow arrows.

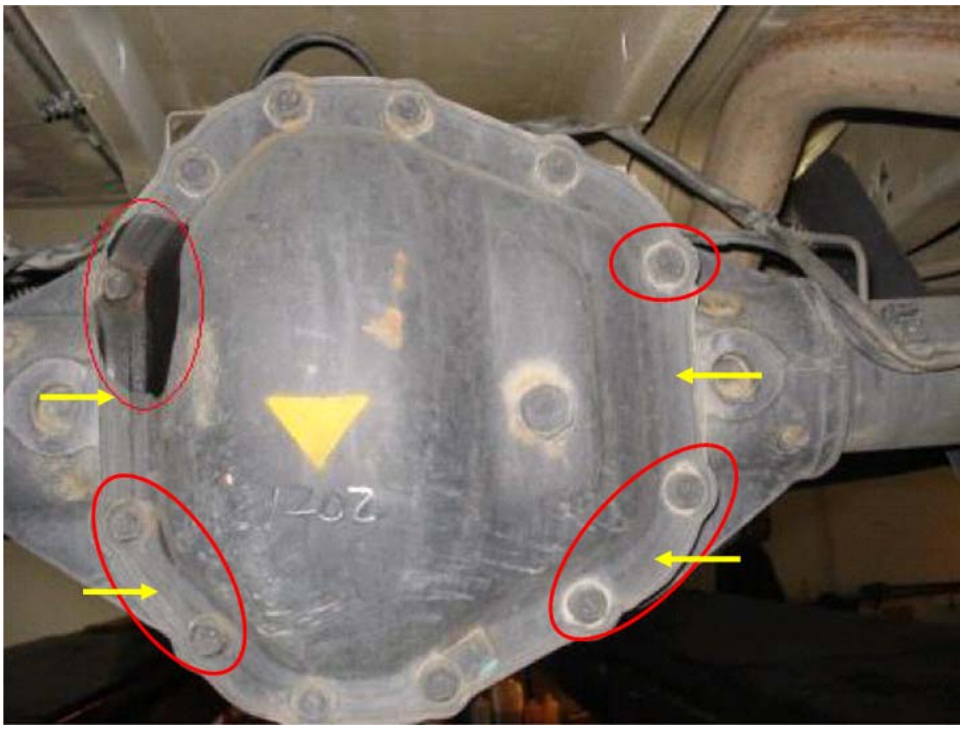

Figure 2.13. Leakage summary of rear axle cover 1 & 2, after TTGD test

2.4 Vertical Beam Fatigue Test Results

View from rear of axle and cover bolt numbering can be seen in Figure 2.14.

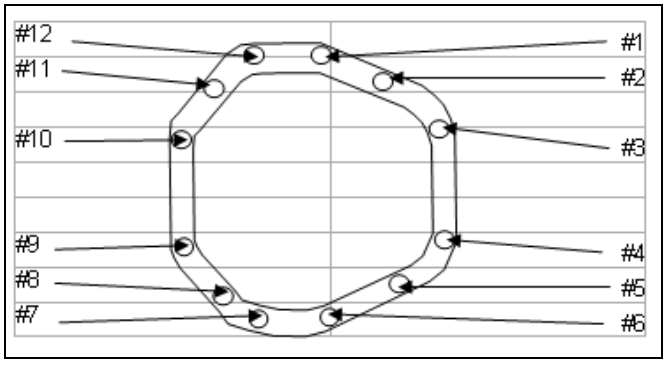

Figure 2.14. View from rear of axle

2.4.1 Vertical Beam Fatigue Test 1

To determine whether cover 1 and cover 2 would perform adequately, a series of tests were performed on the beam fatigue rig in Dana Birmingham. These tests would provide a comparison of the performances of the cover designs.

Five axles were taken from the Birmingham production line, covers are removed and the carrier surfaces are cleaned. Each of the other sourced covers (3 off cover2 and 2 off cover 1) was also cleaned and the Loctite 5900 sealant was applied using the X-Y plotter situated in the production line. Any adjustments required to keep the sealant on the raised section of the cover 2 were made using hand applied sealant. Standard production cover bolts were used to retain the covers. All are torqued to 60 Nm. The axles were then left for a minimum of 24 hours to allow the cover sealant to set. Each axle was then mounted on the beam fatigue rig and subjected to a cyclic loading of 0.5-2.5G. The axle was sealed and pressurized to allow for detection of air loss. Periodically, the cover plate was checked for air loss using a leak detector spray. The tests were suspended at 500,000 cycles if no failure occurred. Test results are shown in Table 2.1.

Table 2.1 Results of vertical beam fatigue test number1

Cover Source	Cycles	Failure mode
Cover 1	513,170	None
Cover 1	500,410	None
Cover 2	455,000 – 461,980	Leak around bolt No 9
Cover 2	373,500 – 382,320	Leak around bolt No 9
Cover 2	323,440 – 332,350	Leak around bolt No 9

As a conclusion, the expected life of an axle at this loading is 300,000-450,000 cycles. All of the axles with cover 2 failed to complete the 500,000 cycles without leaking. For cover 1, both of them completed the test without the cover leakage. The conclusion is that cover 2 is not as robust as cover 1. Although cover 2 did not perform as well as cover 1, the lives of the covers remain close to the expected life of the axle at this loading.

2.4.2 Vertical Beam Fatigue Test 2

Following reported cover 1 leaks in Jumbo vehicles in China, a series of tests were performed on the beam fatigue rig in Dana Birmingham using the mentioned test procedure with cover 2. Additionally, the load was increased by 10%.These tests can be compared with the results from the testing on the previous design. Cover 2 was being contemplated as a replacement for cover 1 currently used in the production.

Test results are shown in table 2.2 :

Table 2.2 Results of vertical beam fatigue test number 2

Sample	Cycles	Failure mode
#1	1,001,530	Cover cracked around bolt No 9
#2	263,510	Cover cracked around bolt No 9
#3	480,000 – 606,220	Cover cracked around bolt No 9

Following this failure it was realized that this crack was only detected when the axle was under heavy loading. All previous checks for air leaks, including those on sample #1 had been performed when the axle was not in a loaded condition. The first sample was then re-mounted on the rig and checked for leaks under load. A crack was found in the cover in the same position as on sample #2 below. Loaded and unloaded conditions for sample 1 is shown in Figure 2.15 and Figure 2.16.It is not possible to determine when this crack occurred in the cover plate and therefore the result from this sample should be ignored.

Figure 2.15. Sample #1 – unloaded condition

Figure 2.16. Sample #1 – loaded condition

The second cover plate cracked on the radius next to bolt number 9. It can be seen in Figure 2.17 and 2.18.

Figure 2.17. Sample #2

Figure 2.18. Sample #2

The cover plate for sample #3 was checked under load prior to test and no cracks were found as can be seen in Figure 2.19 and Figure 2.20. This sample failed during overnight running and so it is not known exactly when the cover cracked. The failed cover is shown in Figure 2.21. For this reason the result of 480,000 cycles will be used.

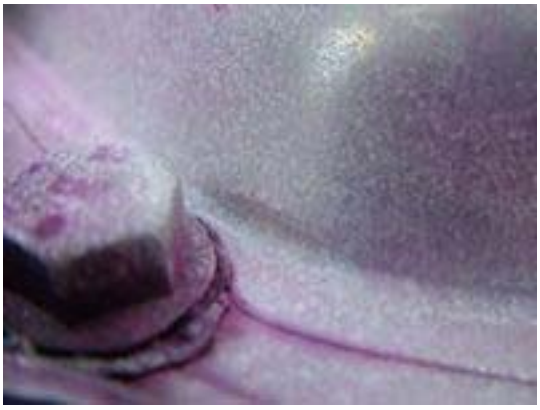

Figure 2.19. Sample #3 – No load prior to test

Figure 2.20. Sample #3 – Under load prior to test

Figure 2.21. Sample #3 – End of test

When comparing the results with those from previous testing it should be remembered that this test was run at an additional 10% load. The new cover design did not perform as well as the old one in previous test, but the increased load my account for this. However, there is insufficient confidence in this cover design.

3. FINITE ELEMENT ANALYSIS OF THE REAR AXLE

In order to save cost and time, one should take advantage of CAE analysis to optimize the rear axle cover design. Vehicle durability test results and vertical beam fatigue test results are available for both of Cover 1 and Cover 2. During the vehicle durability test, torque transmitted from the propeller shaft to the pinion gear is measured and get the maximum torque on pinion shaft as an analysis input.

3.1. FE Model and Inputs for the Analysis

3.1.1 FE Model of the Rear Axle

Figure 3.1 -3.3 show the representative mesh model of the rear axle and its parts. Rear axle tubes, carrier, cover, cover bolts and bearing caps are modeled for this study. There is no need to model the axle shafts as they only transmitted torque to wheels and no effect on force distribution. Moreover, hypoid gear set, differential case and bearings are not modeled, their effects on carrier surfaces are accounted for calculating the reaction forces.

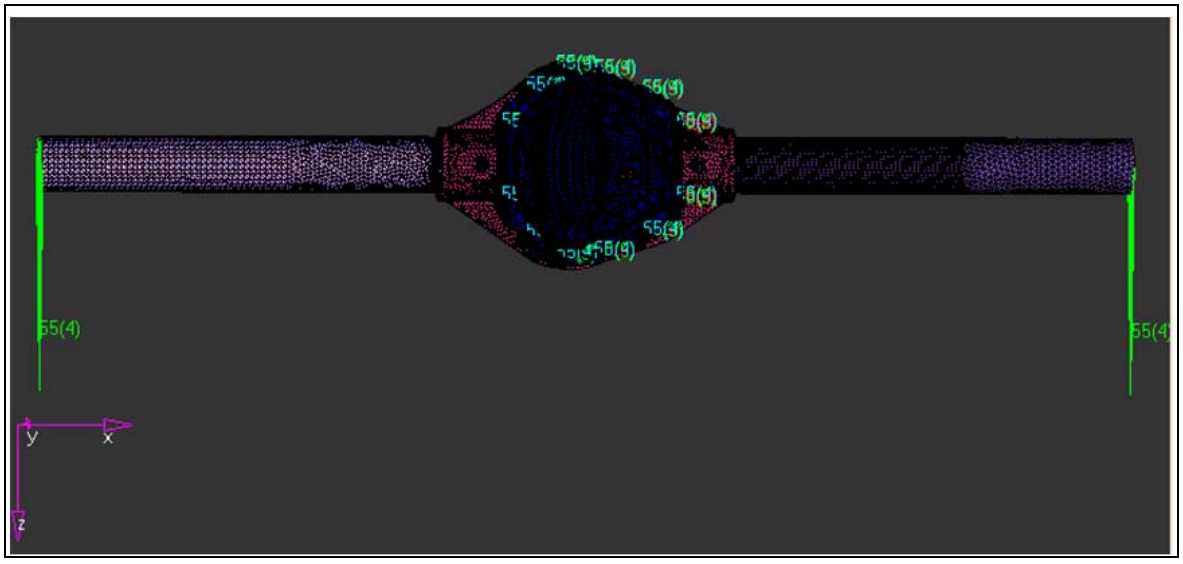

Figure 3.1 Representative mesh model of the rear axle

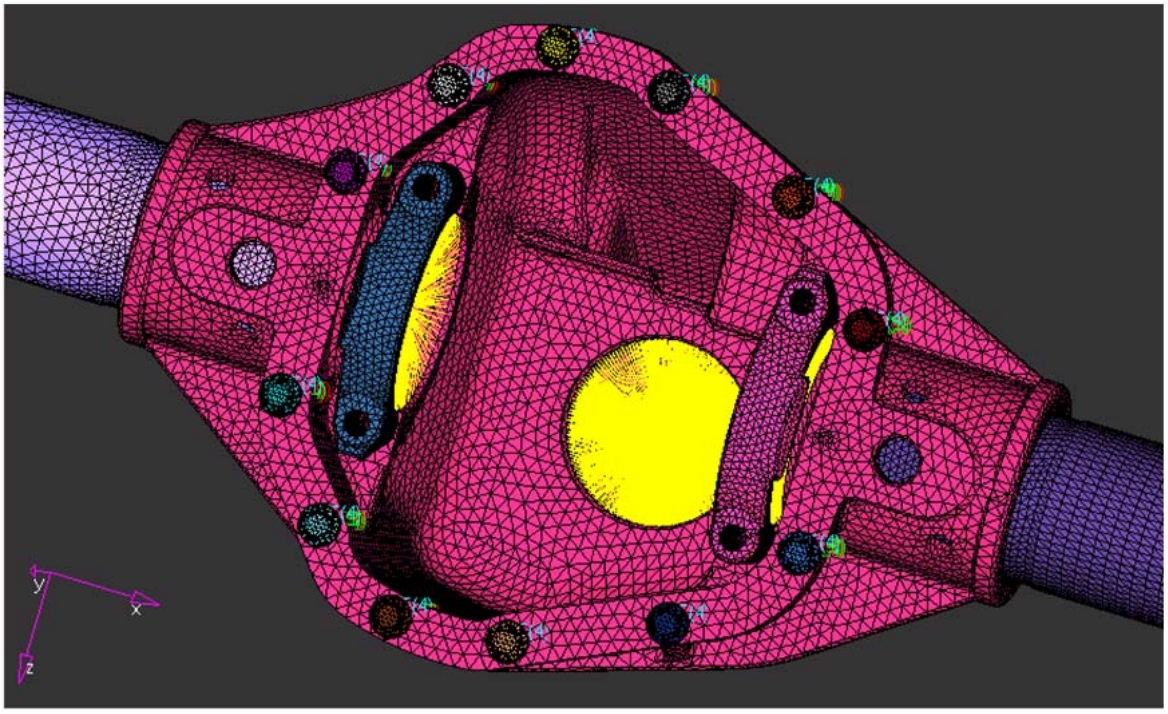

Figure 3.2 Representative mesh model of the rear axle housing (carrier, tube,caps,bolts)

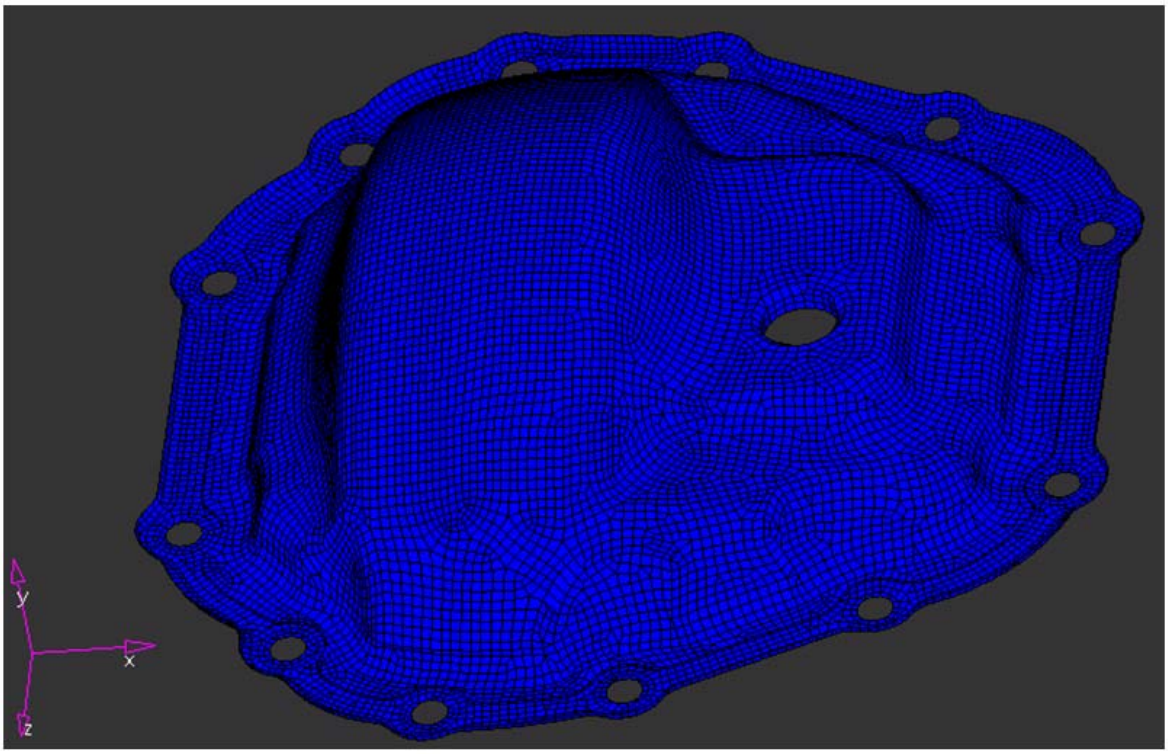

Figure 3.3 Representative mesh model of the rear axle cover

The FE model of the carrier, rear axle tubes and caps are created using 2nd order tetrahedral elements. As shown in Figure 3.4, cover bolt head and carrier are modeled with using solid elements; also the same modeling is used for the bearing caps and the axle tubes. The cover is modeled using first order quad shell elements. There is no need for solid modeling for the cover, because it has 3 mm thickness. Cover bolts are modeled using beam elements. Cover bolts are connected with rigid elements to carrier surface (type of rigid elements is 6 dof RBE2) as shown in Figure 3.5. Also, pretension is defined for each cover bolt in the modeling.

As shown in Figure 3.4, there is a contact between bolt head-cover and carrier-cover. Friction is defined and exponential pressure over closure algorithm is used for the surface behavior. (clearance at 0; contact pressure 0.001 mm and pressure at 0; clearance 10 Pa). Small sliding node to surface algorithm is also used. Friction coefficient for this analysis is taken as 0.1.

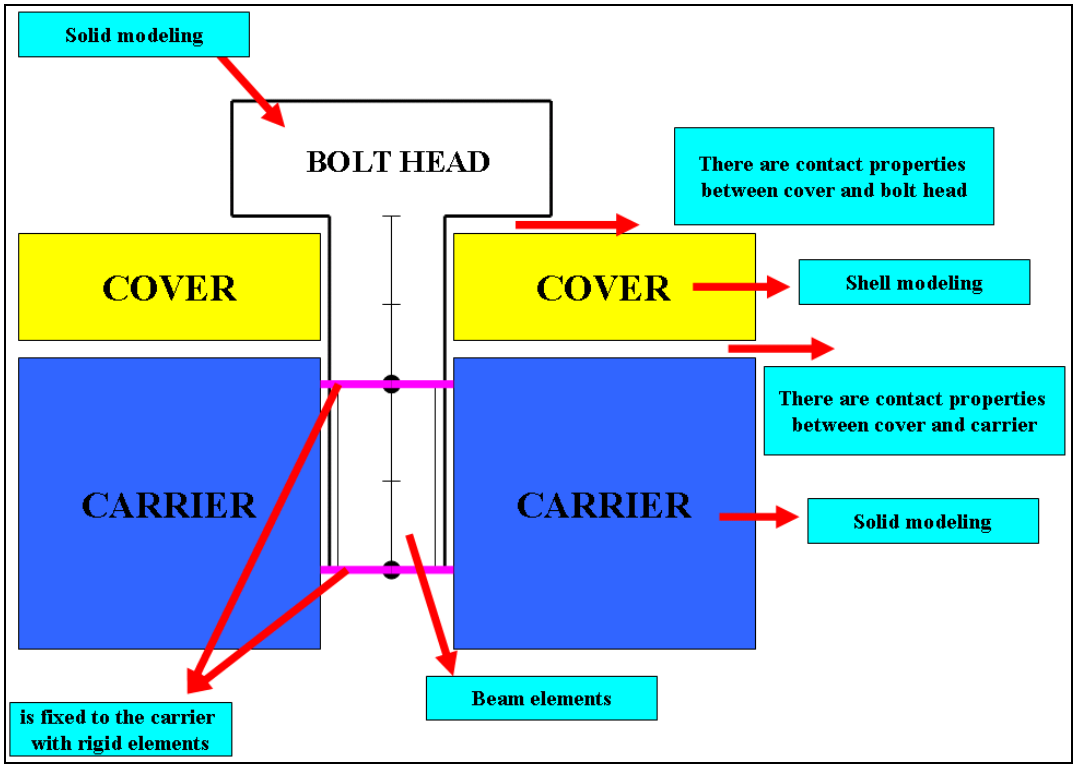

Figure 3.4 FE model of the rear axle cover, carrier and cover bolt

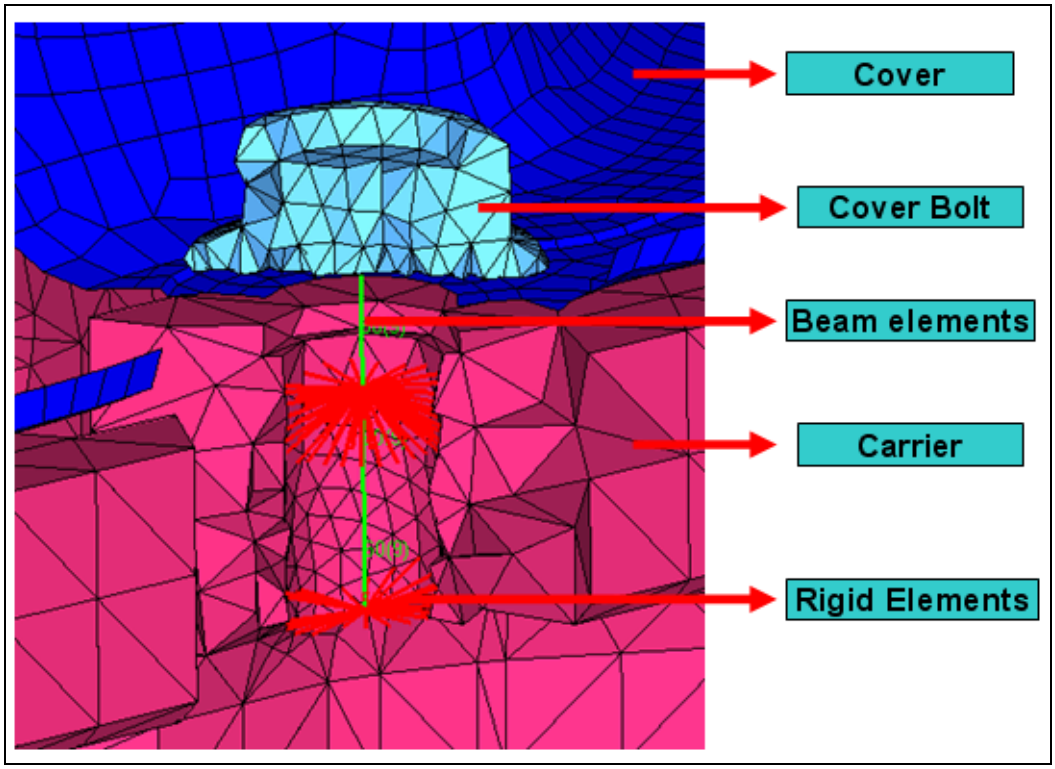

Figure 3.5 FE model of the rear axle cover, carrier and cover bolt (from model view)

In the assembly line carrier and rear axle tubes are fastened with a tight fit. For this, reason tie contact is defined between the carrier and rear axle tubes. It is modeled one to one as a rigid body. Also, the same modeling is applied between carrier and differential bearing cap shown in Figure 3.6.

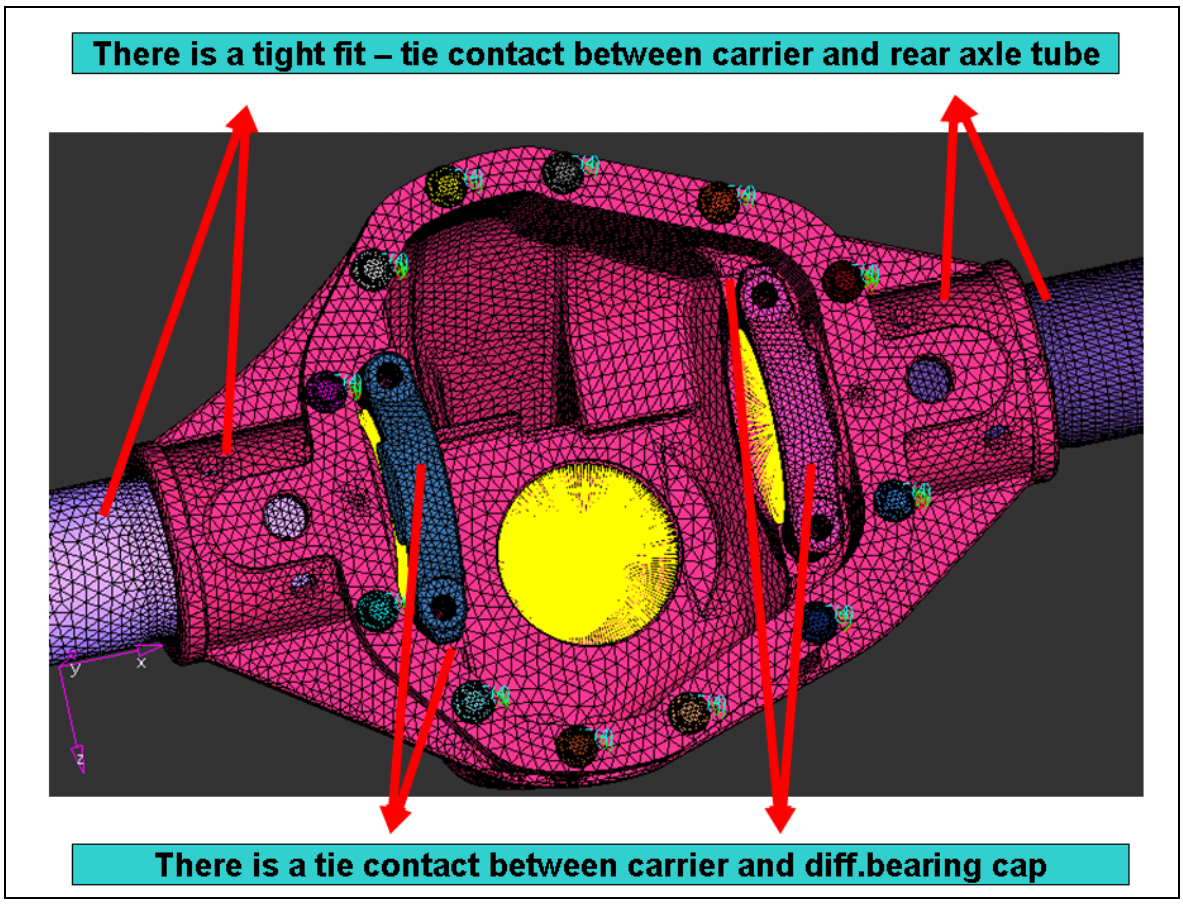

Figure 3.6 FE model of the carrier and rear axle tube & carrier and differential bearing cap (from model view)

As a result of the torque transmitted from the propeller shaft to rear axle, reaction forces develop at the differential and pinion bearings of the rear axle. Instead of including the hypoid gear set and differential case in the model, their effects on the bearing surfaces are accounted for by calculating the reaction forces. Force and pressure are induced on the bearings and on the carrier contact surfaces due to torsional effect. Each bearing center node is defined, then connected with rigid elements to carrier surfaces. Calculated forces are directly applied to this node, so force and pressure are distributed to the bearing carrier surface from the center of the bearings as shown in Figure 3.7.

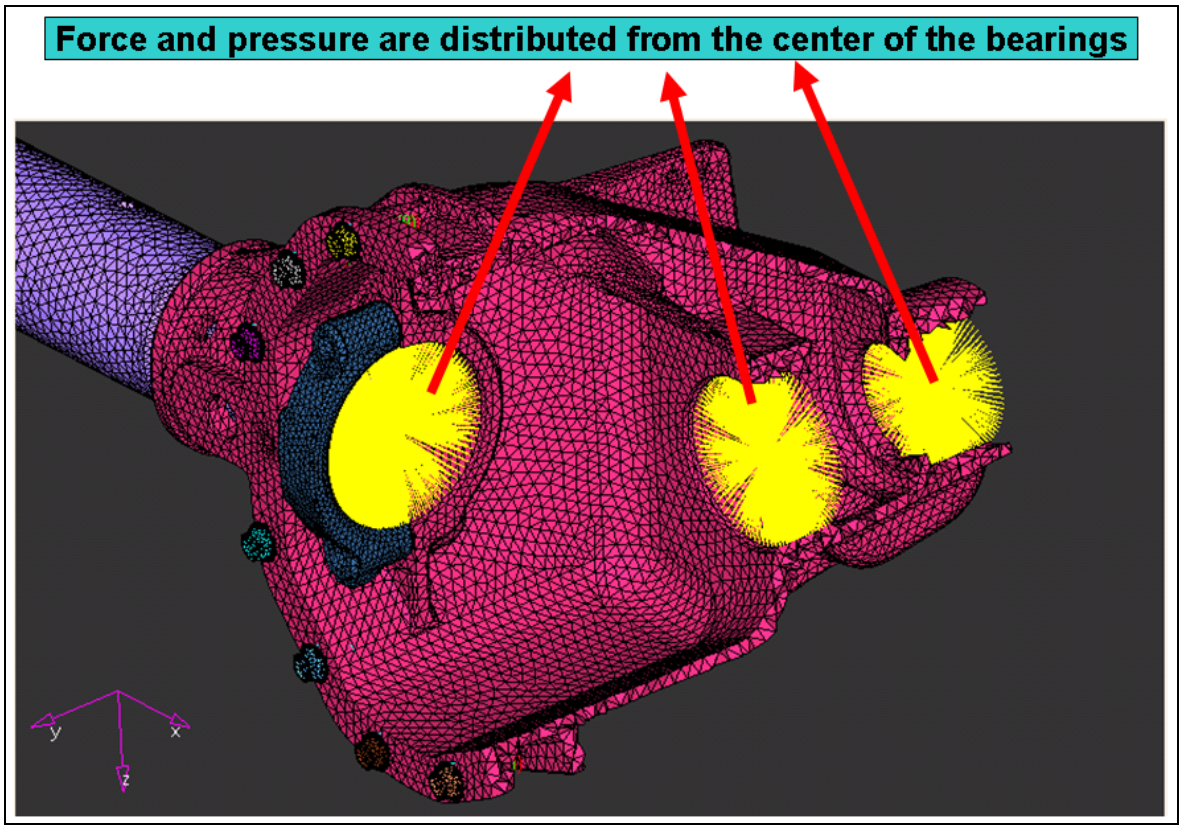

Figure 3.7 FE model of force distribution of the bearings-differential and pinion bearings (from model view)

3.1.2 FE Model Inputs

In the calculations, it is assumed that a 3g wheel load would be reacted by a load split of 1g at the bump stops and 2g at the spring centers as shown in Figure 3.8. This is an assumption based on other typical applications and experience.

1g wheel load is the load calculated by multiplying rear axle load (RAL) with g. Rear axle load can be described as the axle maximum capacity. For this study, the worst case, dual rear wheel is selected and RAL of this type of vehicle is 2950 kg.

1g wheel load = (RAL) * g = 2950 kg * g ~ 28929.6 N

Input loads on the rear axle are given as ;

- Vertical downward load of 28929.6 N on both spring centers.
- Vertical download load of 14464.8 N on both bump centers.

Other inputs shown in Figure 3.8 are;

- Material of the bearing cap and carrier is cast iron and elastic modulus of these parts is 163.3 GPa, and also Poisson's ratio is taken as 0.275.
- Material of the cover, cover bolt and tube is steel and elastic modulus of these parts is 206.8 GPa, and also Poisson's ratio is taken as 0.28.
- Minimum preload of 28491 N is induced in each bolt of carrier and cover during tightening.
- Forward torque is +1800 Nm.

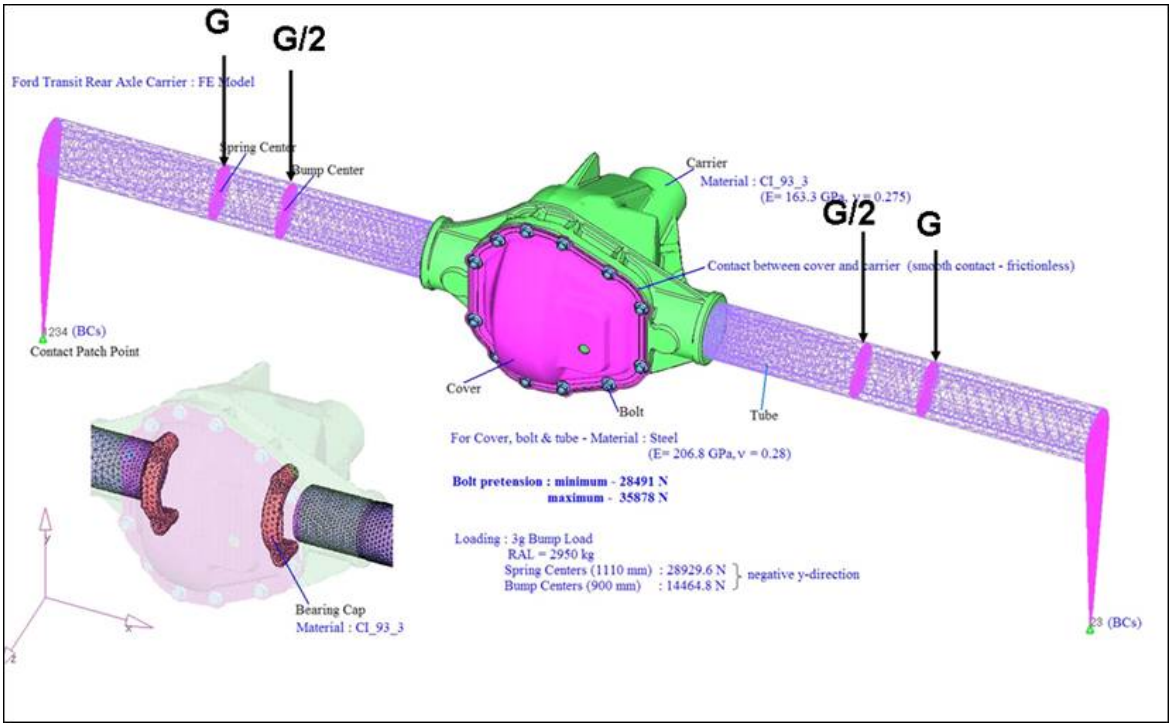

Figure 3.8 FE model of the rear axle and inputs for the analysis

Boundary conditions of the model are shown in Figure 3.9. One side of the rear axle is restrained in x, y and z translation and the other side is constrained in x, z translation and y rotation at tire contact locations. This simulates the rear axle movement under loading.

Moreover, axial forces and resultant forces are shown in Figure 3.9. Calculated resultant forces (R_{ph}, R_{pt}, R_{gl}, R_{gr}) and axial forces (A_{ph}, A_{pt}, A_{gl}, A_{gr}) are shown in Table 3.1. Details of rear axle force analysis can be found in Appendix C & D (FADSIM TOOL BOX & FORMULATIONS).

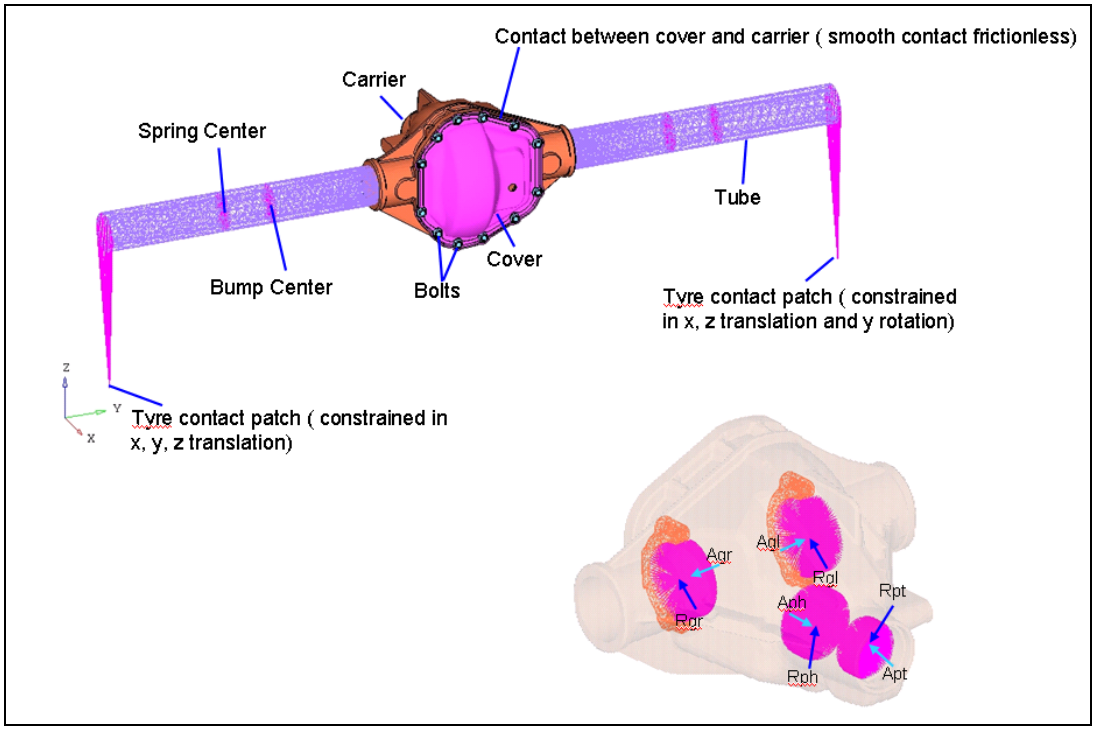

Figure 3.9 FE model of the rear axle with including torsional effects (bearing loads)

Table 3.1 Force and pressure distribution due to torque

	Forward Torque			
Force/Pressure	X	Y	Z	Pressure
Rph (N)		-3757	75527	
Rpt (N)		15768	-15992	
Rgl (N)	52120		-34377	
Rgr (N)	21455		-25125	
Aph (N/mm2)				81.8806
Apt (N/mm2)				37.0373
Agl (N/mm2)				25.3637
Agr (N/mm2)				17.8625

The aim of this study is to correlate the results of the FE model with the test data. The leakage locations are determined by performing several vehicle durability tests and vertical beam fatigue tests. If the model can predict the similar failure modes as observed in the tests, then the model can be used to predict the impact of changes in the cover design on its performance. First, hole locations were modified to improve the design of the cover, so that a smaller gap. Then cover thickness and cover flange design were modified.

3.2. FE Analysis Results for Cover 1, 2 and 3

FE analyses were performed for all 3 covers under 3g beam load and 3g beam load + forward torque. The results of the FE analyses for the cover 1, 2 and 3 are summarized in Table 3.2. As seen in Figures 3.10-3.15, that the critical locations correspond to leakage locations observed in tests. This validates the FE model of the rear axle used in this study.

It can be concluded that the critical loading condition for this analysis is 3g beam load + forward torque load condition. The results can be also seen in Figure 3.10-3.15. Cover design may be improved by changing cover bolt hole locations according to Axle Cover Design Guide released by FORD MOTOR COMPANY. It can be easily seen that cover 3 has the best performance, so cover 3 will be the best choice, at the beginning, to improve the design.

Table 3.2 FE gap analysis results for cover 1, 2 and 3 (all dimensions are in mm)

SUMMARY RESULT TABLE			
Load Condition	Cover 1	Cover 2	Cover 3
3g Beam	0,009325	0,006685	0,00727
3g Beam + Forward Torque	0,08986	0,03601	0,03395

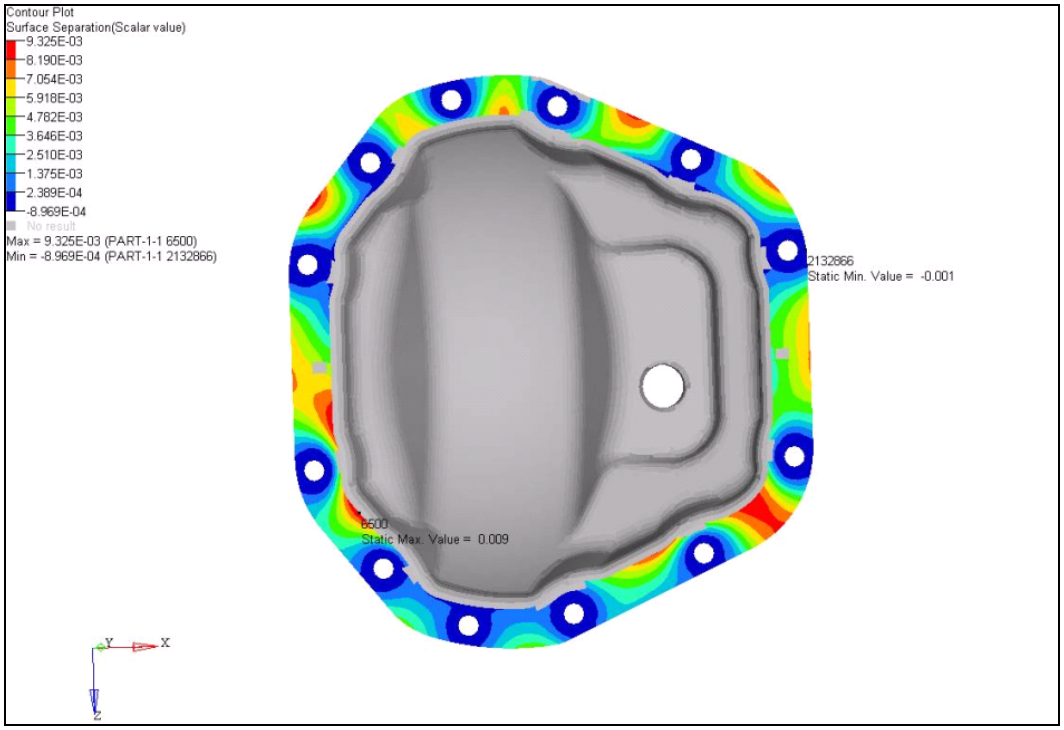

Figure 3.10 FE analysis result of cover 1 with 3g beam load condition

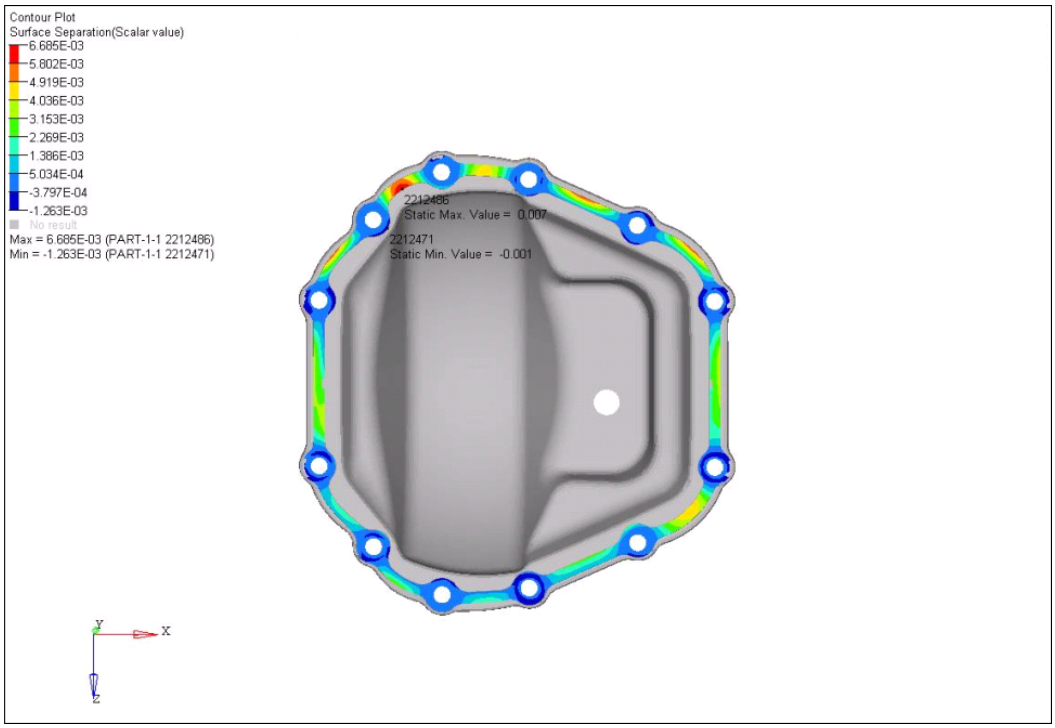

Figure 3.11 FE analysis result of cover 2 with 3g beam load condition

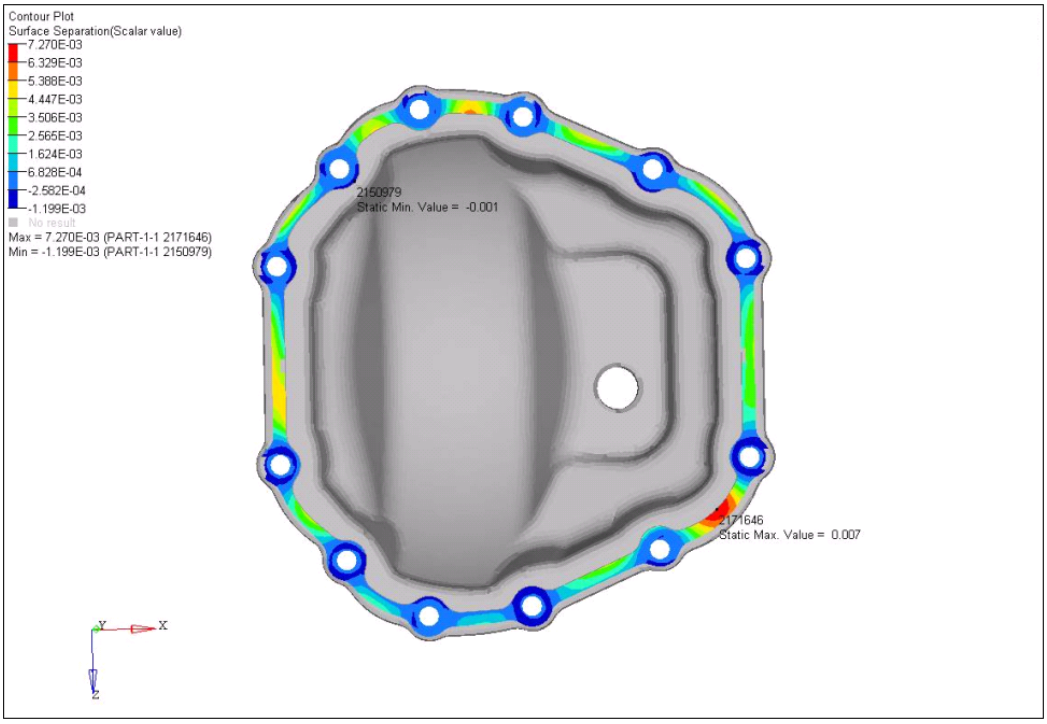

Figure 3.12 FE analysis result of cover 3 with 3g beam load condition

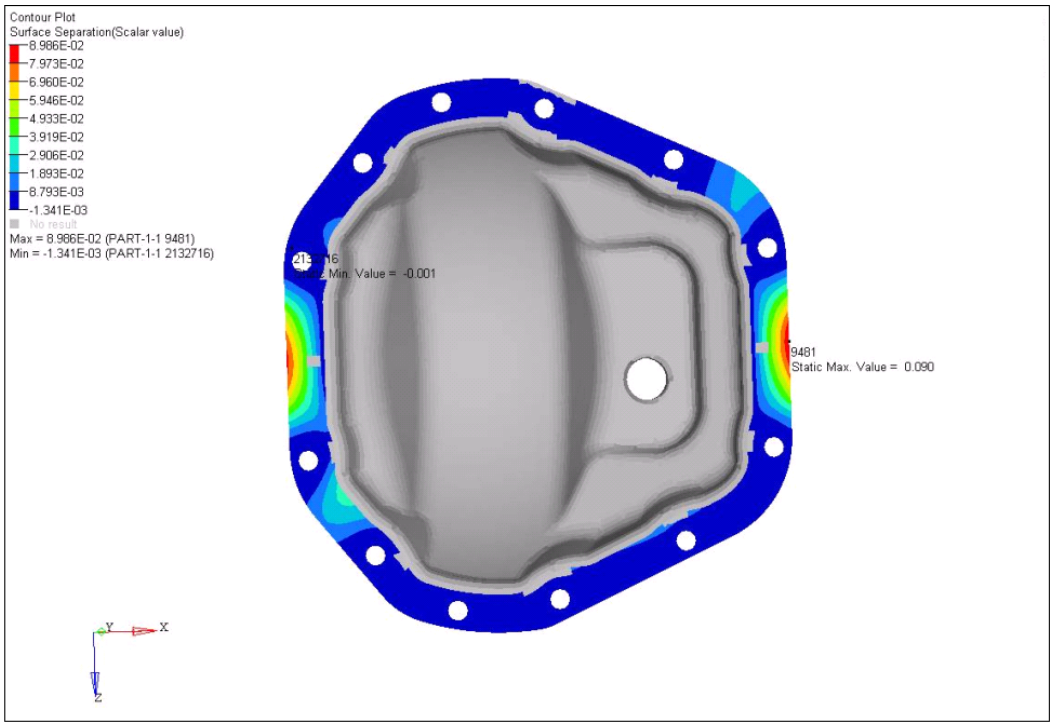

Figure 3.13 FE analysis result of cover 1 with 3g beam load + forward torque condition

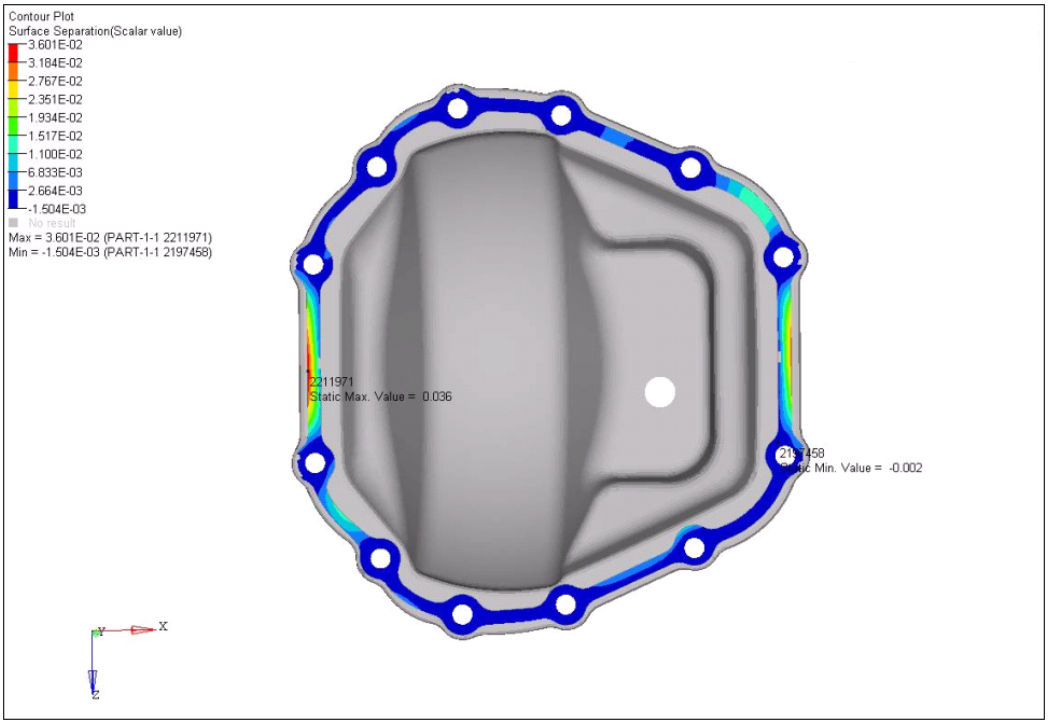

Figure 3.14 FE analysis result of cover 2 with 3g beam load + forward torque condition

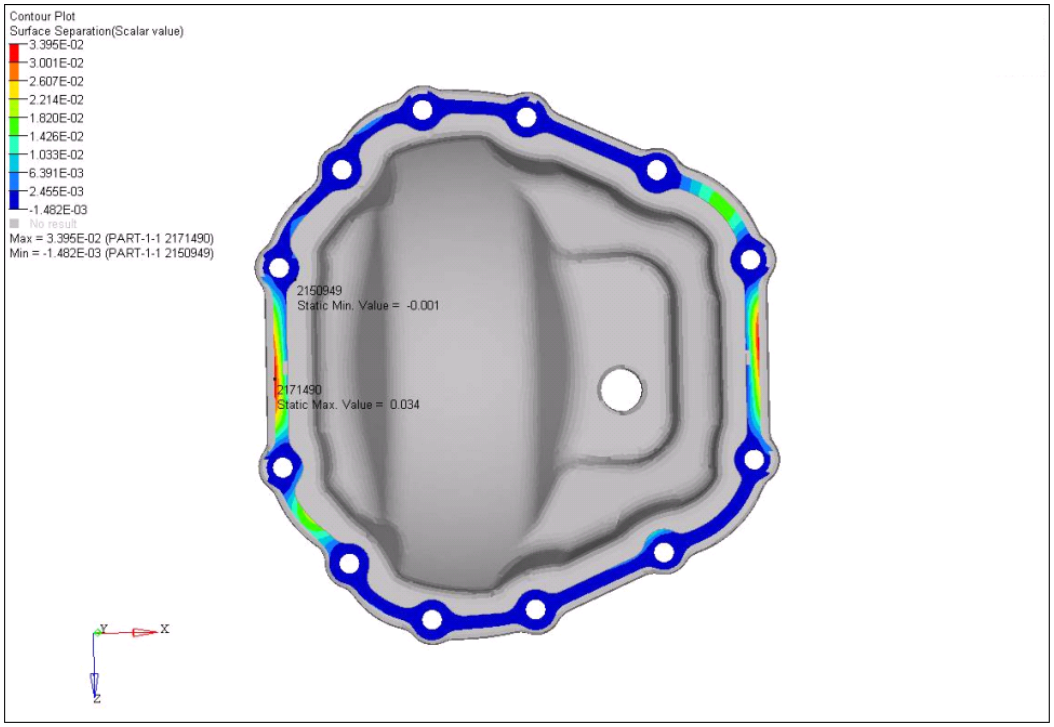

Figure 3.15 FE analysis result of cover 3 with 3g beam load + forward torque condition

3.3. Remodeling of the Bolted Joints with Solid Elements (Comparison between Solid and Beam Modeling)

In obtaining the previous results, the cover bolts were modeled by using beam elements. In order to check the effect of bolt modeling on the FE results, further analysis with solid modeling was also performed. The solid bolt modeling can be seen in Figure 3.16. Same as the previous study, cover bolts are connected with rigid elements to carrier surface and there is a contact between bolt head-cover and carrier-cover

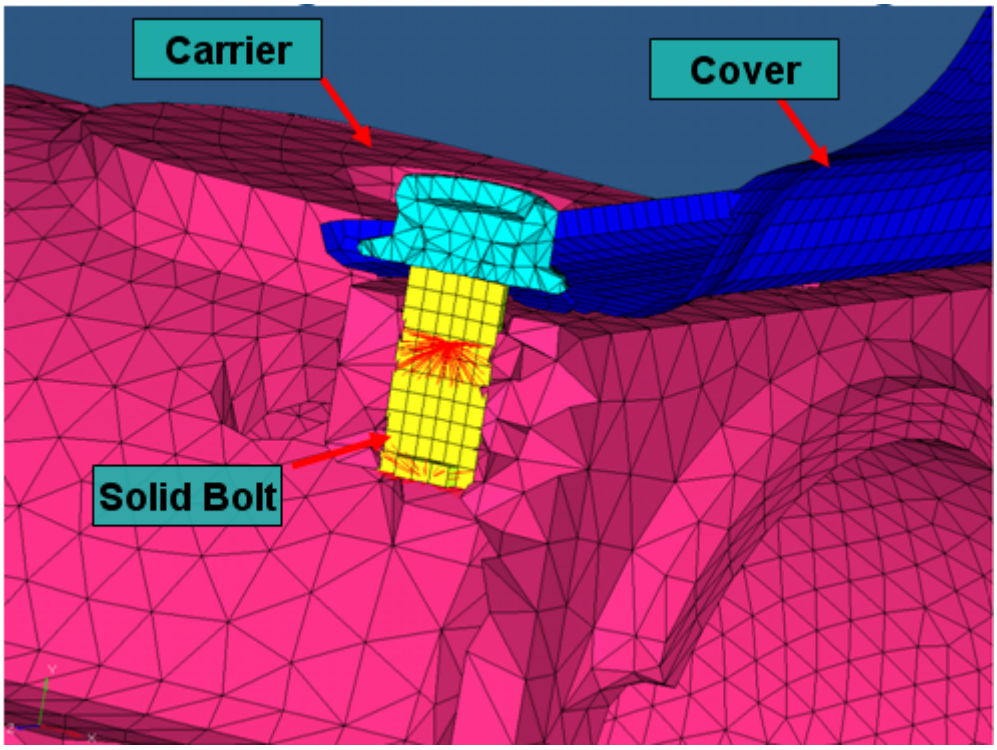

Figure 3.16 FE model of the rear axle cover, carrier and solid cover bolt(from model view)

In this additional study, the rear axle model with rear axle cover 3 is used. The critical load condition for this analysis is 3g beam load + forward torque load condition The maximum gap for cover 3 design with beam modeling is 0.03395 mm. Beside this, the result of maximum gap value for solid modeling study is 0.03424mm. There is a small difference between two different types of modeling. Critical locations are also same for both analyses. FE result of this study can be seen in Figure 3.17. In Cover 3 (3 mm) analysis, cover bolt head was modeled with solid elements and the cover thread is modeled

with beam elements. In the second analysis, cover 3 with solid bolt (3 mm), both cover bolt head and the cover thread are modeled with using solid elements.

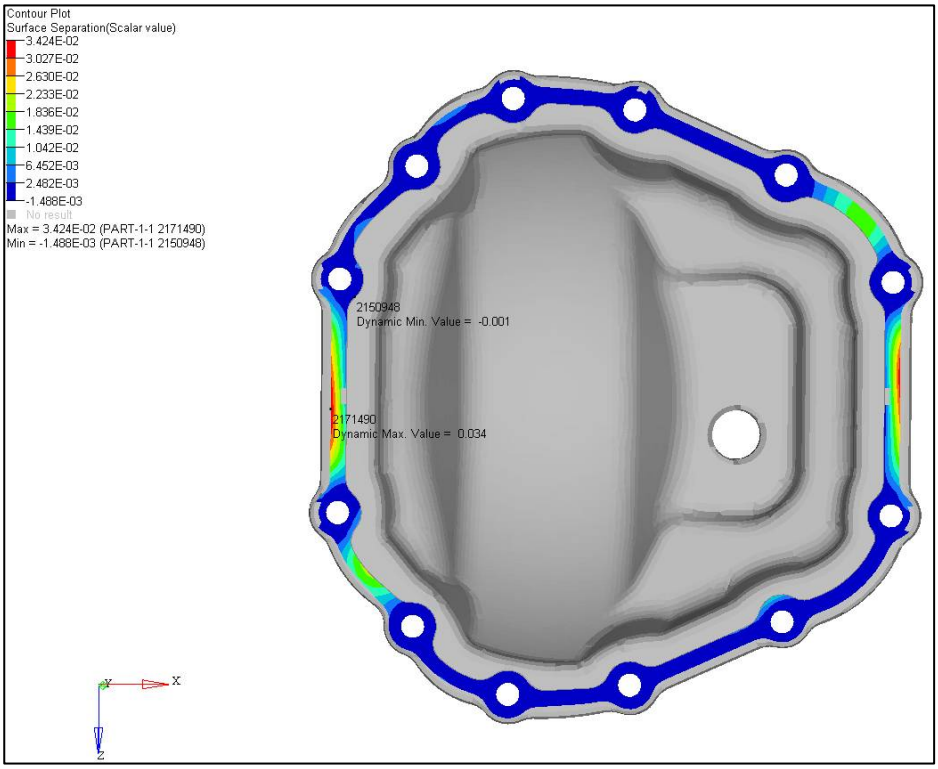

Figure 3.17 FE analysis result of cover 3 with 3g beam load + forward torque condition

In this study, compressive forces at each cover bolt locations are also calculated. As seen in Table 3.3 both modeling yields the same on compressive forces. Cover bolts are also numbered, 1 to 12, during this study as shown in Figure 3.18.

Compressive forces mentioned in the table are the preload values of the cover bolts on 3g beam load + forward torque load condition. The initial value for each cover bolt is 28491N.

Table 3.3 Compressive forces for each cover bolt location (Remodeling Study)

1st - Worst
2nd
3rd
4th
5th
6th - Safe

DESIGN NO (THICKNESS)	COVER BOLT NUMBER & COMP. FORCE (N)											
	1	2	3	4	5	6	7	8	9	10	11	12
COVER 3 (3 mm)	27651	26129	27534	27658	28102	28069	27198	26233	27852	27873	28527	28573
COVER 3 with Solid Bolt (3 mm)	27269	25468	27264	27398	27978	27980	26673	25572	27767	27644	28537	28578

DESIGN NO (THICKNESS)	COVER BOLT NUMBER & NET COMP. FORCE (N)											
	1	2	3	4	5	6	7	8	9	10	11	12
COVER 3 (3 mm)	-840	-2362	-957	-833	-389	-422	-1293	-2258	-639	-618	36	82
COVER 3 with Solid Bolt (3 mm)	-1222	-3023	-1227	-1093	-513	-511	-1818	-2919	-724	-847	46	87

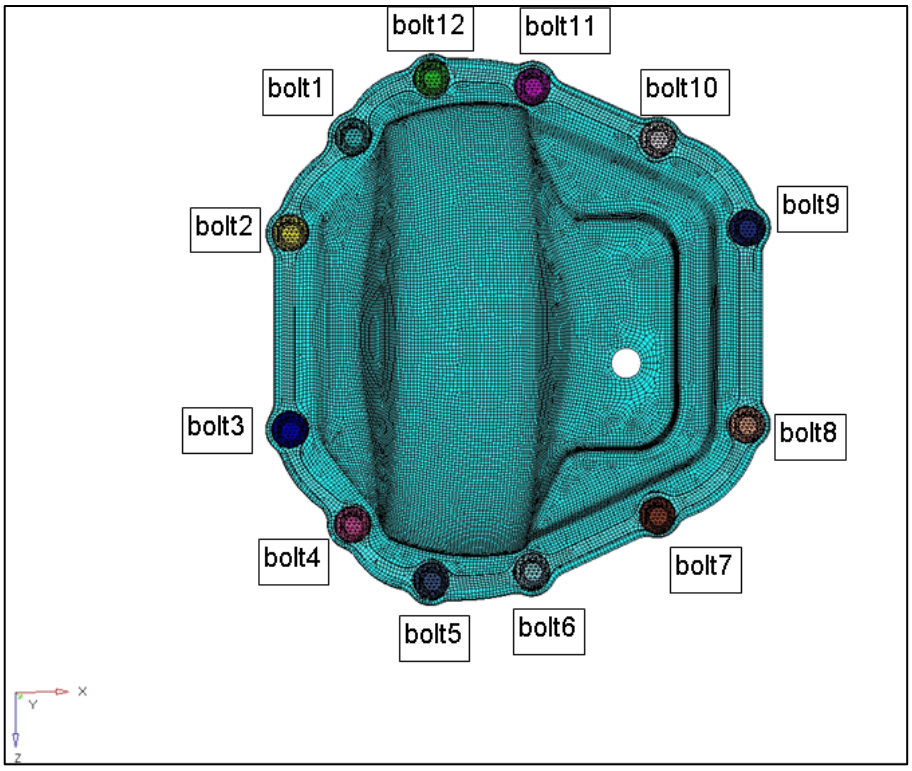

Figure 3.18 Cover bolt numbering on rear axle cover

After all these results, it can be concluded that the difference of both modeling is very small and can be neglected. Both solid and beam modeling gives similar results. In

order to perform the analysis in a shorter time, beam modeling can be used for rear cover bolts.

3.4. Design Improvement Proposals for Cover 3 (Different Hole Locations)

According to the Axle Design Guide [23] released by Ford Motor Company, cover bolt hole locations are very important parameters for the design. Bolt spacing shown in Figure 3.19 is an important parameter and as a design requirement the distance between two neighbouring holes should be within a specific range. They should not be far away. Then, it is considered that cover 3 design may be improved by changing the locations of the critical holes shown in Figure 3.20. A parametric study is conducted to determine the effects of bolt hole locations. The modifications in bolt positions are indicated in Table 3.3.

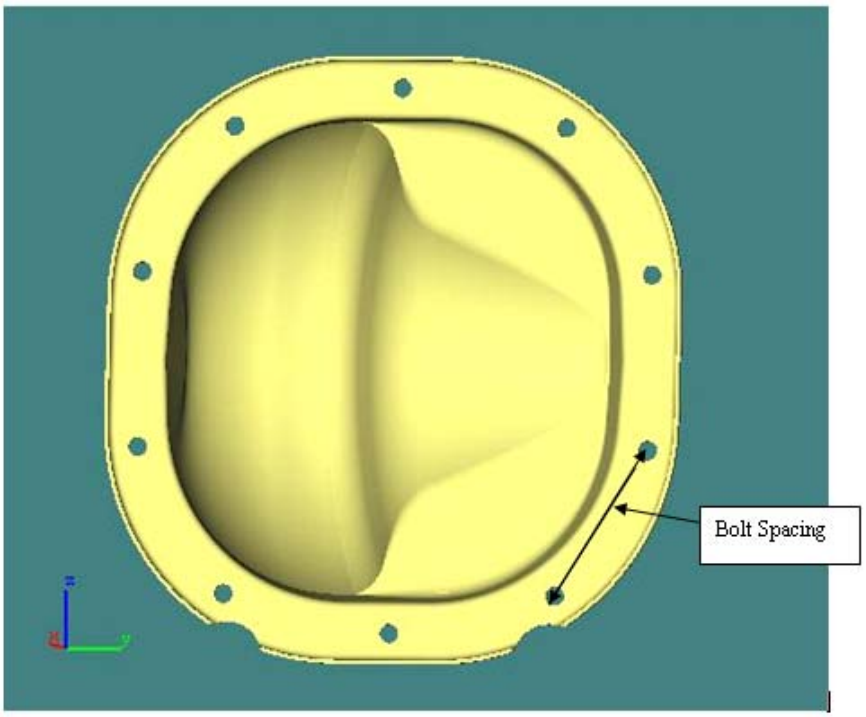

Figure 3.19 Bolt spacing

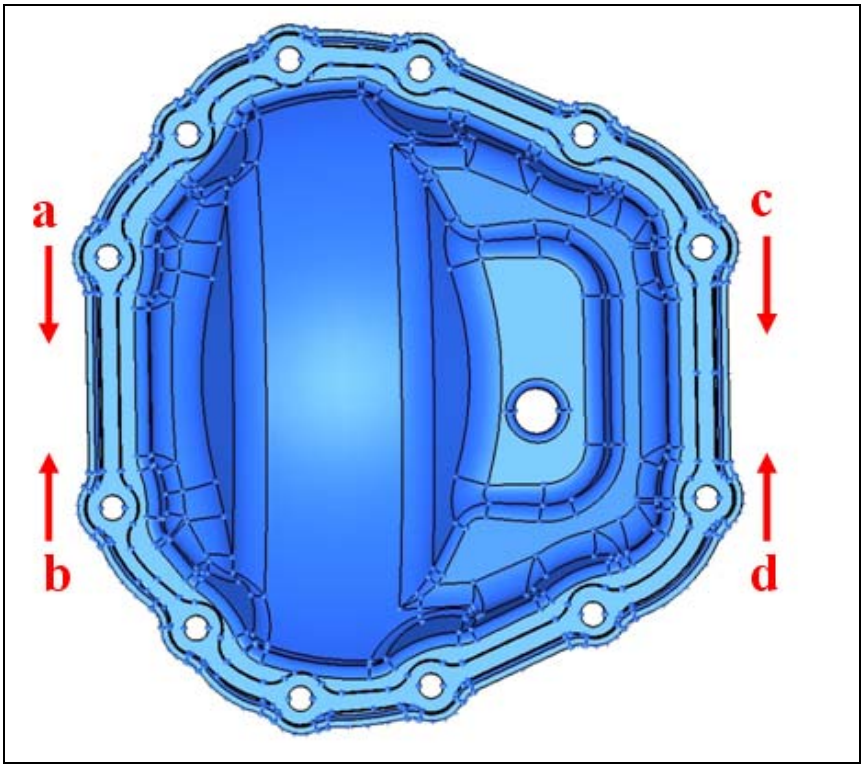

Figure 3.20 (Cover 3) Modified bolt holes

Table 3.4 (Cover 3) Positional changes tried for design improvement (in mm)
[(-) sign means opposite direction]

	a (↓)	b (↑)	c (↓)	d (↑)
Design 1	5	5	5	5
Design 2	10	10	10	10
Design 3	15	15	15	15
Design 4	5	5	10	0
Design 5	10	10	10	0
Design 6	15	15	10	0
Design 7	-2	-2	-2	-2
Design 8	-4	-4	-4	-4
Design 9	2	2	2	2
Design 10	4	4	4	4

3.5. FE Analysis Results of Cover 3 for Different Hole Locations

FE analyses were carried out for all 10 different cover designs with 3g beam load and 3g beam load + forward torque. The results of the FE analysis for the cover design 1-10 are summarized in Table 3.4 and shown in Figure 3.21-3.30.

The gap results for each cover are shown in Table 3.4. As sees in the table, no improvement is obtained by modifying bolt holes. This can be due to asymmetric current design of the cover. Because, it is also stated in the design guide that cover should be symmetric to get the best performance. But, due to design limitations, it is not possible to change the asymmetric cover to symmetric design.

It can be easily seen that cover 3 has the best performance, so cover 3 will be the best choice to improve the design. For the further studies, thickness of the cover and cover bead dimension will be investigated.

Table 3.5 FE gap analysis results for design 1-10

SUMMARY RESULT TABLE (DESIGN IMPROVEMENT-PROPOSAL)		
	MAX. GAP	
Load Conditon	3g Beam	3g Beam + Forward Torque
COVER 3	0.007 mm	0.03395 mm
Design 1	0.008 mm	0.04248 mm
Design 2	0.009 mm	0.04440 mm
Design 3	0.011 mm	0.05393 mm
Design 4	0.007 mm	0.04104 mm
Design 5	0.007 mm	0.04401 mm
Design 6	0.007 mm	0.05396 mm
Design 7	N/A	0.05177 mm
Design 8	N/A	0.05443 mm
Design 9	N/A	0.03898 mm
Design 10	N/A	0.04188 mm

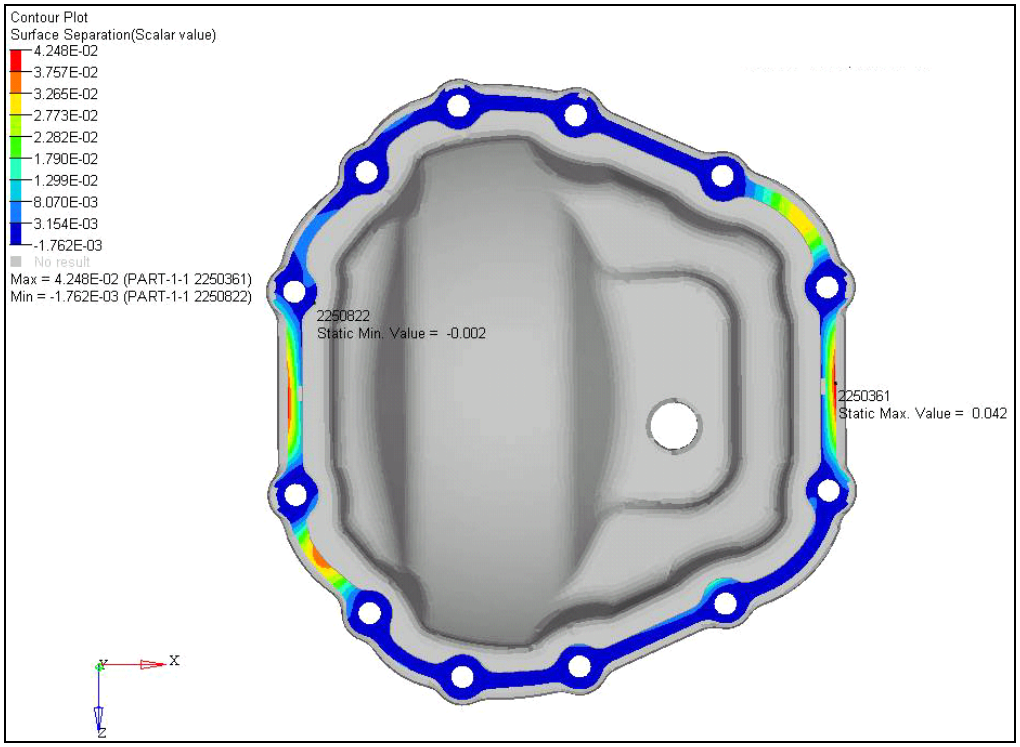

Figure 3.21 FE analysis result of design 1 with 3g beam load + forward torque condition

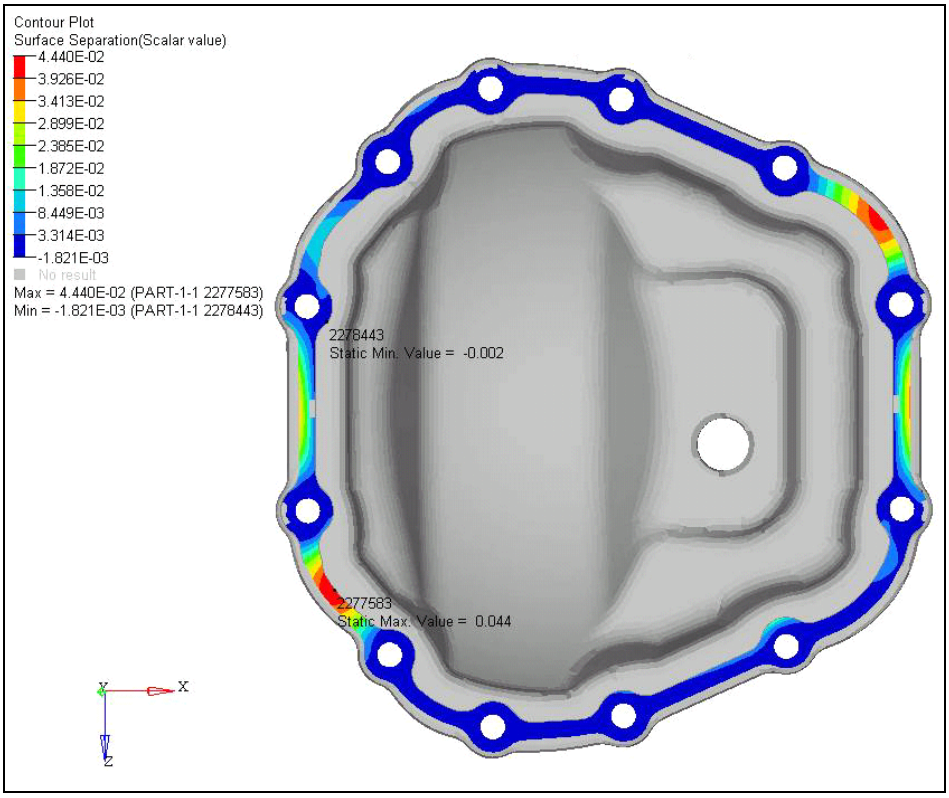

Figure 3.22 FE analysis result of design 2 with 3g beam load + forward torque condition

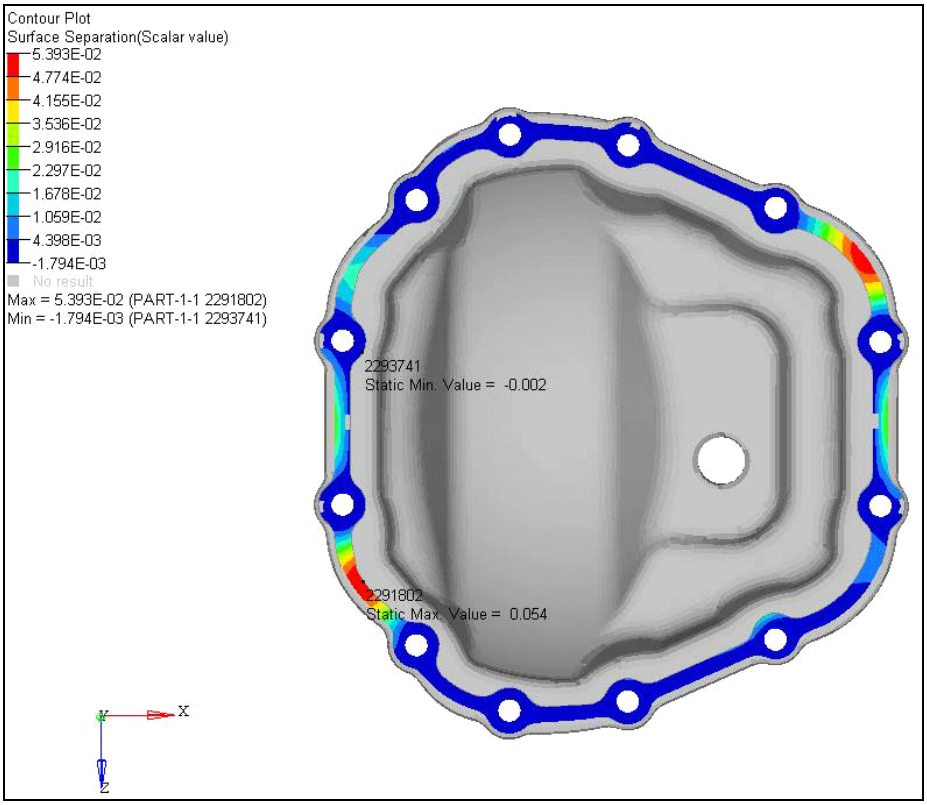

Figure 3.23 FE analysis result of design 3 with 3g beam load + forward torque condition

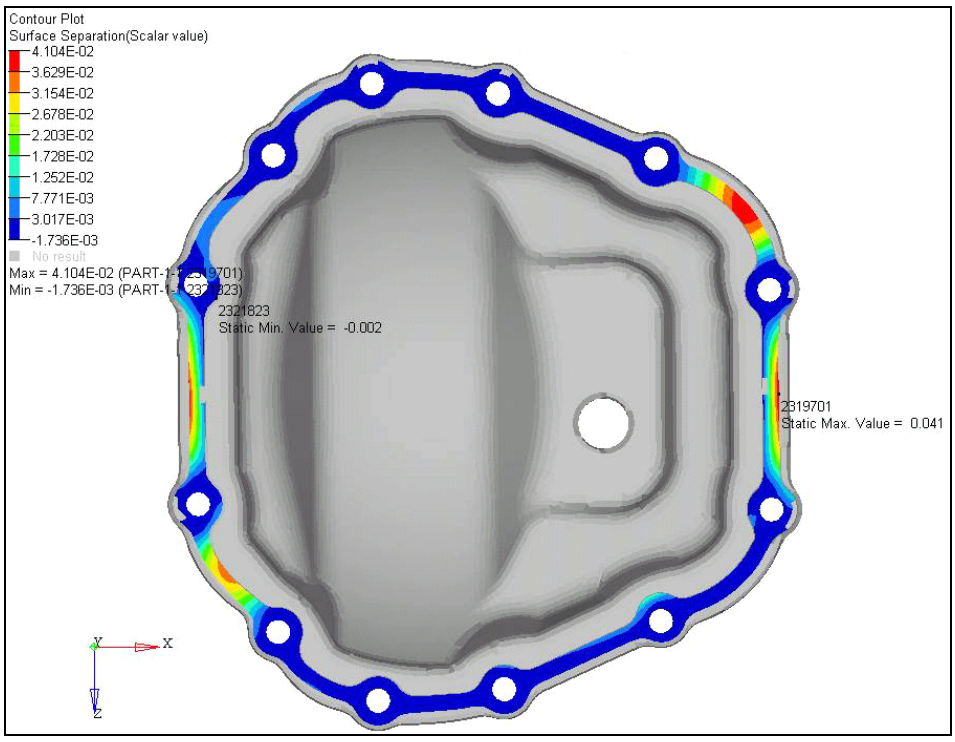

Figure 3.24 FE analysis result of design 4 with 3g beam load + forward torque condition

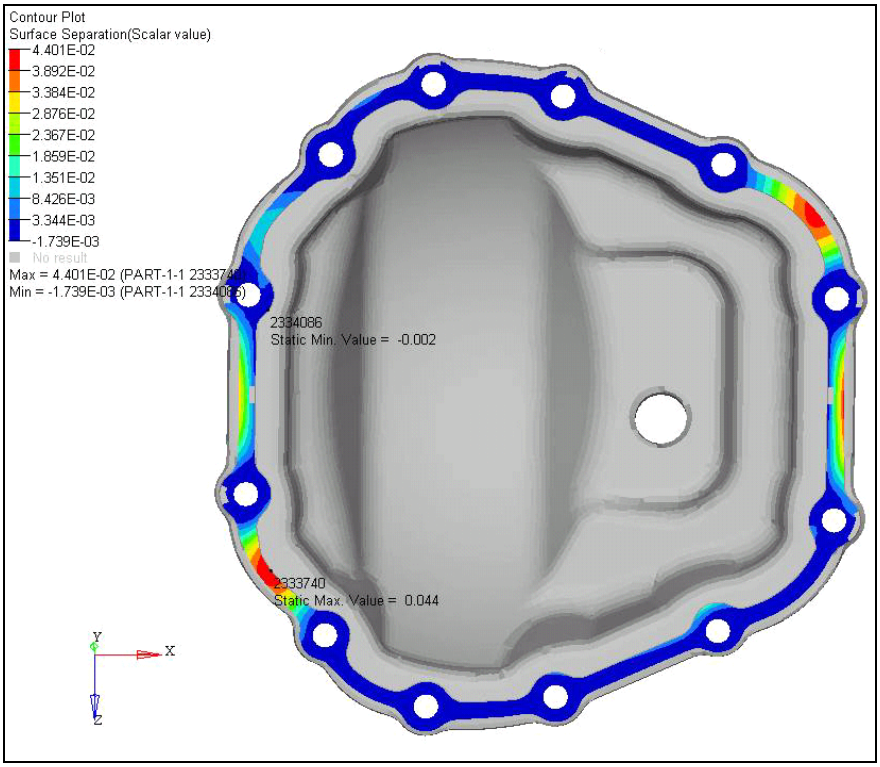

Figure 3.25 FE analysis result of design 5 with 3g beam load + forward torque condition

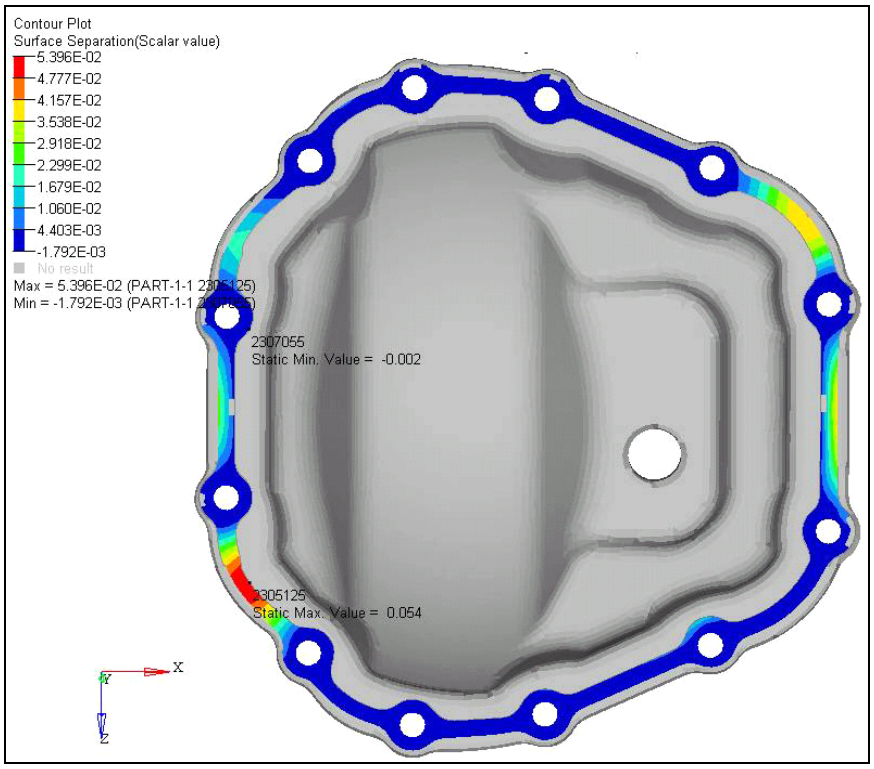

Figure 3.26 FE analysis result of design 6 with 3g beam load + forward torque condition

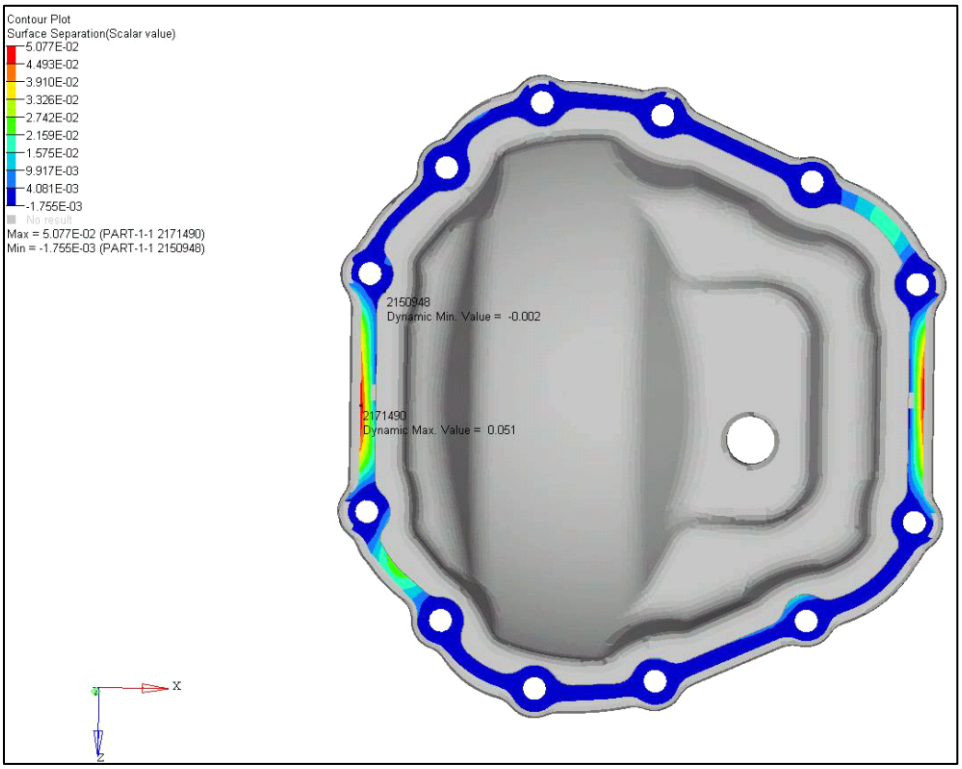

Figure 3.27 FE analysis result of design 7 with 3g beam load + forward torque condition

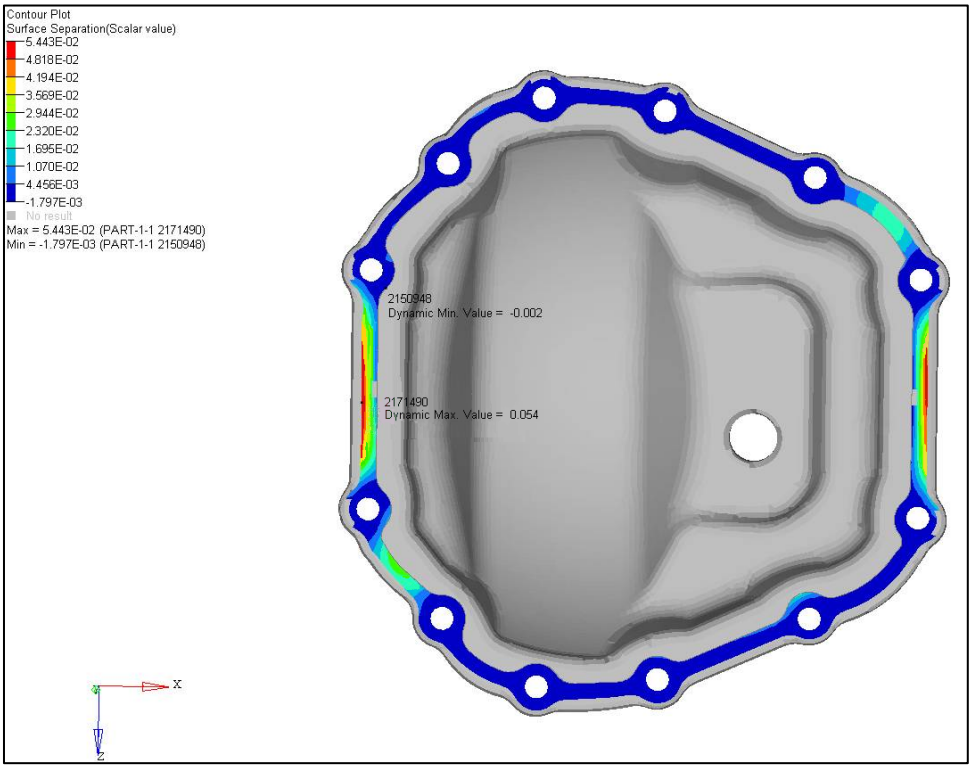

Figure 3.28 FE analysis result of design 8 with 3g beam load + forward torque condition

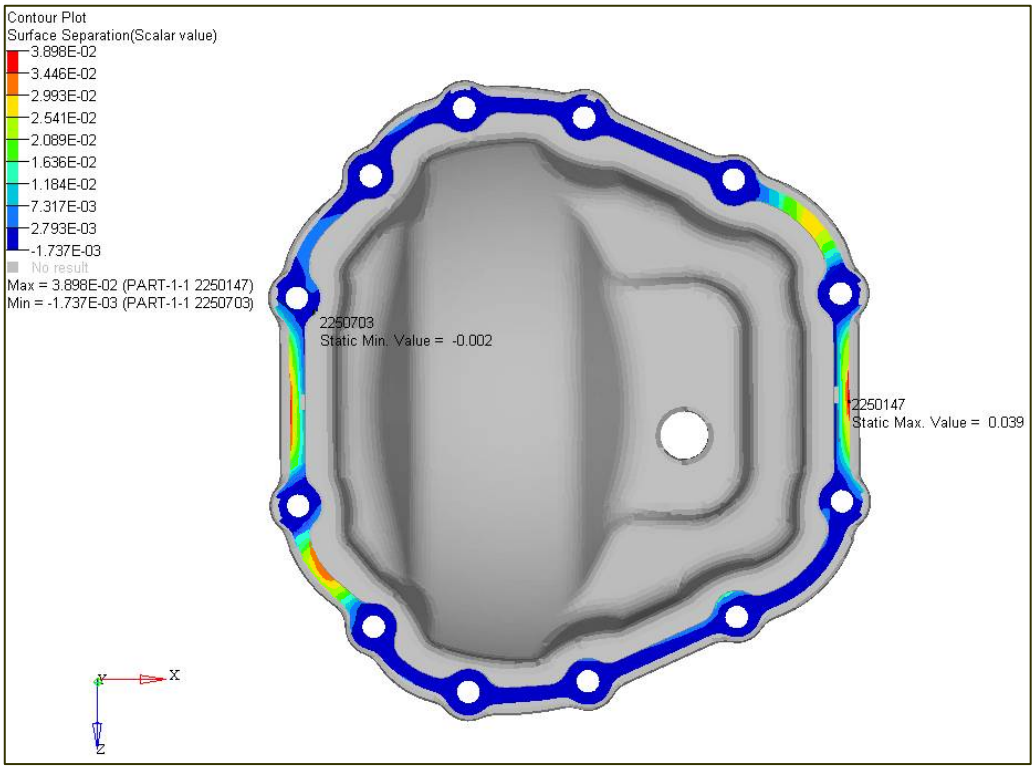

Figure 3.29 FE analysis result of design 9 with 3g beam load + forward torque condition

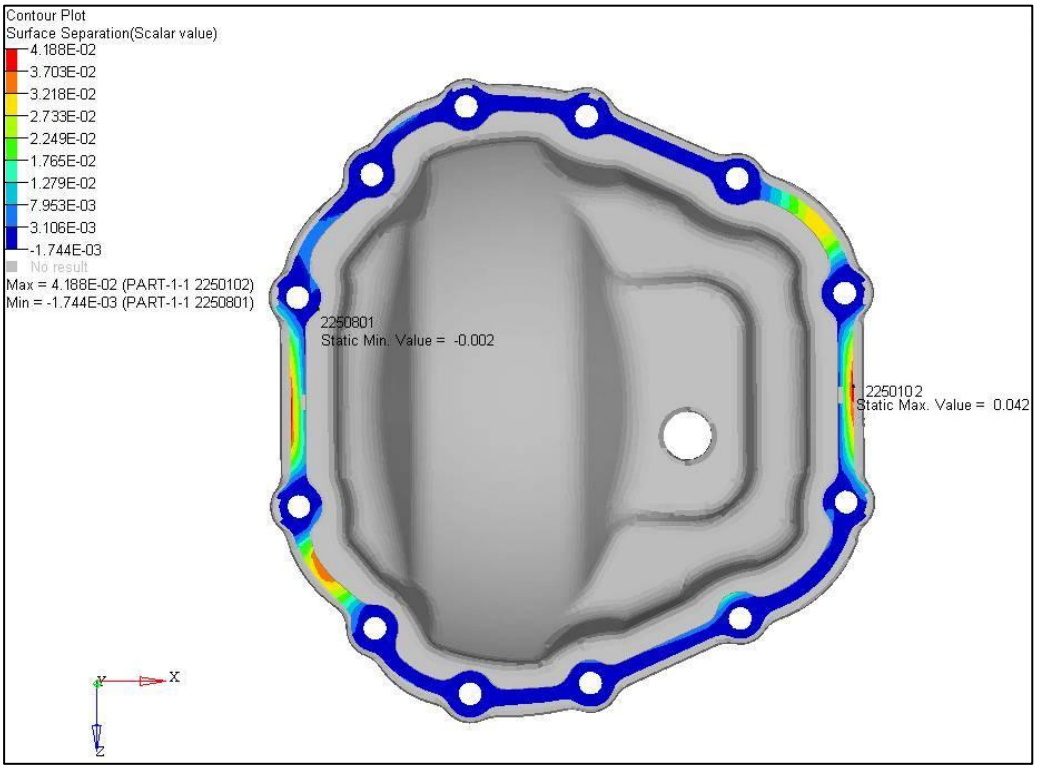

Figure 3.30 FE analysis result of design 10 with 3g beam load + forward torque condition

Similar to the previous study, compressive forces for each cover bolt locations are also calculated. Table 3.6 shows the compressive forces for each cover bolt location for this study. It can be seen that location 2 is the most critical location for all design proposals. Also, location 8 is the second one at all. More, location 12 is the safest area for all design covers. At vehicle tests, leakages were seen generally from these areas. This shows the validity of the model.

If we reduce the distance between bolt locations 2-3 and 8-9, critical bolt locations become as 2,8,7,1 and 4 respectively.

If we increase the distance between bolt locations 2-3 and 8-9, critical bolt locations changes to 2,8,3,7 and 9 respectively.

Although location 1 is not critical, reducing distance between holes makes this area critical. Similarly, increasing distance makes location 3 critical.

Table 3.6 Compressive forces for each cover bolt location (Design 1-10)

1st - Worst
2nd
3rd
4th
5th
6th - Safe

DESIGN NO (THICKNESS)	COVER BOLT NUMBER & COMP. FORCE (N)											
	1	2	3	4	5	6	7	8	9	10	11	12
DESIGN 8 (-4mm)	27095	24348	26487	27412	28027	28040	26883	24642	26946	27182	28522	28670
DESIGN 7 (-2mm)	27374	25060	26815	27420	28035	28048	26913	25237	27313	27572	28525	28661
Hybrid Cover (COVER 3)	27651	26129	27534	27658	28102	28069	27198	26233	27852	27873	28527	28573
DESIGN 9 (2mm)	27501	25517	28117	27608	28058	28049	26999	26200	27701	27519	28522	28647
DESIGN 10 (4mm)	27406	25048	28387	27457	28055	28030	26901	26189	27584	27522	28520	28658
DESIGN 1 (5mm)	27382	24887	28495	27438	28054	28024	26875	26164	27525	27515	28520	28665
DESIGN 2 (10mm)	27413	24692	28898	27424	28057	28024	26802	25238	28418	27510	28520	28650
DESIGN 3 (15mm)	27348	23823	28333	27461	28049	28051	26809	24460	28397	27519	28506	28645
DESIGN 4 (cons 5mm)	27362	24879	28513	27441	28055	28028	26873	25343	28425	27522	28519	28677
DESIGN 5 (cons 10mm)	27386	24667	28875	27419	28056	28063	26795	27318	28410	27510	28519	28666
DESIGN 6 (cons 15mm)	27399	23806	28292	27451	28067	28077	26819	26898	28422	27515	28511	28662

DESIGN NO (THICKNESS)	COVER BOLT NUMBER & NET COMP. FORCE (N)											
	1	2	3	4	5	6	7	8	9	10	11	12
DESIGN 8 (-4 mm)	-1396	-4143	-2004	-1079	-464	-451	-1608	-3849	-1545	-1309	31	179
DESIGN 7 (-2 mm)	-1117	-3431	-1676	-1071	-456	-443	-1578	-3254	-1178	-919	34	170
Hybrid Cover (COVER 3)	-840	-2362	-957	-833	-389	-422	-1293	-2258	-639	-618	36	82
DESIGN 9 (2mm)	-990	-2974	-374	-883	-433	-442	-1492	-2291	-790	-972	31	156
DESIGN 10 (4mm)	-1085	-3443	-104	-1034	-436	-461	-1590	-2302	-907	-969	29	167
DESIGN 1 (5mm)	-1109	-3604	4	-1053	-437	-467	-1616	-2327	-966	-976	29	174
DESIGN 2 (10mm)	-1078	-3799	407	-1067	-434	-467	-1689	-3253	-73	-981	29	159
DESIGN 3 (15mm)	-1143	-4668	-158	-1030	-442	-440	-1682	-4031	-94	-972	15	154
DESIGN 4 (cons 5mm)	-1129	-3612	22	-1050	-436	-463	-1618	-3148	-66	-969	28	186
DESIGN 5 (cons 10mm)	-1105	-3824	384	-1072	-435	-428	-1696	-1173	-81	-981	28	175
DESIGN 6 (cons 15mm)	-1092	-4685	-199	-1040	-424	-414	-1672	-1593	-69	-976	20	171

3.6. Design Improvement Proposals for Cover 3 (Different Thickness and Curvature Height)

There are some control factors which are defined as cover design features. Thicknesses of the cover, curvature height, bead width, radius of the curvature, bead height, and shape of the bead are some of the design features of the cover design.

It is considered that thickness of the cover and curvature of the flange surface has more effect on the stiffness and performance of the cover design. So, it is beneficial to check the design proposal with FE analysis.

In this section, thickness of the cover and curvature height effects on the cover design will be investigated. For further analysis, thickness of the cover is changed to 2.5mm to 4mm, by the way current cover thickness is 3 mm. Moreover, curvature of the flange surface is increased to 5.5 mm where current cover design has 5 mm curvature which can be seen in Figure 3.31.

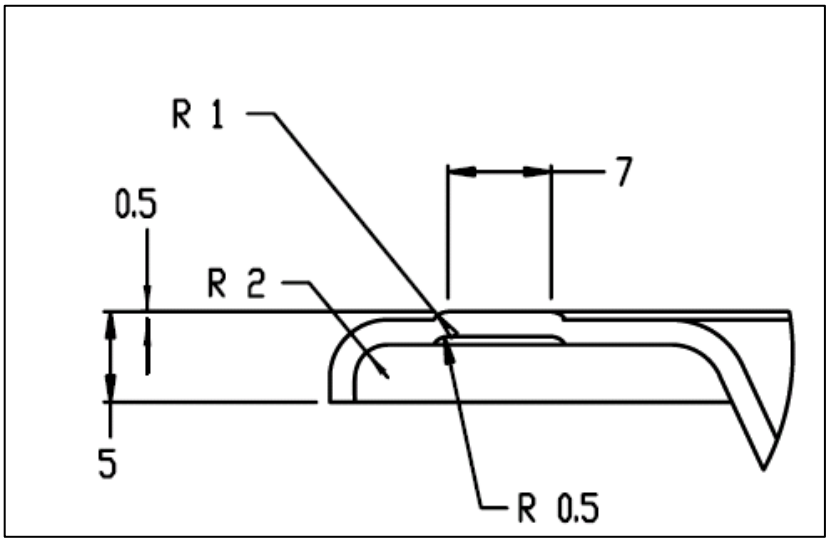

Figure 3.31 Figure of cover flange design

3.7. FE Analysis Results of Cover 3 for Different Thickness and Curvature Height

The results of the FE analysis for the cover design 11-16 are summarized in Table 3.5. The critical holes regions and gap dimensions can be seen in Figure 3.35-3.40.

The gap results for each cover are shown in Table 3.5. Increasing flange length of the design results in improvement on the maximum gap values. But, it is not very significant. After comparing the thickness of the design, it is revealed that there is an optimum thickness value which is 3 mm. Decreasing thickness of the cover does not give better results, it increases the maximum gap. Increasing thickness of the cover does not have significant effect on the maximum gap values. It slightly changes and can be assumed as having no effect on the design.

Table 3.7 FE gap analysis results for design 11-16

SUMMARY RESULT TABLE (DESIGN IMPROVEMENT-PROPOSAL)			
	HEIGHT	THICKNESS	MAX. GAP
COVER 3	5 mm	3 mm	0.03395 mm
Design 11	5.5 mm	3 mm	0.03321 mm
Design 12	5 mm	2.5 mm	0.03754 mm
Design 13	5.5 mm	2.5 mm	0.03624 mm
Design 14	5 mm	2 mm	0.04281 mm
Design 15	5 mm	3.5 mm	0.03398 mm
Design 16	5 mm	4 mm	0.03481 mm

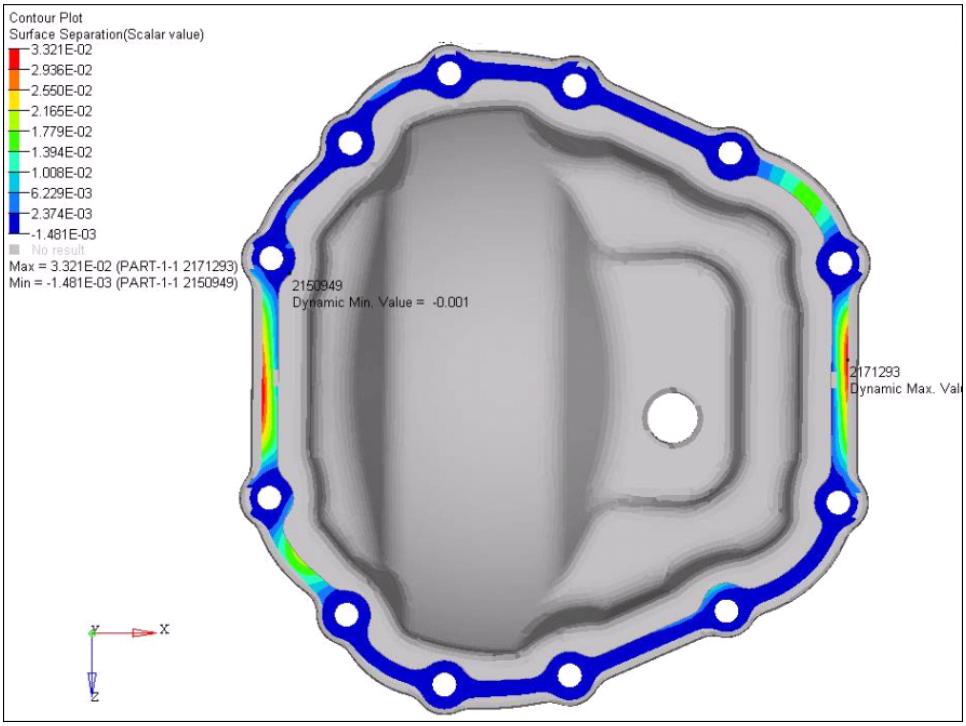

Figure 3.32 FE analysis result of design 11 with 3g beam load + forward torque condition

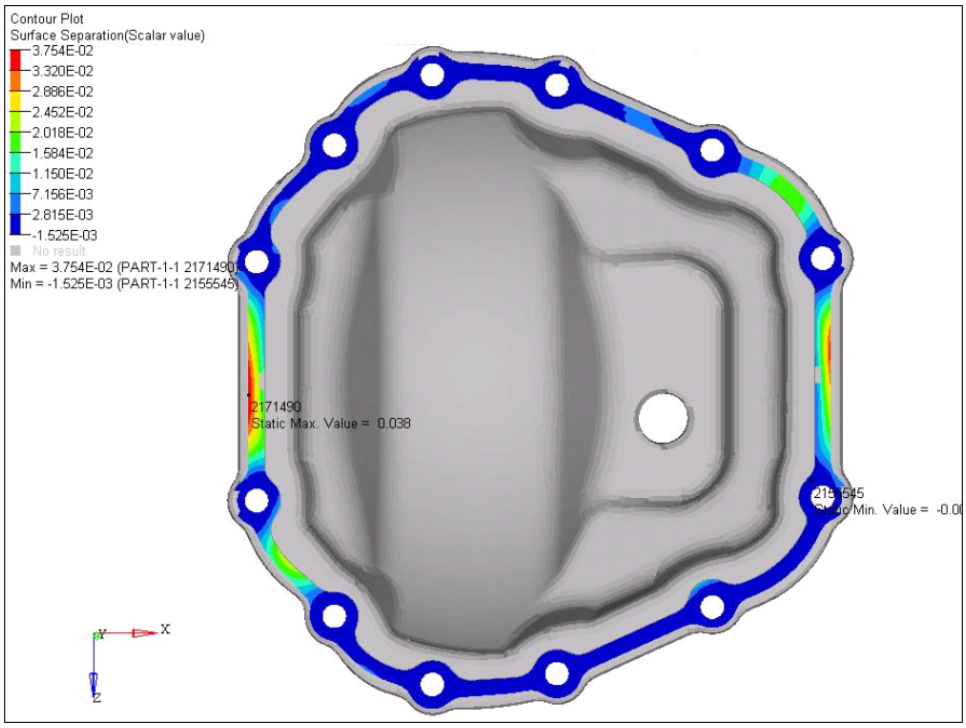

Figure 3.33 FE analysis result of design 12 with 3g beam load + forward torque condition

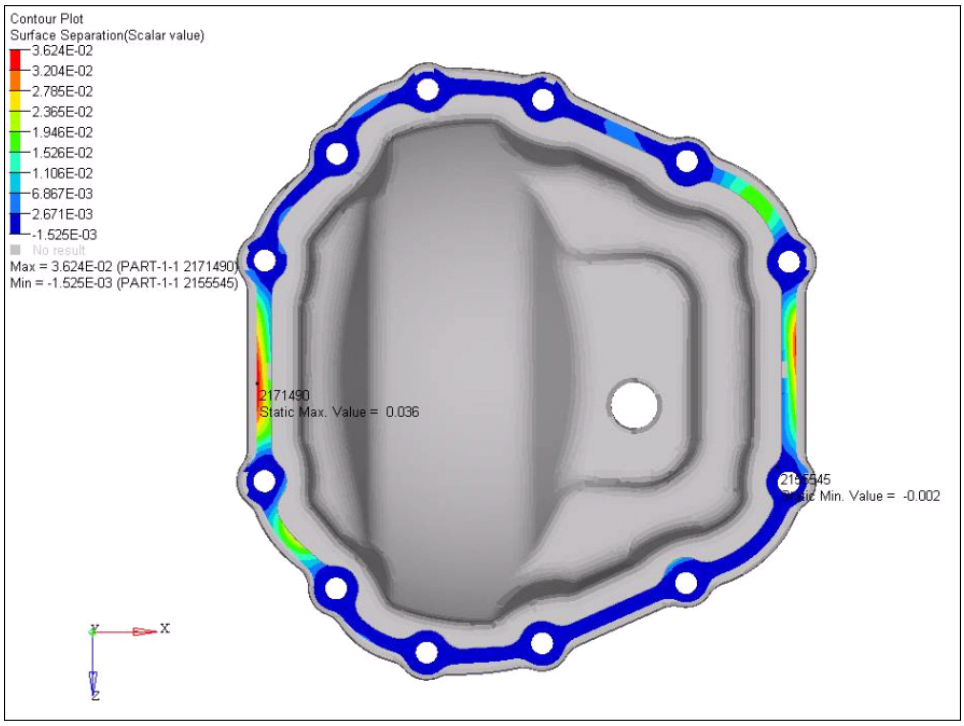

Figure 3.34 FE analysis result of design 13 with 3g beam load + forward torque condition

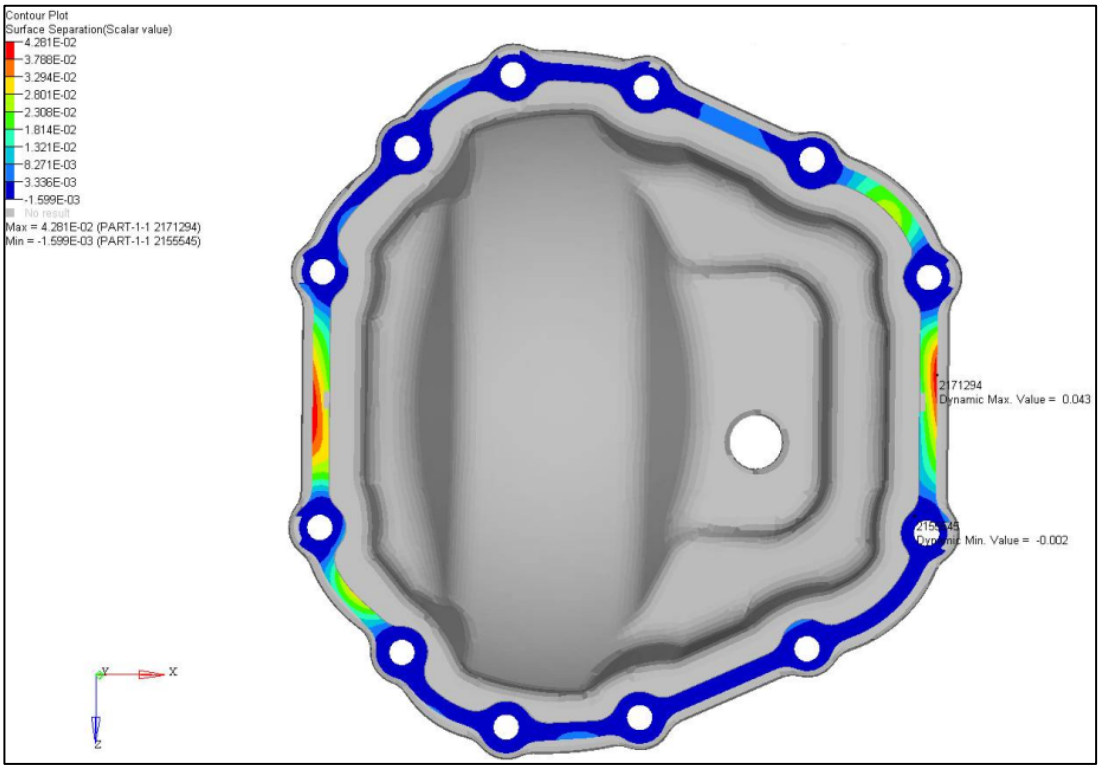

Figure 3.35 FE analysis result of design 14 with 3g beam load + forward torque condition

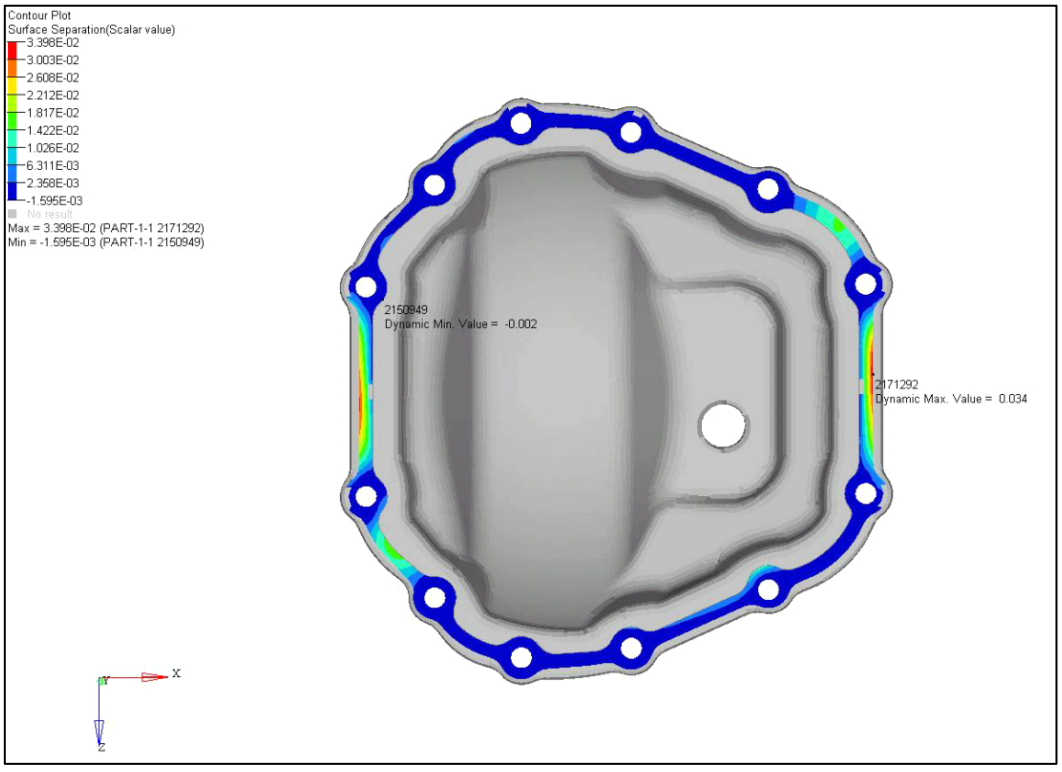

Figure 3.36 FE analysis result of design 15 with 3g beam load + forward torque condition

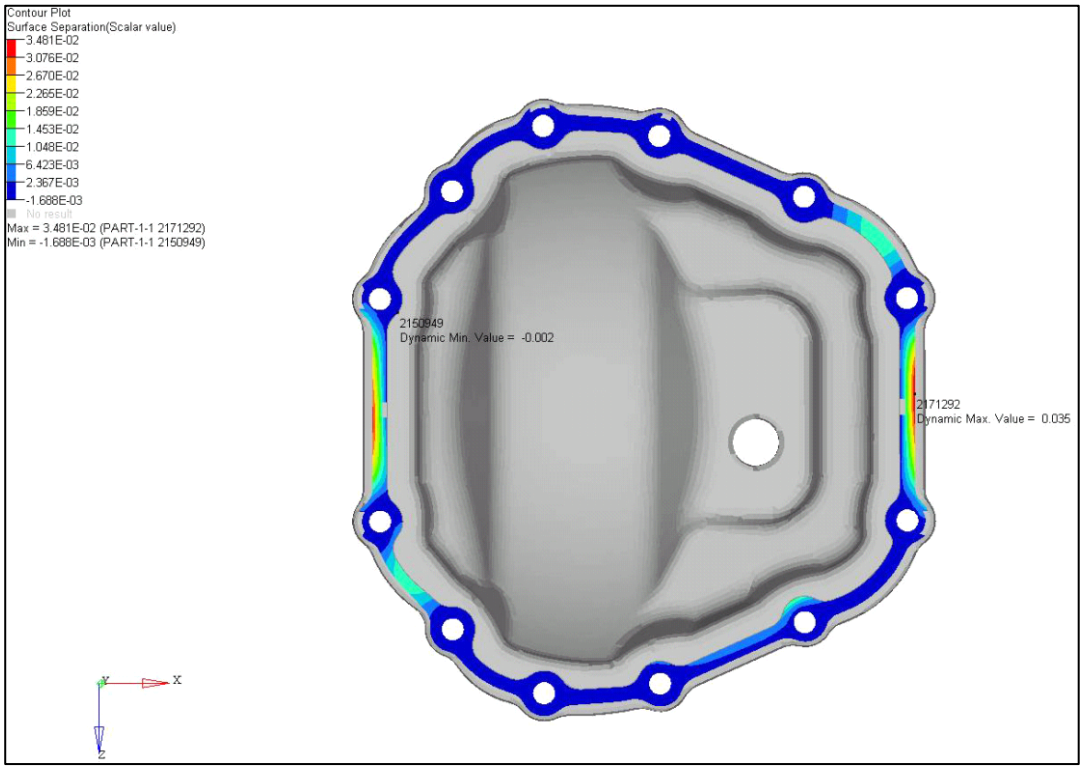

Figure 3.37 FE analysis result of design 16 with 3g beam load + forward torque condition

Clamping forces at each cover bolt locations were also calculated for different cover thicknesses. Table 3.8 shows the clamping forces at each cover bolt location for this study. It can be seen that location 2 is the most critical location for all design proposals. Also, location 8 is the second one. Moreover, location 12 is the safest area for all design covers. It follows exactly the same trend as the previous ones.

As stated before, at vehicle tests, leakages were seen generally from these areas. This shows the validity of the model.

Whether increasing or reducing the thickness of the cover, the critical locations are not changed. Location 2,8,7,3 and 1 are most critical areas at all for each design.

Table 3.8 Compressive forces for each cover bolt location (Design 12-16)

1st - Worst
2nd
3rd
4th
5th
6th - Safe

DESIGN NO (THICKNESS)	COVER BOLT NUMBER & COMP. FORCE (N)											
	1	2	3	4	5	6	7	8	9	10	11	12
DESIGN 14 (2 mm)	27663	26095	27537	27667	28137	28090	27168	26205	27838	27883	28536	28604
DESIGN 12 (2.5 mm)	27655	26110	27537	27661	28119	28078	27182	26222	27845	27878	28531	28589
COVER 3 (3 mm)	27651	26129	27534	27658	28102	28069	27198	26233	27852	27873	28527	28573
DESIGN 15 (3.5 mm)	27641	26152	27547	27657	28085	28069	27230	26253	27869	27869	28521	28560
DESIGN 16 (4 mm)	27630	26181	27569	27655	28069	28077	27269	26276	27892	27864	28515	28550

DESIGN NO (THICKNESS)	COVER BOLT NUMBER & NET COMP. FORCE (N)											
	1	2	3	4	5	6	7	8	9	10	11	12
DESIGN 14 (2 mm)	-828	-2396	-954	-824	-354	-401	-1323	-2286	-653	-608	45	113
DESIGN 12 (2.5 mm)	-836	-2381	-954	-830	-372	-413	-1309	-2269	-646	-613	40	98
COVER 3 (3 mm)	-840	-2362	-957	-833	-389	-422	-1293	-2258	-639	-618	36	82
DESIGN 15 (3.5 mm)	-850	-2339	-944	-834	-406	-422	-1261	-2238	-622	-622	30	69
DESIGN 16 (4 mm)	-861	-2310	-922	-836	-422	-414	-1222	-2215	-599	-627	24	59

4. COVER BOLT STUDIES & TESTS

Beside cover design, cover bolt performance is another important factor for leakage problem. Paint on cover bolt paint, sealer, sealer process, sealer quantity and tightening torque are the parameters which are directly affect cover bolt performance. To reveal the effect of these parameters effect on bolt performance several tests were performed such as clamp load testing, elongation study and torque & angle study for various conditions.

4.1. Effect of Paint on Cover Bolt Face (Clamp Load Test)

Cover is painted by dipping the paint bath, so all faces including cover bolt faces are painted. Paint causes a drop on the friction coefficient between the bolt heads and the cover, results in excessive load and hence, excessive elongation on cover bolts. Clamp load test is performed with painted and unpainted bolt face at different torque values to determine the effect of torque and paint on these locations.

Clamp load test was performed with painted and unpainted cover to determine the effect of paint on cover bolt face. Test set up is shown in Figure 4.1. There is a connector, which is put in through the load cell clamped with the screw vice. Cover is located on top of load cell and there is a ring between load cell and cover. Bolt is tightened and clamp load is measured with the help of load cell apparatus.

Figure 4.1 Load cell test set up

Clamp load test results are shown in the below table 4.1 and table 4.2.

Table 4.1 Clamp load of bolts (for painted cover) at different torque values

Cover Bolt (Grade 8) - Painted Cover			
Bolt No	**54 Nm**	***61Nm***	**68Nm**
1	2,22	***2,40***	2,64
2	2,58	***2,73***	2,97
3	2,43	***2,58***	2,81
4	2,48	***2,59***	2,82
5	2,34	***2,52***	2,71
6	2,58	***2,79***	2,96
7	2,34	***2,53***	2,68
8	2,86	***3,09***	3,47
9	2,27	***2,43***	2,62
10	2,20	***2,38***	2,60
11	2,57	***2,74***	2,97
12	2,00	***2,23***	2,56
Load (kN)	2,41	***2,58***	2,82

Table 4.2 Clamp load of bolts (for unpainted bolt face) at different torque values

Cover Bolt (Grade 8) - Cover without paint			
Bolt No	**54 Nm**	***61Nm***	**68Nm**
1	3,00	***3,23***	3,66
2	2,61	***2,94***	3,36
3	3,06	***3,45***	3,86
4	2,70	***3,11***	3,54
5	2,67	***2,93***	3,31
6	2,71	***3,00***	3,32
7	3,16	***3,52***	3,86
8	2,97	***3,36***	3,70
9	2,73	***2,98***	3,42
10	2,93	***3,20***	3,55
11	2,95	***3,29***	3,65
12	2,89	***3,28***	3,81
Load (kN)	2,87	***3,19***	3,59

Clamp load testing was performed with painted and unpainted cover at 54, 61 and 68 Nm, respectively. Bolts are tightened and loads are measured.

As expected, increasing torque values results in an increase on bolt loads. Friction coefficient variation is also caused a variation on loads at the same torque values.

When comparing the painted vs. unpainted test results at same torque values, it is seen that load on unpainted cover is higher than the painted one. As paint reduces the friction, torque effect on bolt increases that results in an increase on clamp load and excessive elongation. If bolt elongation exceeds the elastic region, plastic deformation occurs. After plastic deformation, load on bolt is decreased. It can be concluded that paint on bolt face reduces friction and cause excessive elongation on bolt due to plastic deformation. So, clamp load on bolt is also reduced.

4.2. Effect of Sealer on Cover Bolt (Clamp Load Test)

In assembly process, sealer is used between cover and carrier. So, cover bolts are directly contact with some amount of sealer during assembly. It is known that sealer reduces the friction coefficient if it is stuck to bolt threads. This may affect the bolt performance.

Clamp load test was performed with sealed and nonsealed sample plates to determine the effect of sealer on bolt performance. The load cell and ring plate which are used in these test shown in Figure 4.2. There is an a connector which is put in through the load cell is clamped with the screw vise. Test sample plates (50x160x3mm) are prepared. These plates which are sealed or nonselaed located on top of load cell and there is a ring between load cell and plates. Bolt is tightened and clamp load is measured with the help of load cell apparatus.

Figure 4.2 Load cell and ring plate

Clamp load testing results are shown in Table 4.3.

Table 4.3 Clamp load variation of bolts with / without sealer

	Torque(Nm)	Load(kN)	
1	60	4,37	Current Level Cover (Without Sealer)
2	60	4,34	"
3	60	4,60	"
4	60	4,98	"
5	60	4,64	"
6	60	4,62	"
7	60	4,36	"
1	60	4,17	Current Level Cover (With Sealer)
2	62	4,03	"
3	60	4,15	"
4	61	3,67	"
5	61	3,96	"

Clamp load test was performed with 7 sample bolts without sealer and 5 sample bolts with sealer. Bolts are tightened and loads are measured.

It is seen that there is a variation on load values at the same torque for both tests. Friction coefficient variation is also caused a variation on loads at the same torque values.

When comparing these two tests, it is seen that load on cover without sealer is higher. As sealer reduces the friction, torque effect on bolt increases which in turn results in an increase on the clamp load and excessive elongation of the bolt. If bolt elongation exceeds the elastic region, plastic deformation occurs. After plastic deformation, load on bolt is decreased. It can be concluded that sealer effect on bolt reduces friction and cause excessive elongation due to plastic deformation. So, clamp load on bolt is also reduced.

4.3. Determining Effect of Sealer Process

As expected, sealer has an effect on bolt performance. Amount of sealer in contact with cover bolt thread affects bolt performance. It is known that sealer process directly affects the amount of sealer which is used at assembly line. Elongation of bolt study was performed to determine the effect of sealer process.

Figure 4.3 Comparison between DANA sealer process vs Inonu sealer process

Rear axle is produced by DANA and Inonu. They use different sealer application processes at assembly lines. DANA and Inonu sealer application patterns are shown in Figure 4.3. It can be easily seen that heavy sealer process is using at Inonu.

Bolt elongation study was performed for each sealer process. Initial length of the bolts are measured. All bolts were tightened and after a while they are unscrewed. After that final lengths of the bolts are measured. The difference between initial and final measurements gives the elongation of each bolt. Results are shown in Table 4.4 and 4.5. It should noted that maximum elongation limit for the bolts are 0.021 mm.

Table 4.4 Results of bolt elongation study with Inonu sealer process

Current	Initial Length (mm)	Final Length (mm)	Elongation (mm)
1	27.394	27.427	0.033
2	27.258	27.324	0.066
3	27.329	27.345	0.016
4	27.286	27.298	0.012
5	27.357	27.365	0.008
6	27.268	27.272	0.004
7	27.257	27.262	0.005
8	27.346	27.353	0.007
9	27.276	27.298	0.022
10	27.400	27.421	0.021
11	27.450	27.462	0.012
12	27.334	27.351	0.017

Current	Initial Length (mm)	Final Length (mm)	Elongation (mm)
1	27.273	27.342	0.069
2	27.328	27.334	0.006
3	27.380	27.392	0.012
4	27.177	27.181	0.004
5	27.308	27.311	0.003
6	27.208	27.218	0.010
7	27.408	27.414	0.006
8	27.298	27.317	0.019
9	27.315	27.359	0.044
10	27.350	27.364	0.014
11	27.479	27.490	0.011
12	27.331	27.344	0.013

Table 4.4 Results of bolt elongation study with Inonu sealer process (continued)

Current	Initial Length (mm)	Final Length (mm)	Elongation (mm)
1	27.243	27.315	0.072
2	27.403	27.418	0.015
3	27.371	27.421	0.050
4	27.208	27.219	0.011
5	27.354	27.360	0.006
6	27.200	27.224	0.024
7	27.303	27.362	0.059
8	27.440	27.483	0.043
9	27.285	27.292	0.007
10	27.330	27.361	0.031
11	27.349	27.388	0.039
12	27.179	27.226	0.047

Current	Initial Length (mm)	Final Length (mm)	Elongation (mm)
1	27.346	27.389	0.043
2	27.258	27.282	0.024
3	27.249	27.276	0.027
4	27.570	27.579	0.009
5	27.457	27.467	0.010
6	27.135	27.143	0.008
7	27.330	27.341	0.011
8	27.444	27.484	0.040
9	27.328	27.343	0.015
10	27.302	27.335	0.033
11	27.353	27.413	0.060
12	27.248	27.290	0.042

Table 4.5 Results of bolt elongation study with Dana sealer process

DANA	Initial Length (mm)	Final Length (mm)	Elongation (mm)
1	27.233	27.242	0.009
2	27.382	27.384	0.002
3	27.420	27.427	0.007
4	27.319	27.327	0.008
5	27.170	27.182	0.012
6	27.270	27.296	0.026
7	27.263	27.284	0.021
8	27.385	27.398	0.013
9	27.294	27.307	0.013
10	27.291	27.295	0.004
11	27.251	27.260	0.009
12	27.398	27.400	0.002

DANA	Initial Length (mm)	Final Length (mm)	Elongation (mm)
1	27.245	27.258	0.013
2	27.375	27.385	0.010
3	27.261	27.276	0.015
4	27.385	27.390	0.005
5	27.346	27.360	0.014
6	27.284	27.302	0.018
7	27.416	27.423	0.007
8	27.317	27.329	0.012
9	27.126	27.126	0.000
10	27.332	27.354	0.022
11	27.304	27.309	0.005
12	27.422	27.443	0.021

Table 4.5 Results of bolt elongation study with Dana sealer process(continued)

DANA	Initial Length (mm)	Final Length (mm)	Elongation (mm)
1	27.338	27.352	0.014
2	27.335	27.340	0.005
3	27.491	27.498	0.007
4	27.244	27.252	0.008
5	27.348	27.354	0.006
6	27.259	27.283	0.024
7	27.367	27.374	0.007
8	27.284	27.295	0.011
9	27.333	27.338	0.005
10	27.217	27.228	0.011
11	27.328	27.333	0.005
12	27.378	27.391	0.013

DANA	Initial Length (mm)	Final Length (mm)	Elongation (mm)
1	27.334	27.360	0.026
2	27.404	27.410	0.006
3	27.396	27.398	0.002
4	27.466	27.472	0.006
5	27.265	27.290	0.025
6	27.188	27.214	0.026
7	27.315	27.315	0.000
8	27.345	27.364	0.019
9	27.364	27.403	0.039
10	27.294	27.298	0.004
11	27.254	27.263	0.009
12	27.392	27.435	0.043

Table 4.4 and 4.5 show that the DANA sealer process gives better results than the Inonu process. It can be concluded that heavy sealer application causes excessive bolt elongation and decreases bolt clamp load.

4.4. Effect of Sealer & Torque (Torque vs. Angle Test)

Sealer and torque are two parameters which directly affect the bolt performance. Torque vs. angle tests are performed with various torque values and sealer conditions to determine the effect of sealer and torque on bolt performance.

4 studies were performed,

- Study 1 - 61 Nm torque with Inonu (current) sealer process.
- Study 2 - 68 Nm torque without sealer.
- Study 3 - 68 Nm torque with Inonu (current) sealer process.
- Study 4 - 68 Nm torque with heavy sealer process.

Bolts are tightened with the help of torque equipment which is shown in Figure 4.4.

Figure 4.4 Bolt tightening process and torque equipment

Torque wrench is connected to the torque measurement equipment (ACTA 3000) which is shown in Figure 4.5. Torque is measured and controlled with this equipment. Torque value should be in the range of 61 ± 1 Nm.

Figure 4.5 Bolt torque measurement equipment - ACTA 3000

Torque measurement equipment is connected to a computer system which is shown in Figure 4.6. A special program is used and torque vs angle values are taken from the computer program as an output. Results are given in the next sections.

Figure 4.6 Torque vs. angle measurement equipment

4.4.1 61Nm Torque with Inonu(current) Sealer Process (Study 1)

Study 1 is performed with current sealer process at 61Nm torque value. Results are shown in Figure 4.7.

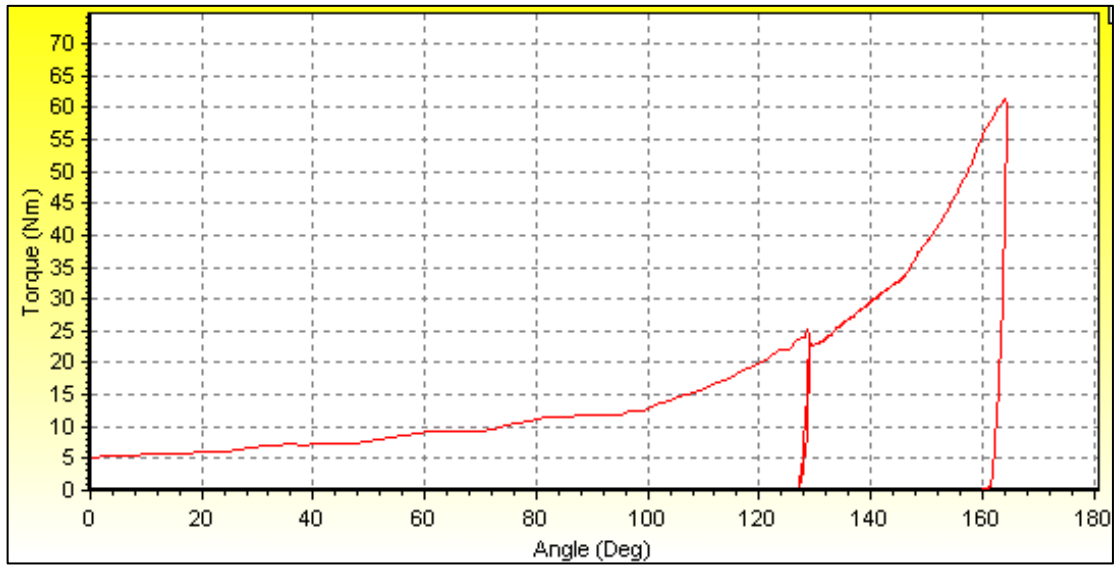

(a)

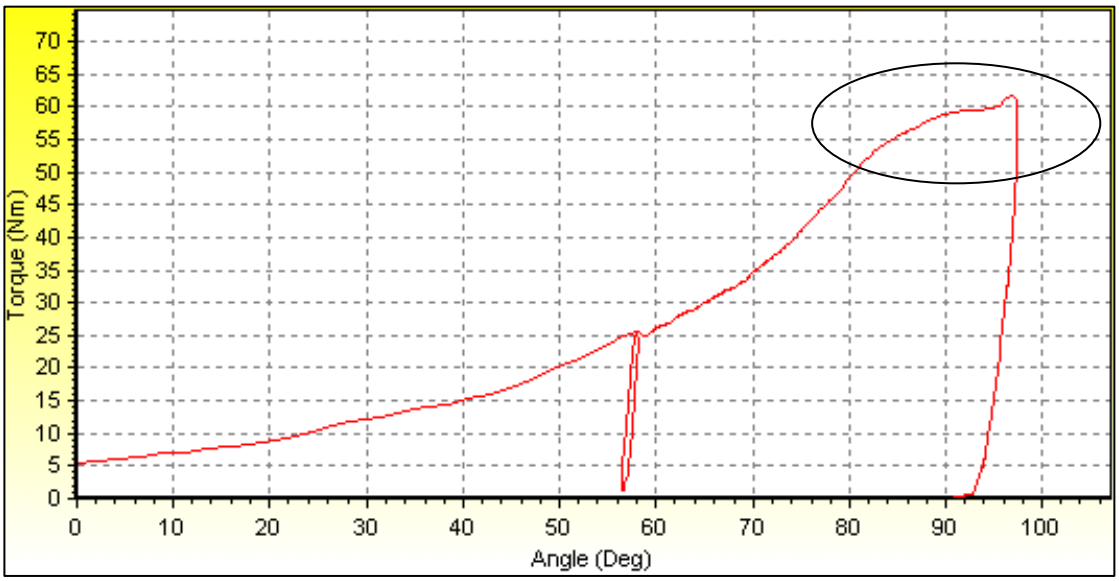

(b)

Figure 4.7 Bolt torque vs. angle results for Study 1

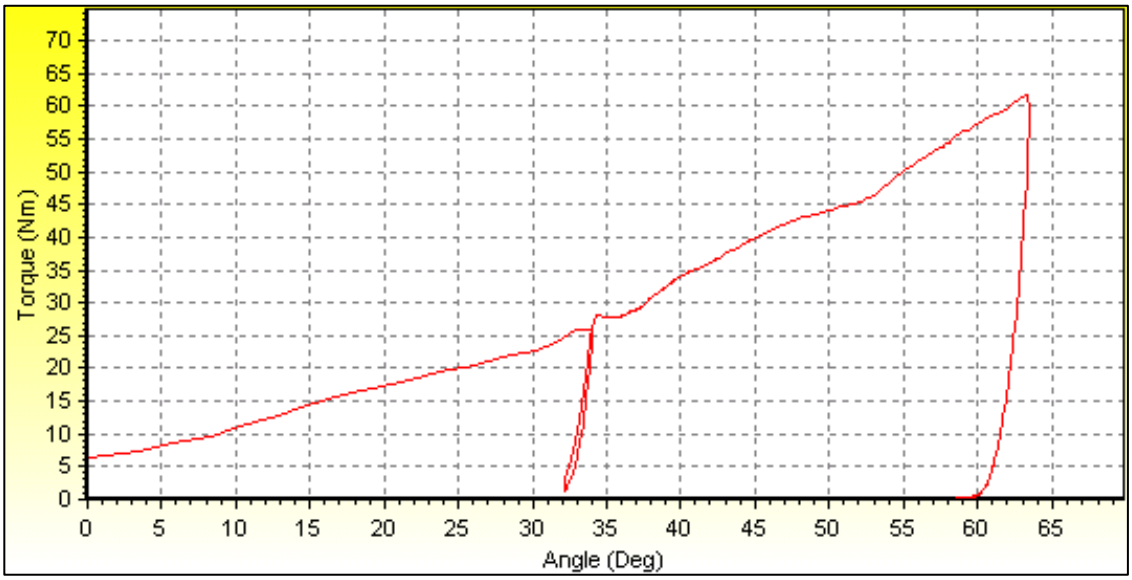

(c)

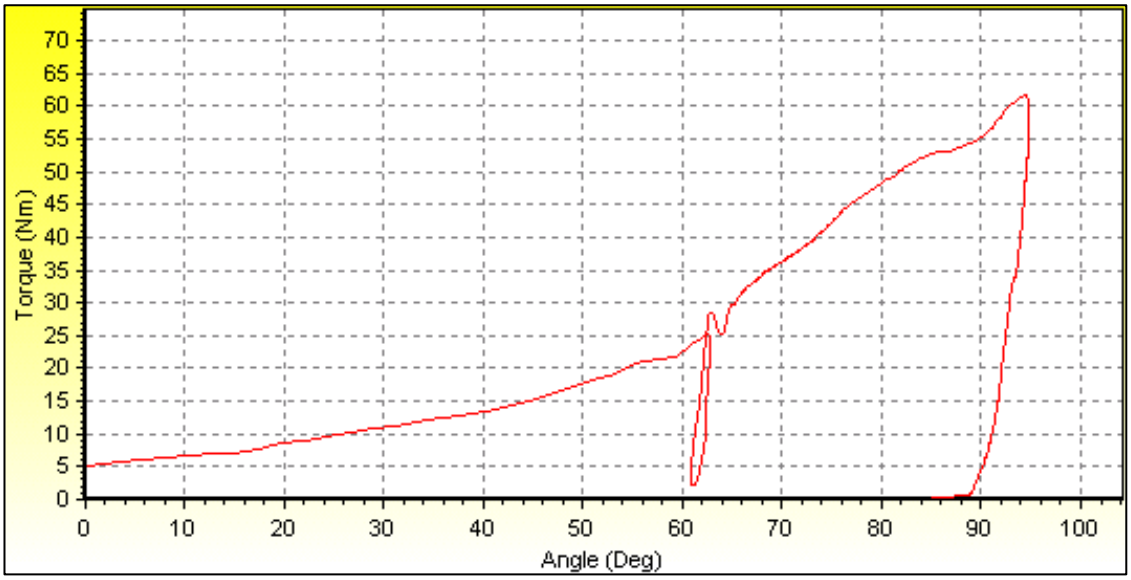

(d)

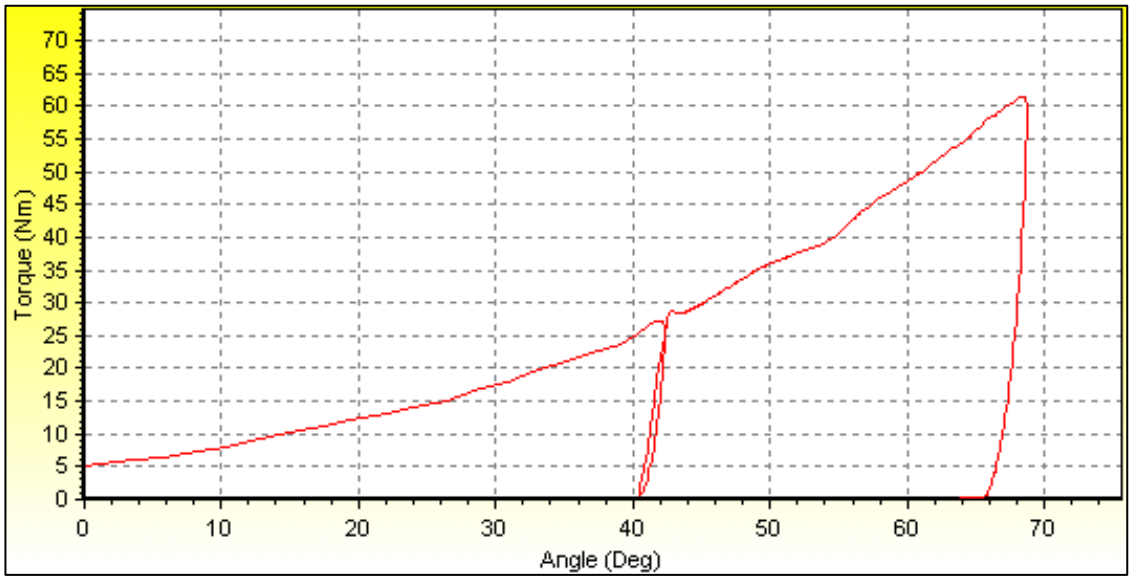

(e)

Figure 4.7 Bolt torque vs. angle results for Study 1 (continued)

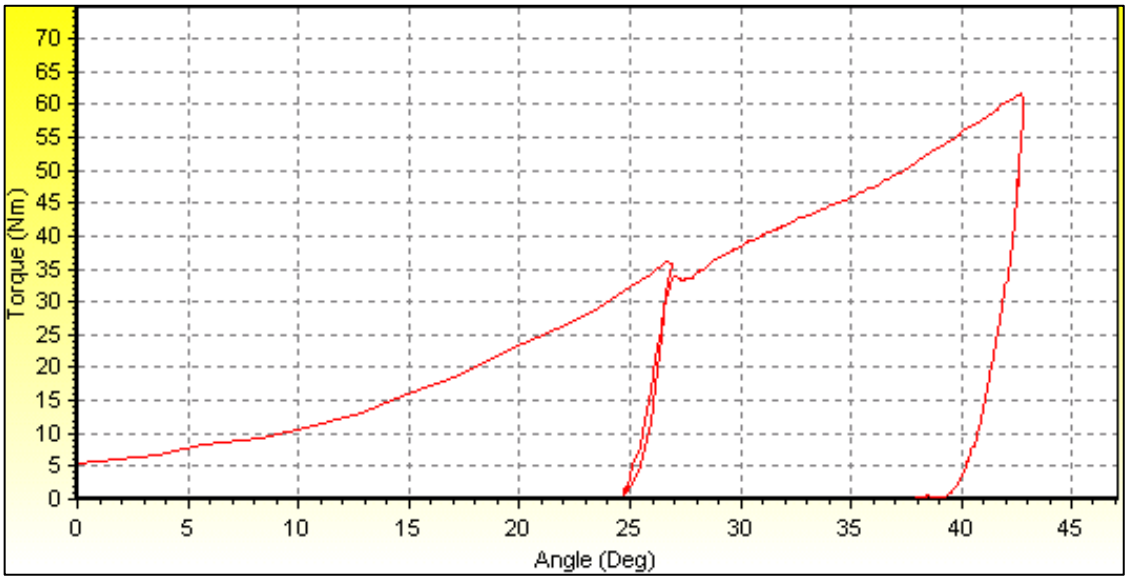

(f)

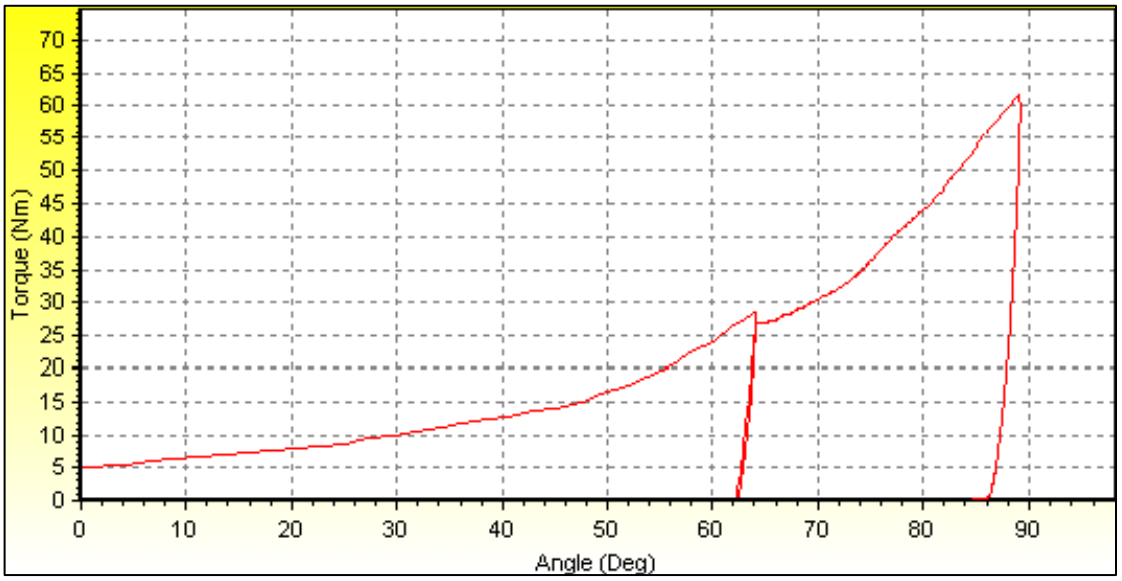

(g)

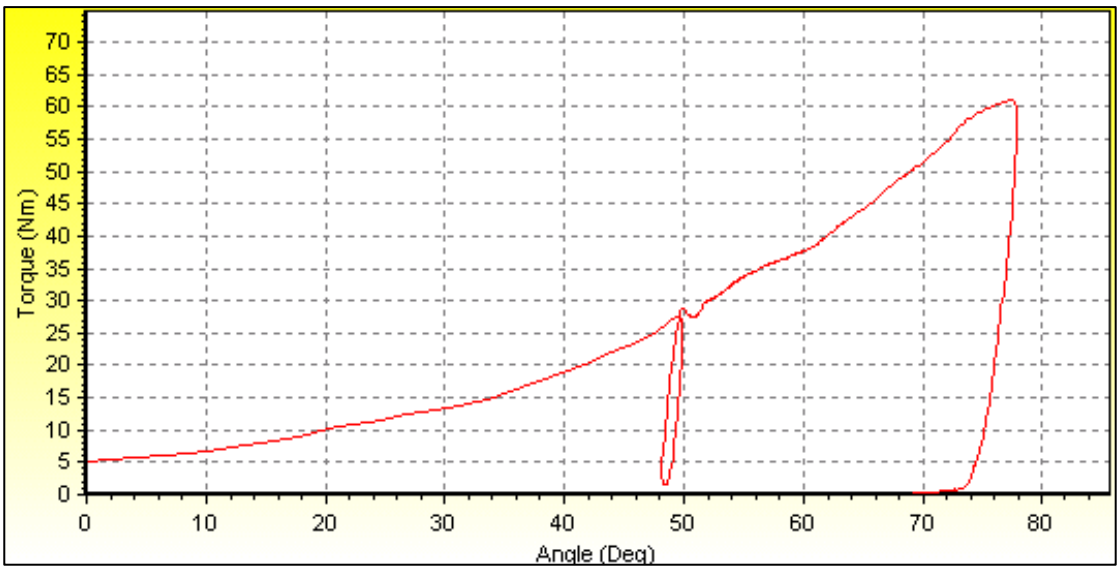

(h)

Figure 4.7 Bolt torque vs. angle results for Study 1 (continued)

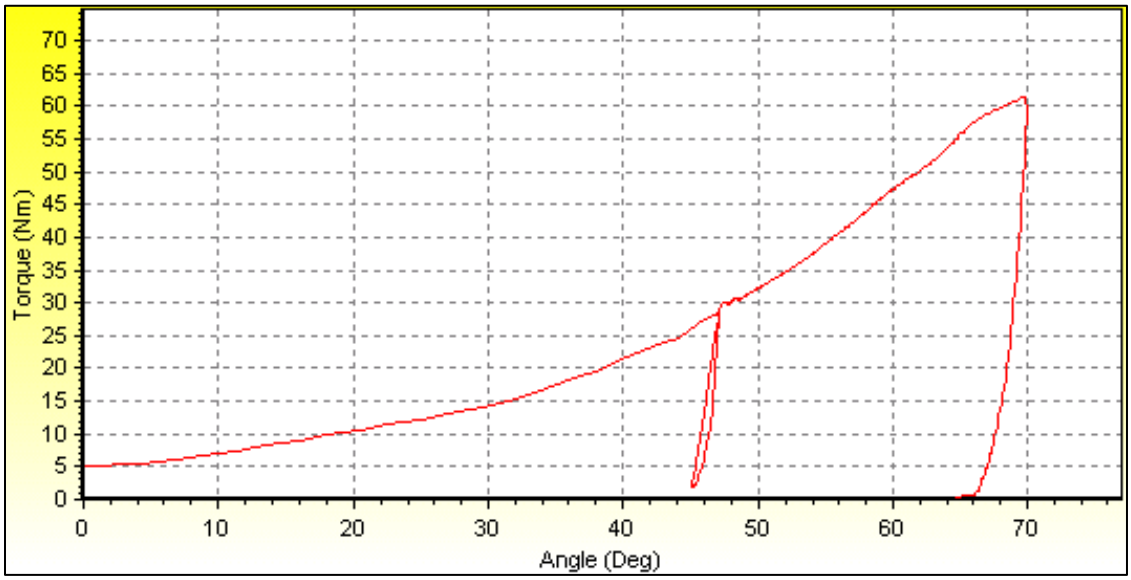

(i)

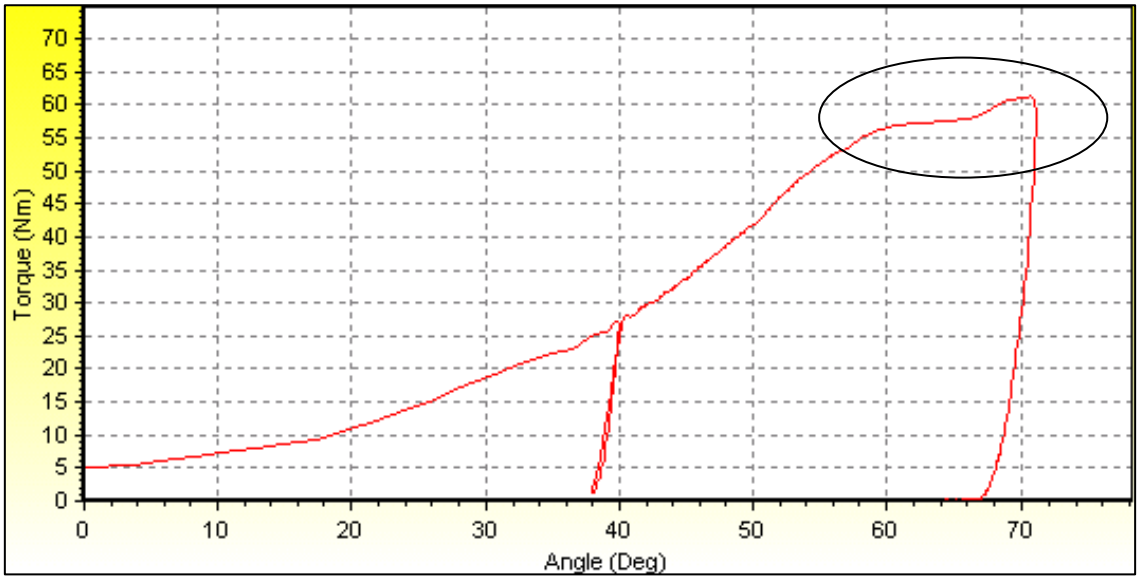

(j)

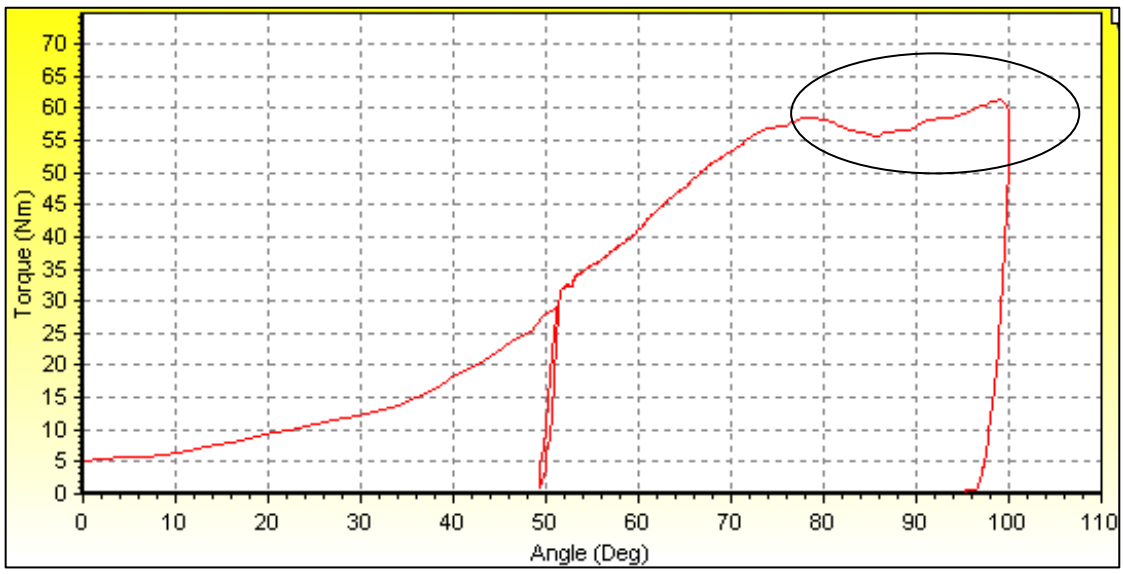

(k)

Figure 4.7 Bolt torque vs. angle results for Study 1 (continued)

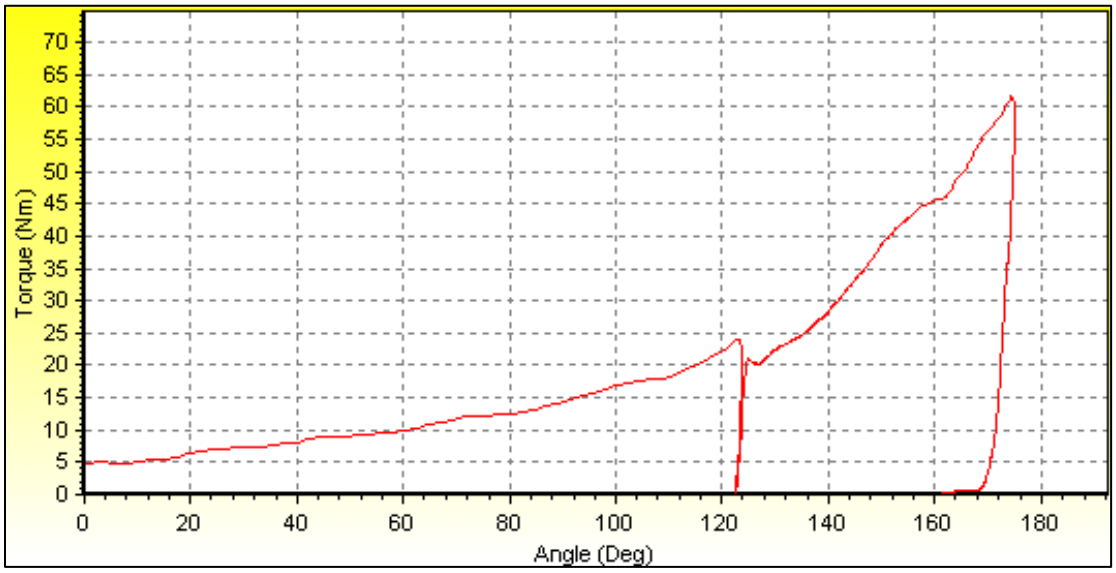

(l)

Figure 4.7 Bolt Torque vs Angle results for Study 1 (continued)

It is seen that yielding occurs at 3 bolts shown in Figure 4.7 b, j and k, two at 58Nm and one at 60Nm.

4.4.2 61Nm Torque without Sealer (Study 2)

Study 2 is performed without sealer process at 61Nm torque value. Results are shown in Figure 4.8.

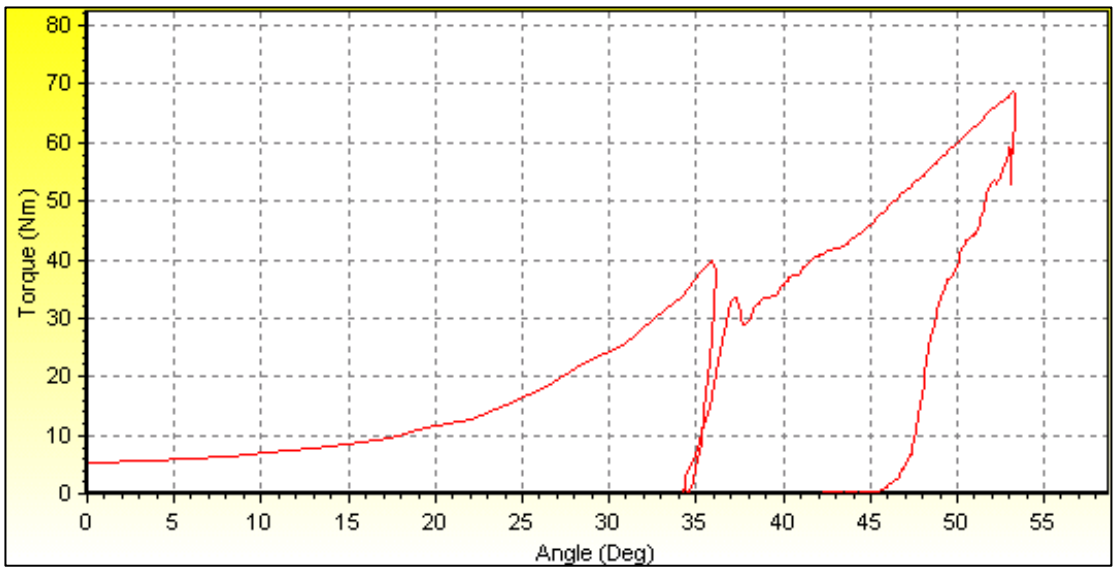

(a)

Figure 4.8 Bolt torque vs. angle results for Study 2

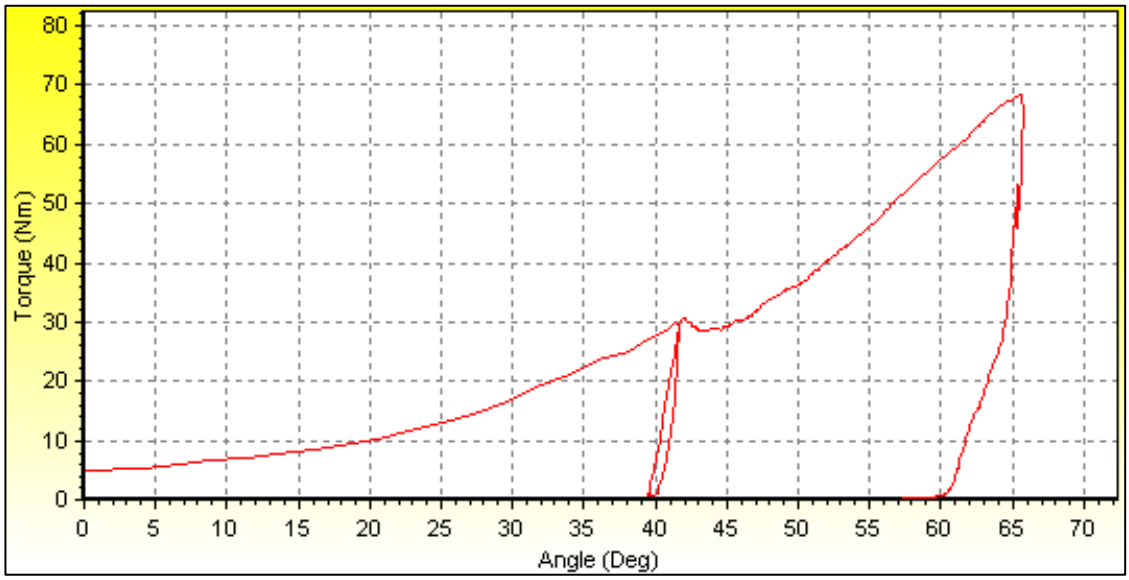

(b)

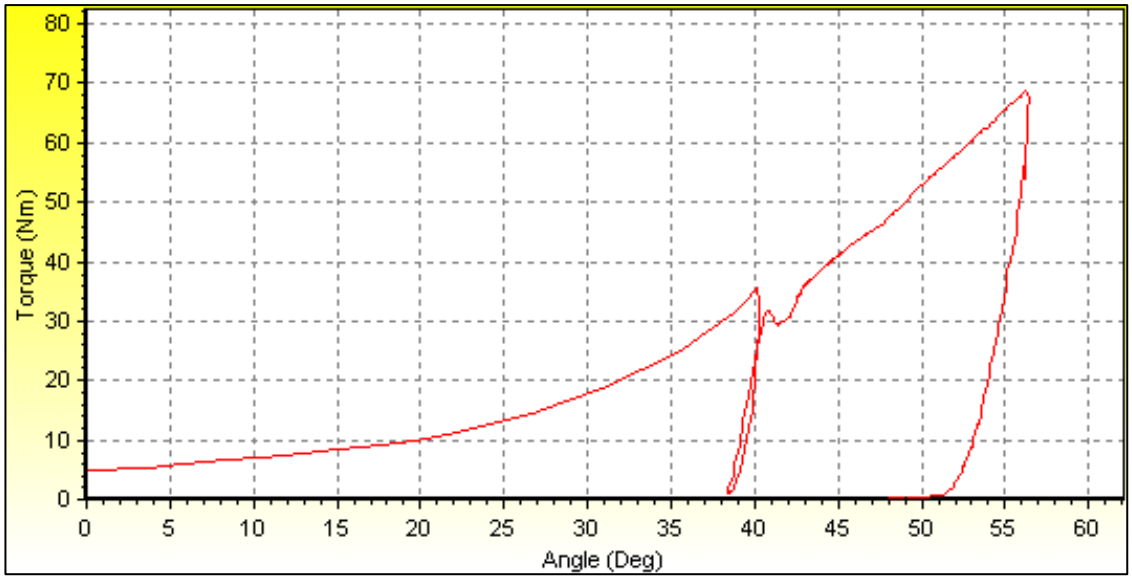

(c)

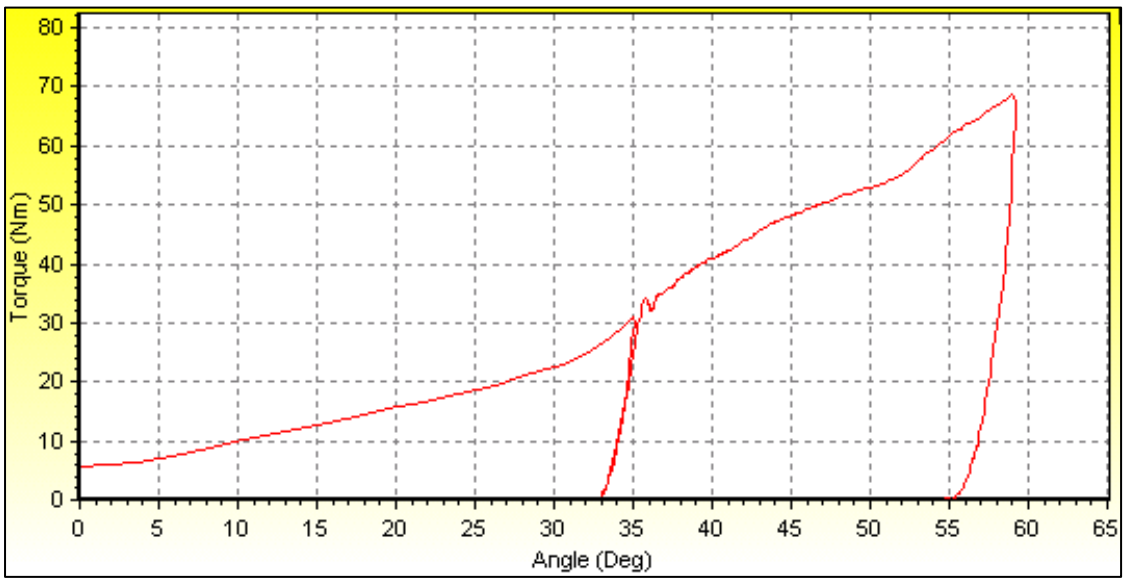

(d)

Figure 4.8 Bolt torque vs. angle results for Study 2 (continued)

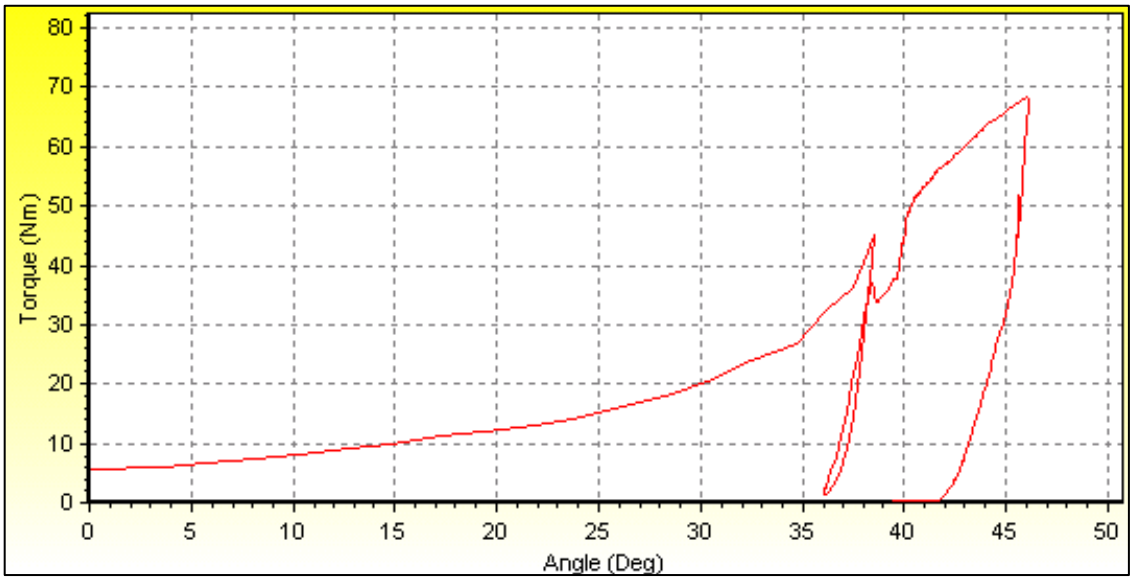

(e)

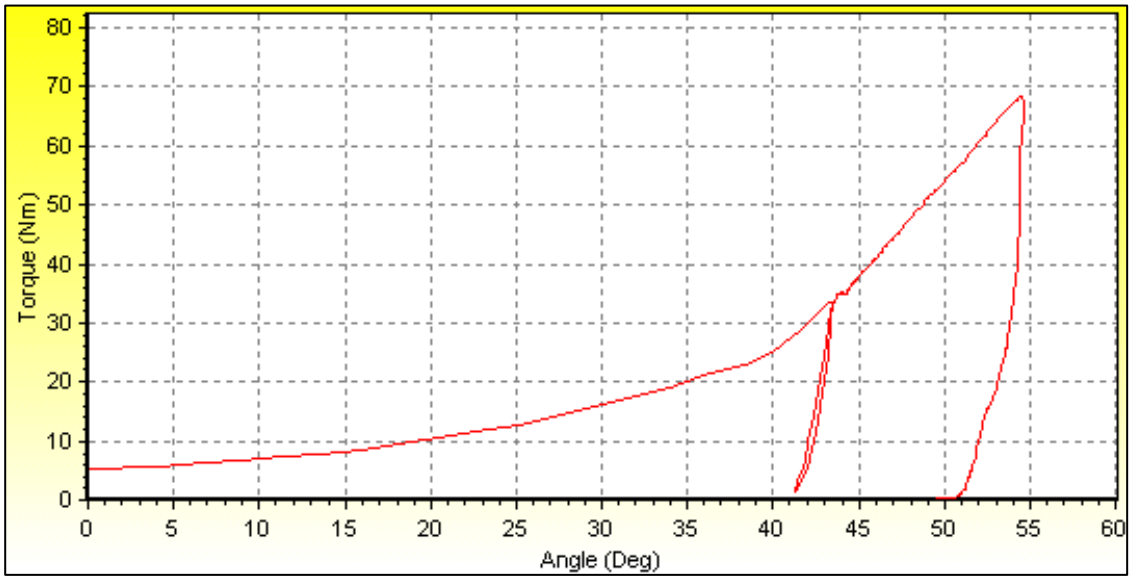

(f)

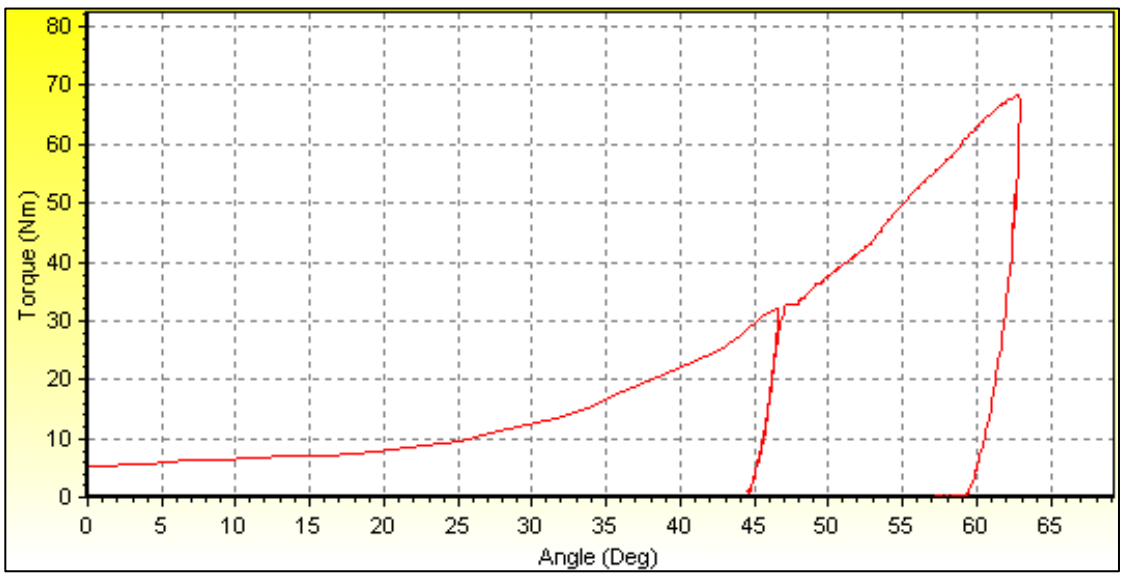

(g)

Figure 4.8 Bolt torque vs. angle results for Study 2 (continued)

(h)

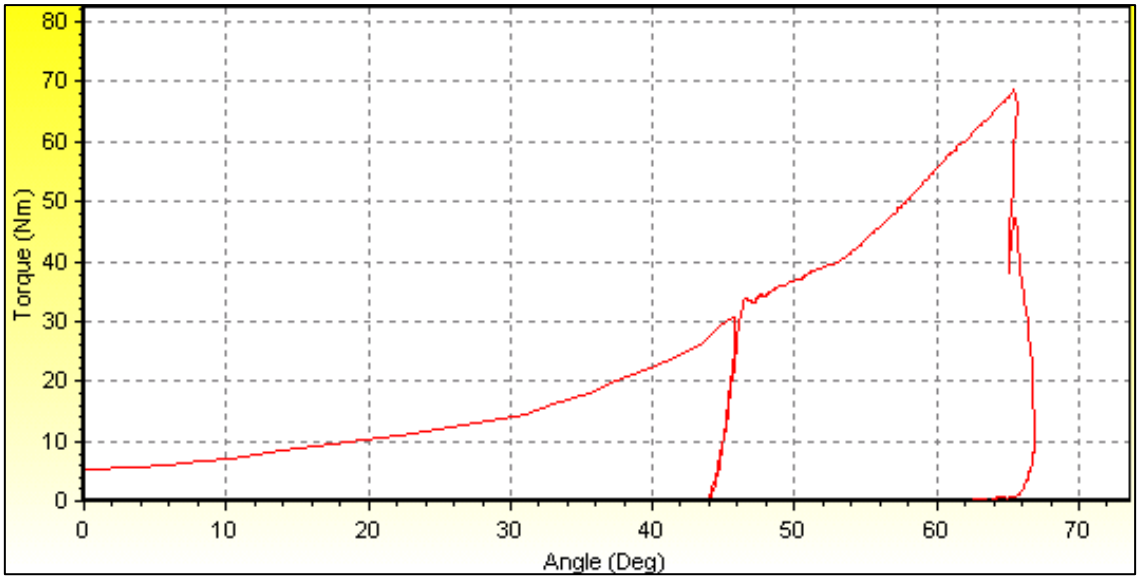

(i)

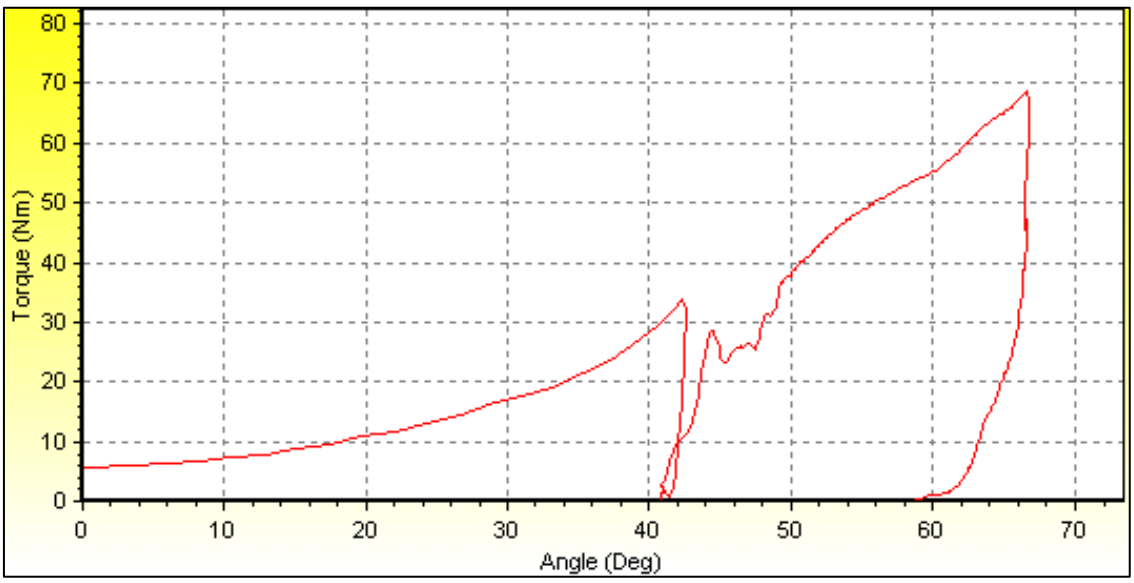

(j)

Figure 4.8 Bolt torque vs. angle results for Study 2 (continued)

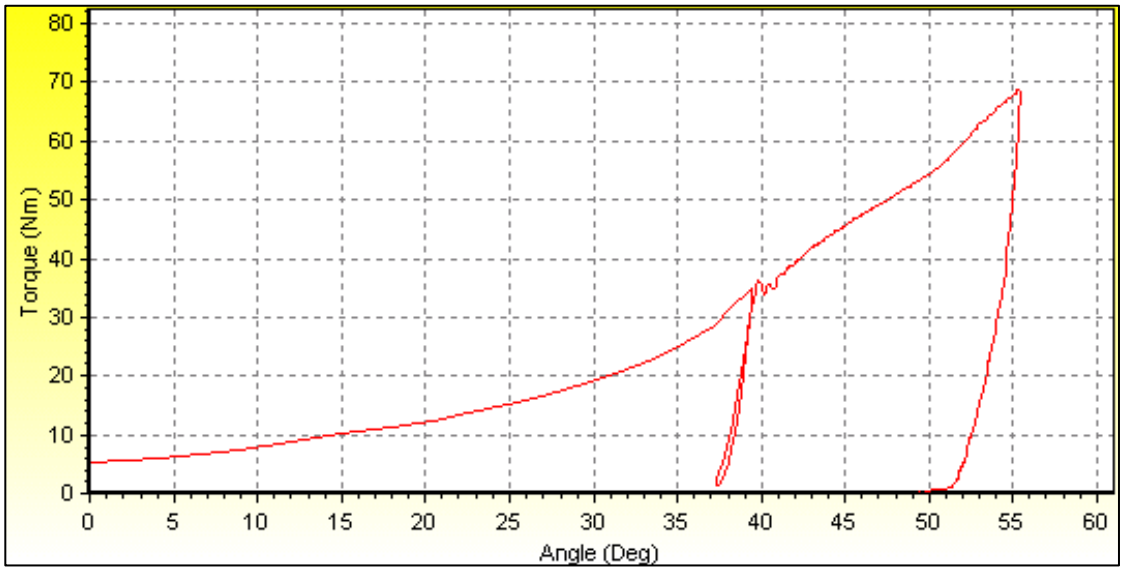

(k)

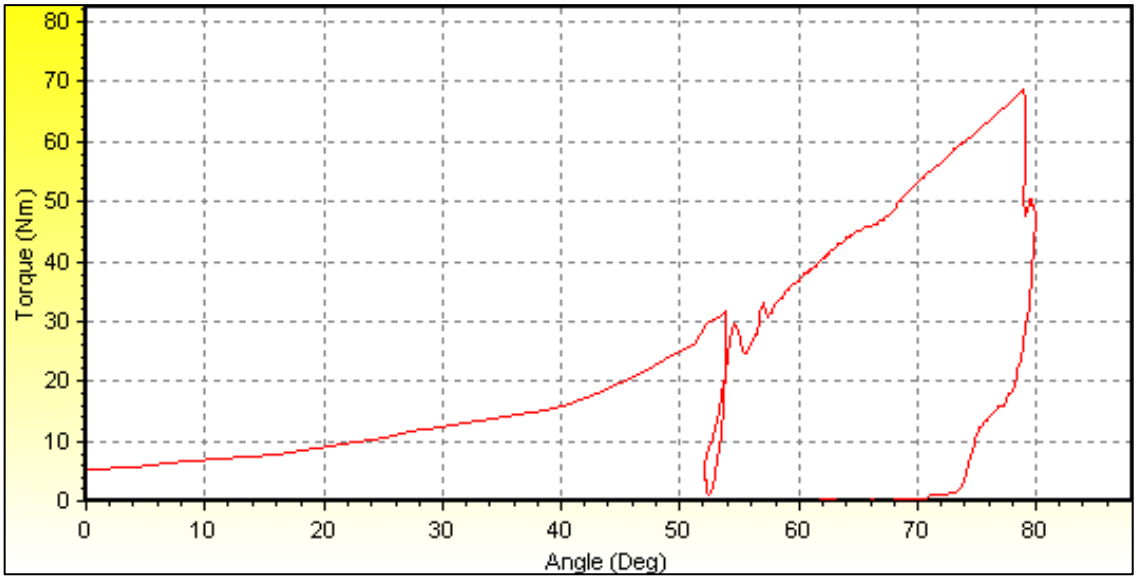

(l)

Figure 4.8 Bolt torque vs. angle results for Study 2 (continued)

There is no yieldint at any of the cover bolts for stuy 2.

4.4.3 68Nm Torque with Inonu(current) Sealer Process (Study 3)

Study 3 is performed with current sealer process at 68Nm torque value. Results are shown in Figure 4.9.

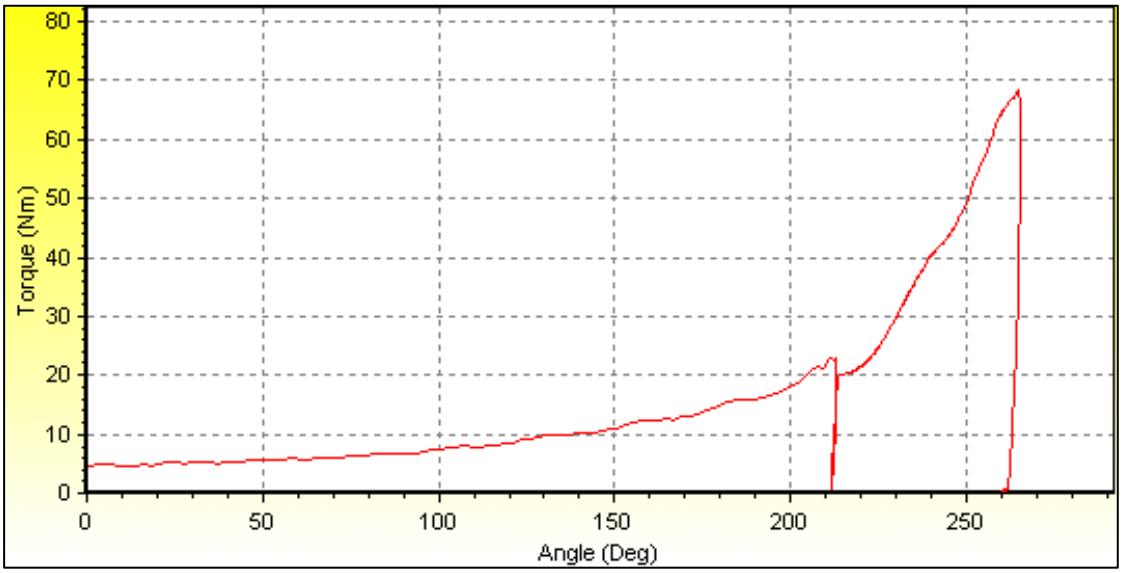

(a)

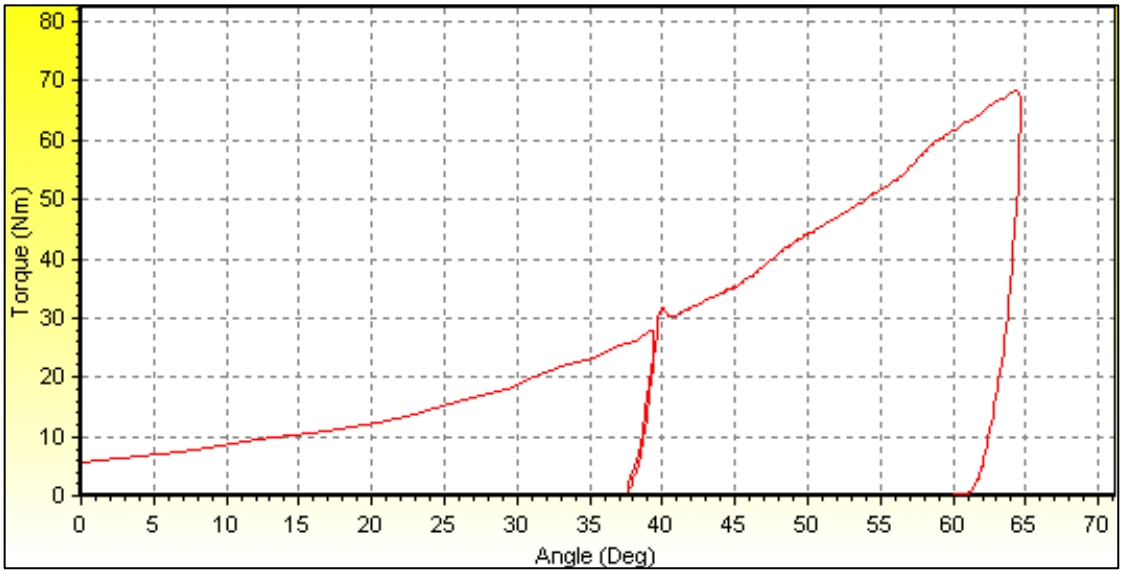

(b)

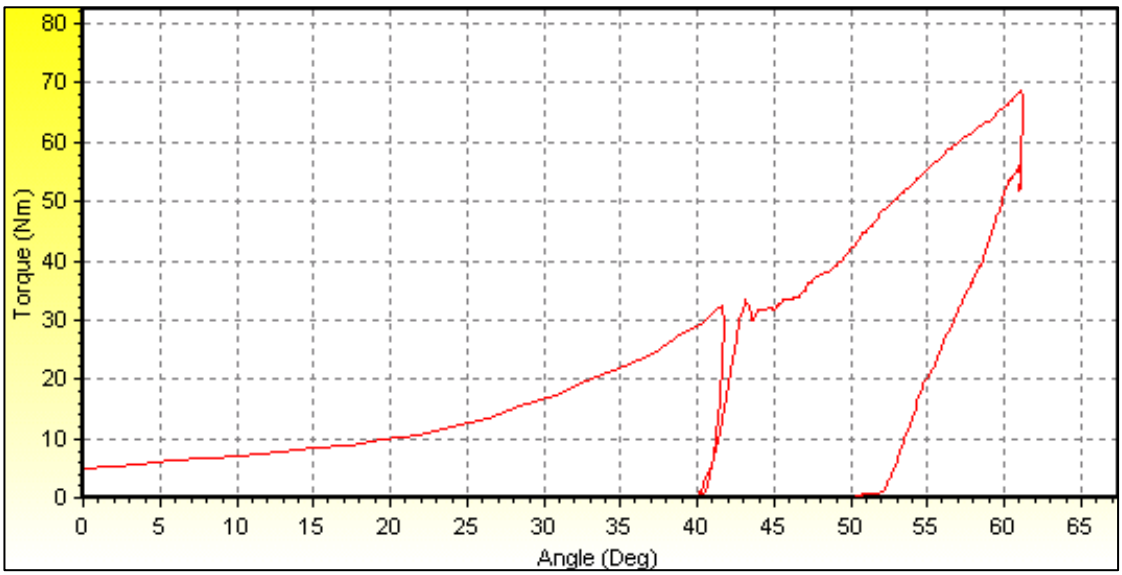

(c)

Figure 4.9 Bolt torque vs. angle results for Study 3

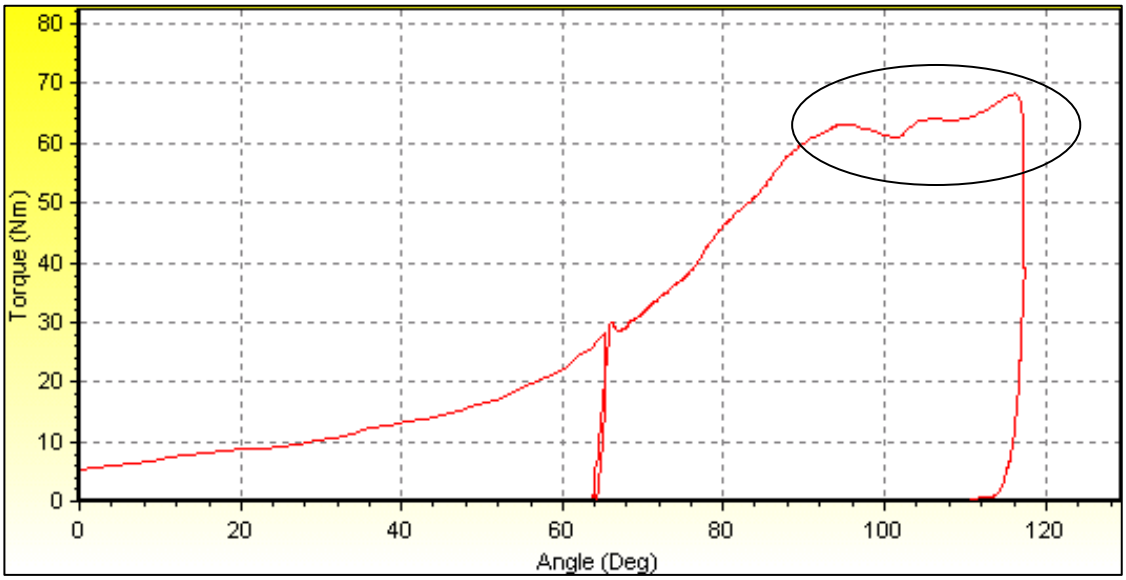

(d)

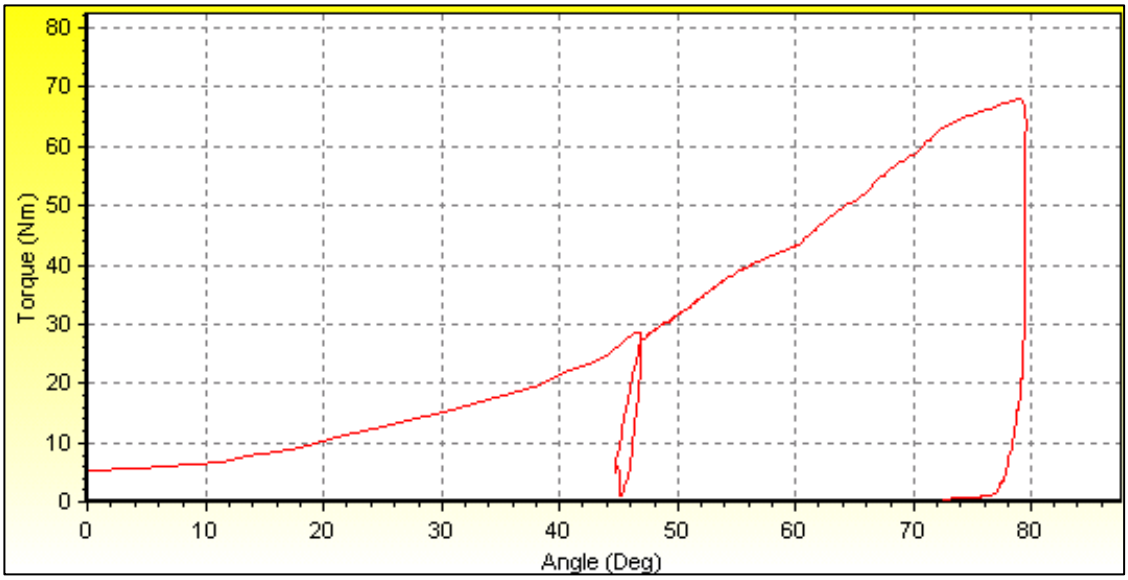

(e)

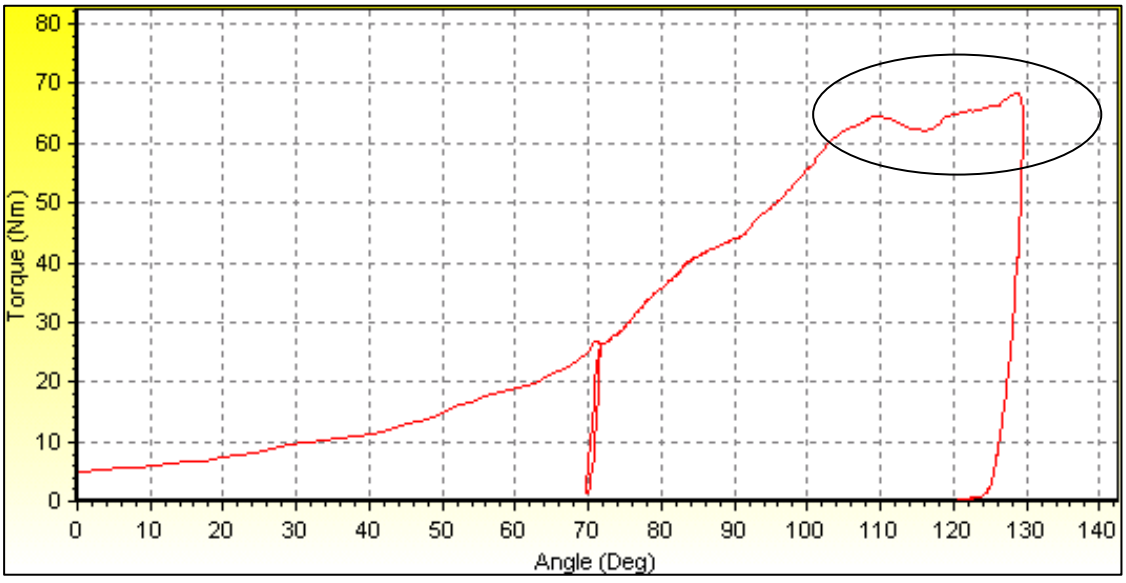

(f)

Figure 4.9 Bolt torque vs. angle results for Study 3 (continued)

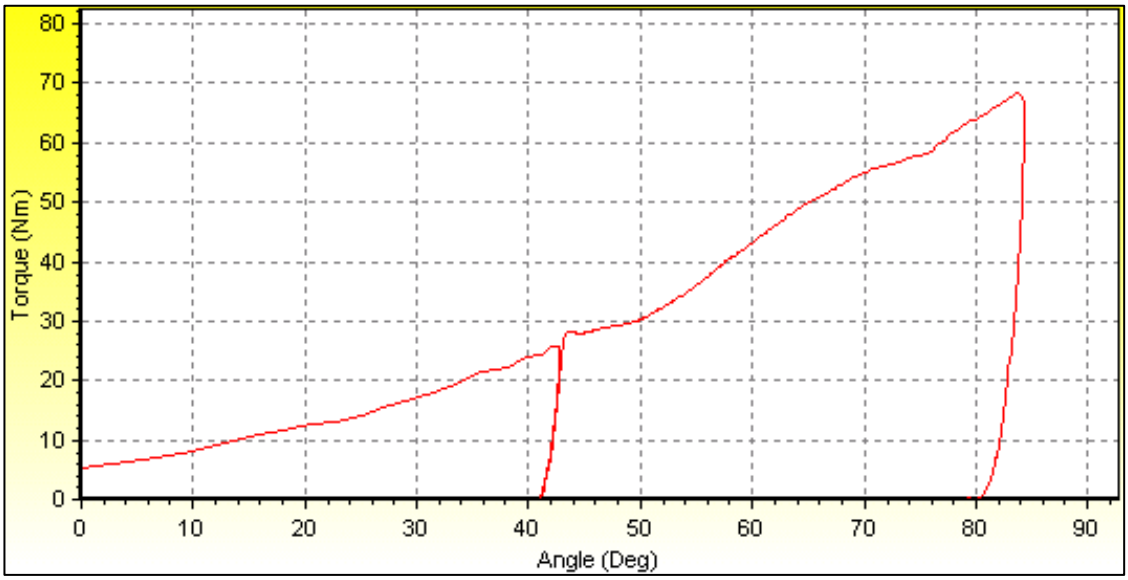

(g)

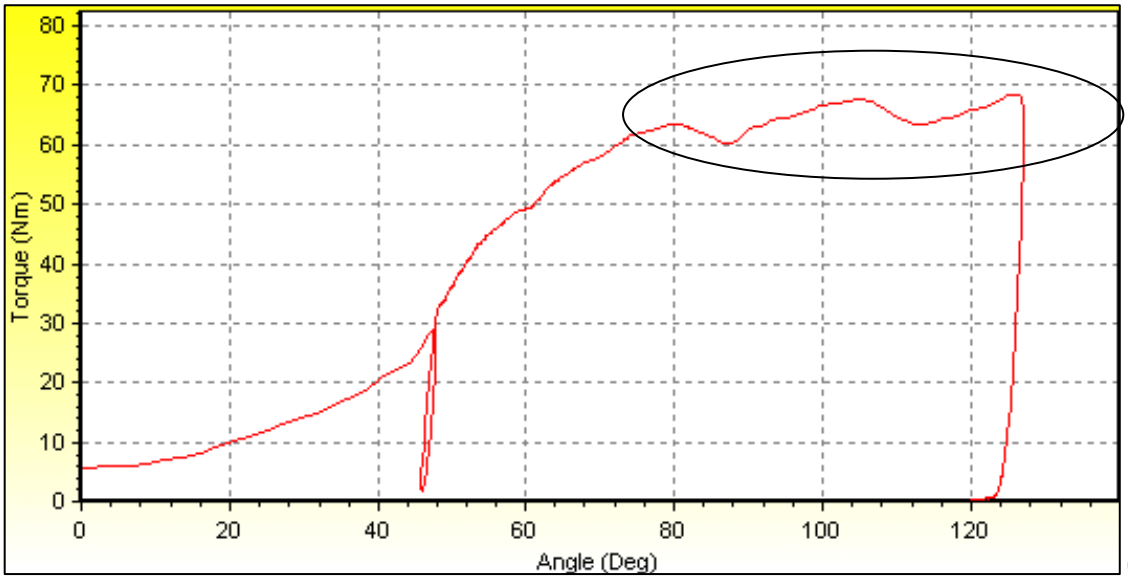

(h)

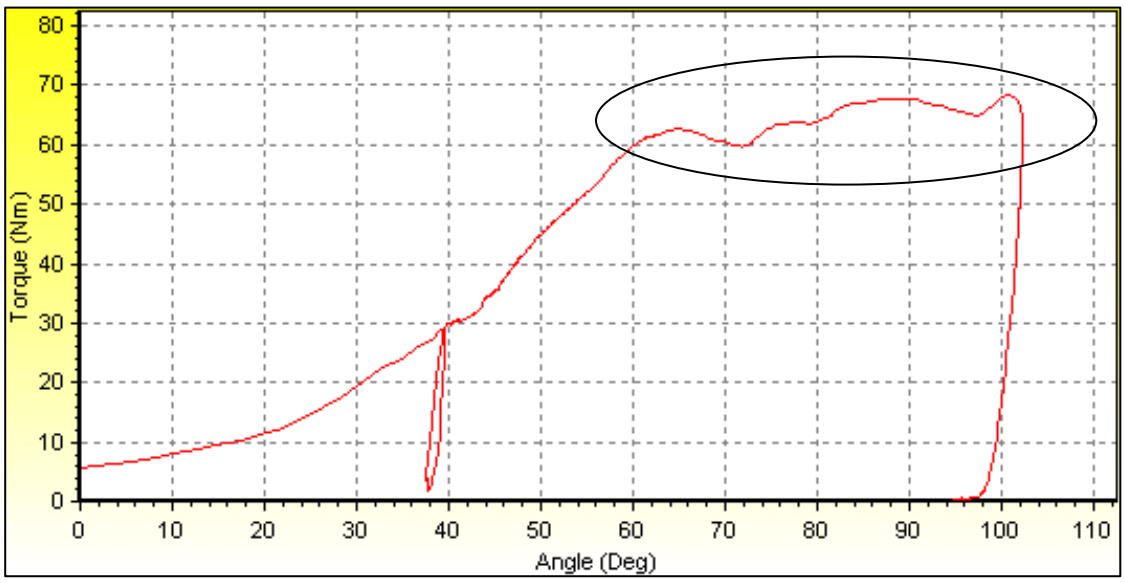

(i)

Figure 4.9 Bolt torque vs. angle results for Study 3 (continued)

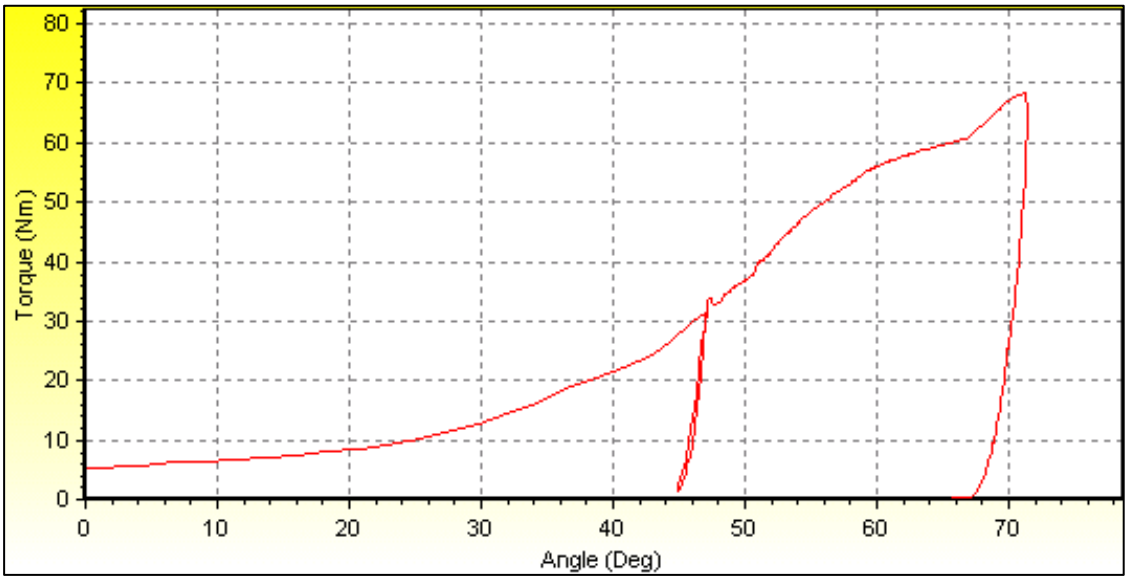

(j)

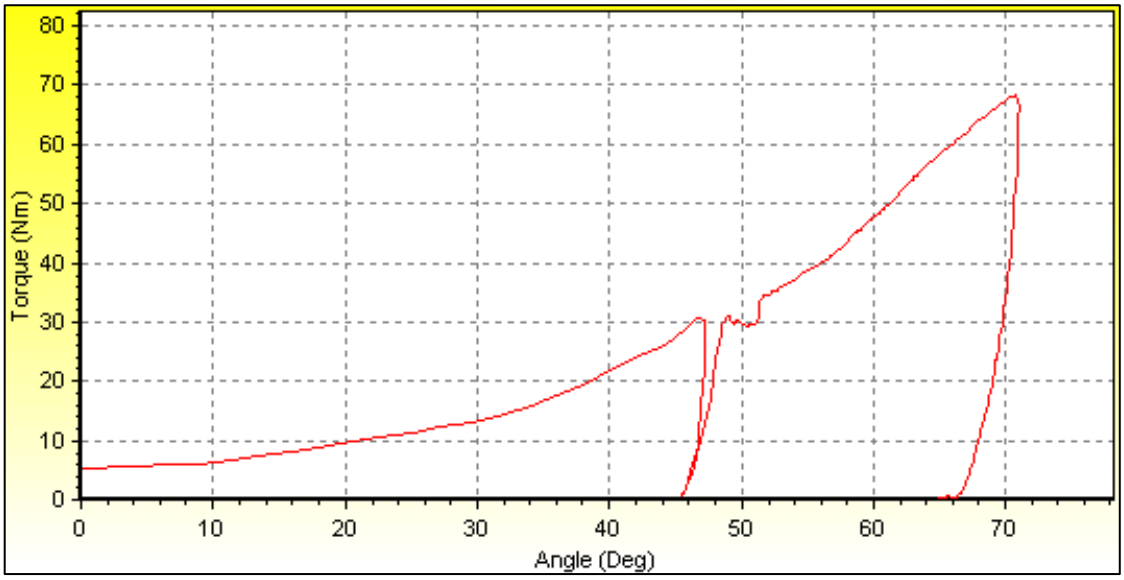

(k)

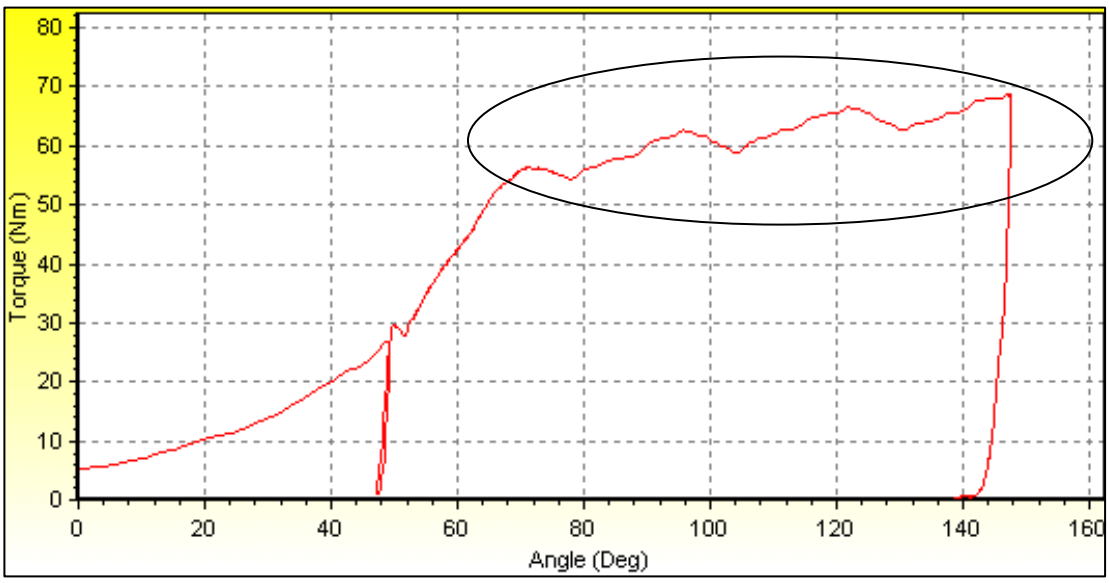

(l)

Figure 4.9 Bolt torque vs. angle results for Study 3 (continued)

It is seen that yielding occurs at 5 bolts shown in Figure 4.9 d, f, h, i and l, four above 61Nm and one at 57Nm.

4.4.4 68Nm Torque with Heavy Sealer Process (Study 4)

Study 4 is performed with heavy sealer process at 68Nm torque value. Results are shown in Figure 4.10.

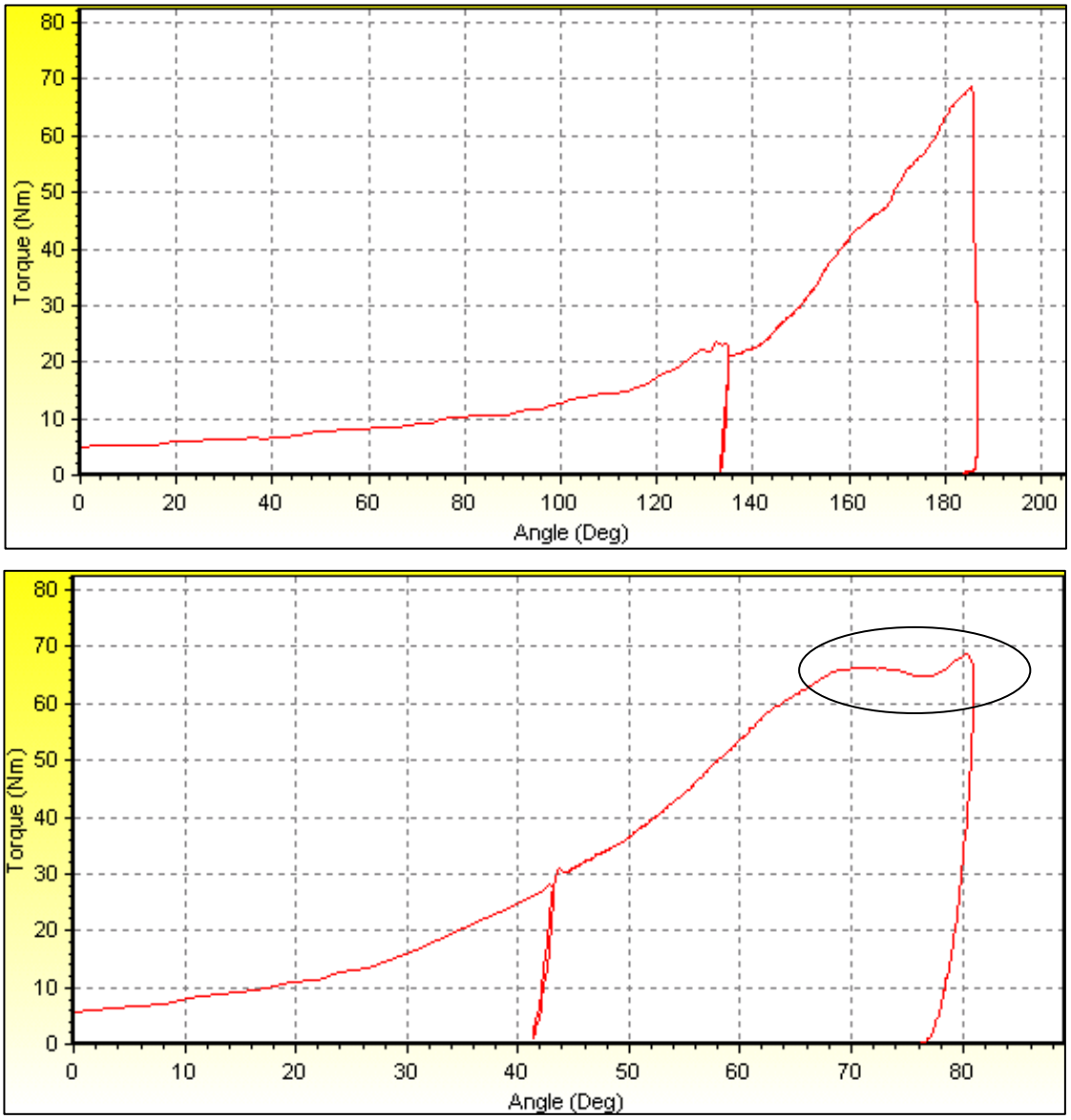

Figure 4.10 Bolt torque vs. angle results for Study 4

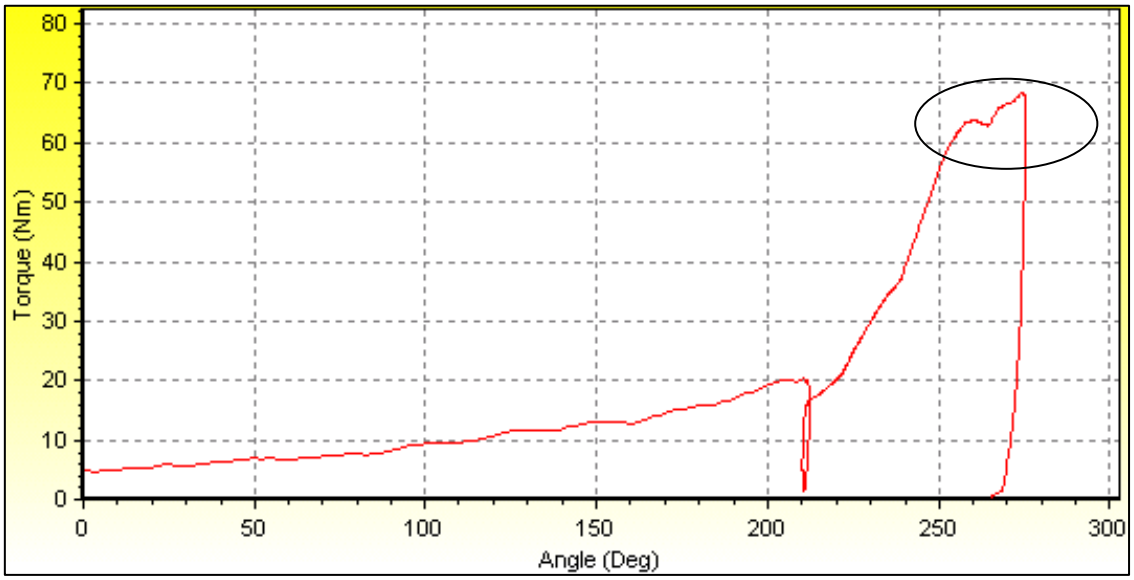

(c)

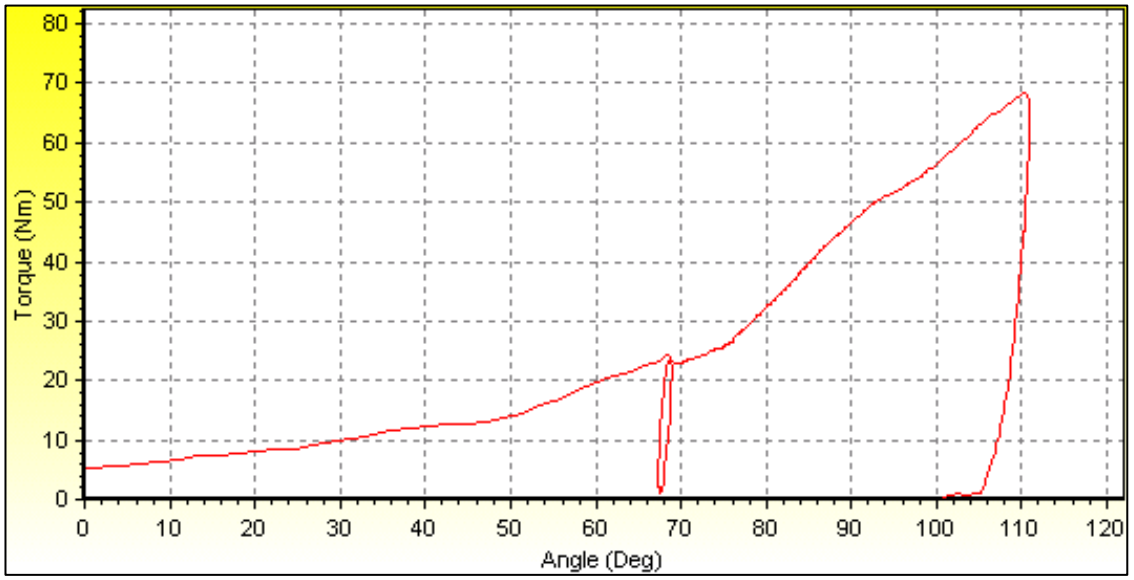

(d)

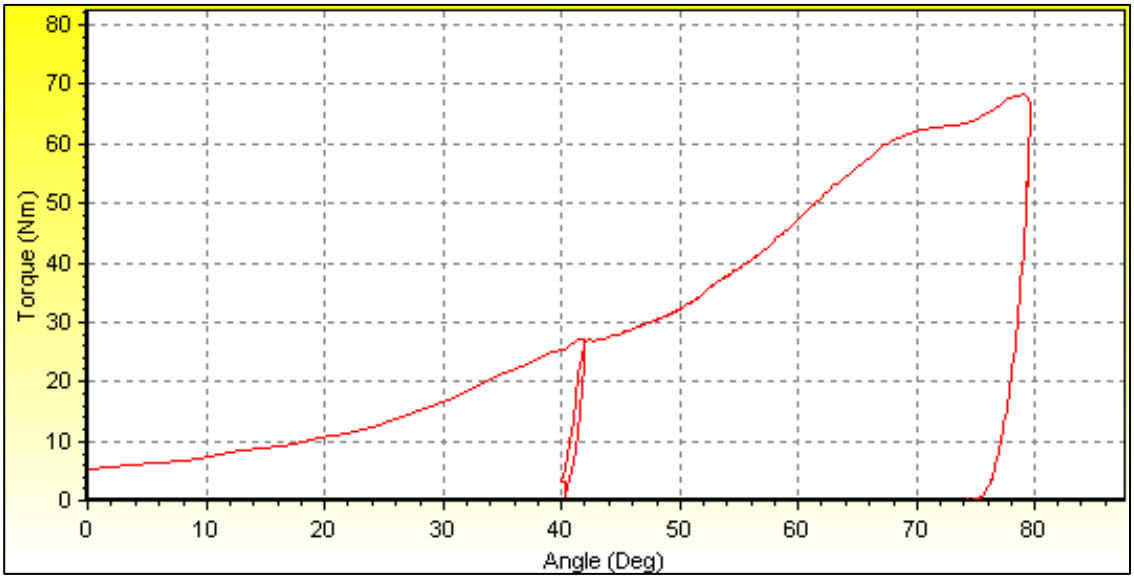

(e)

Figure 4.10 Bolt torque vs. angle results for Study 4 (continued)

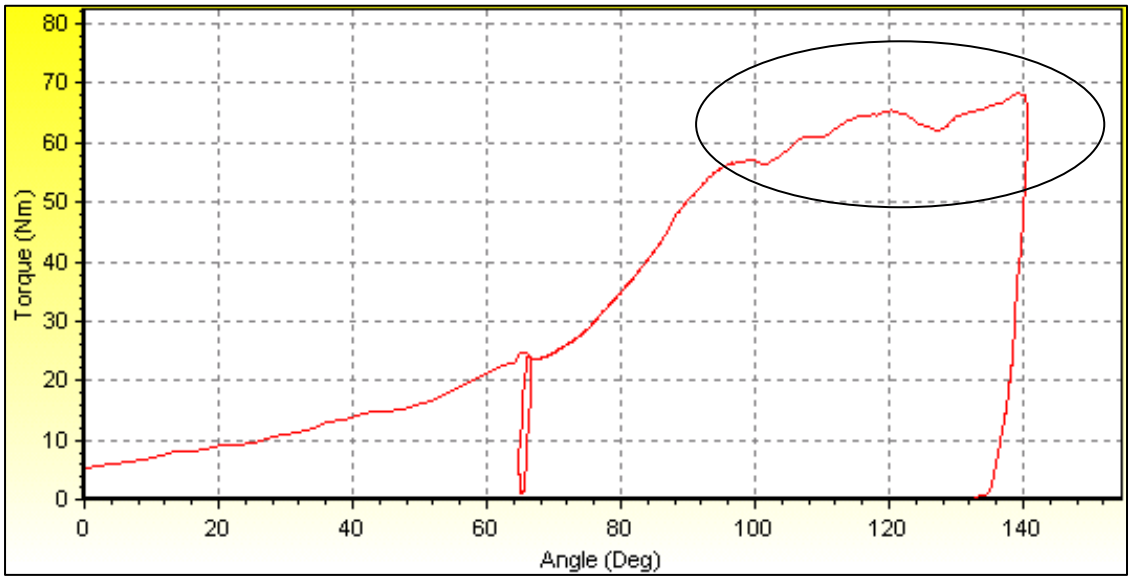

(f)

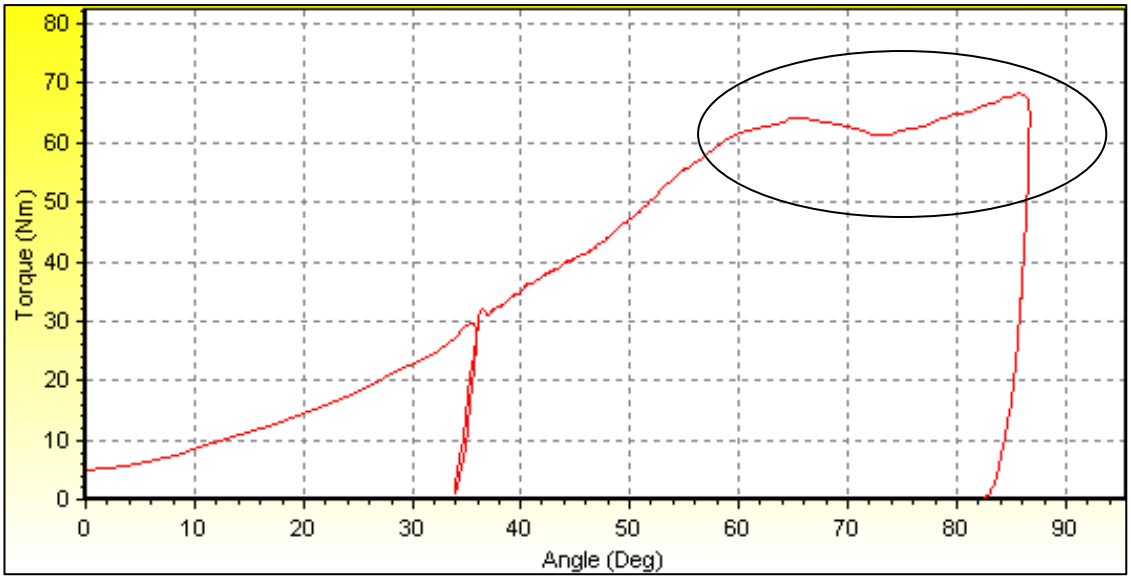

(g)

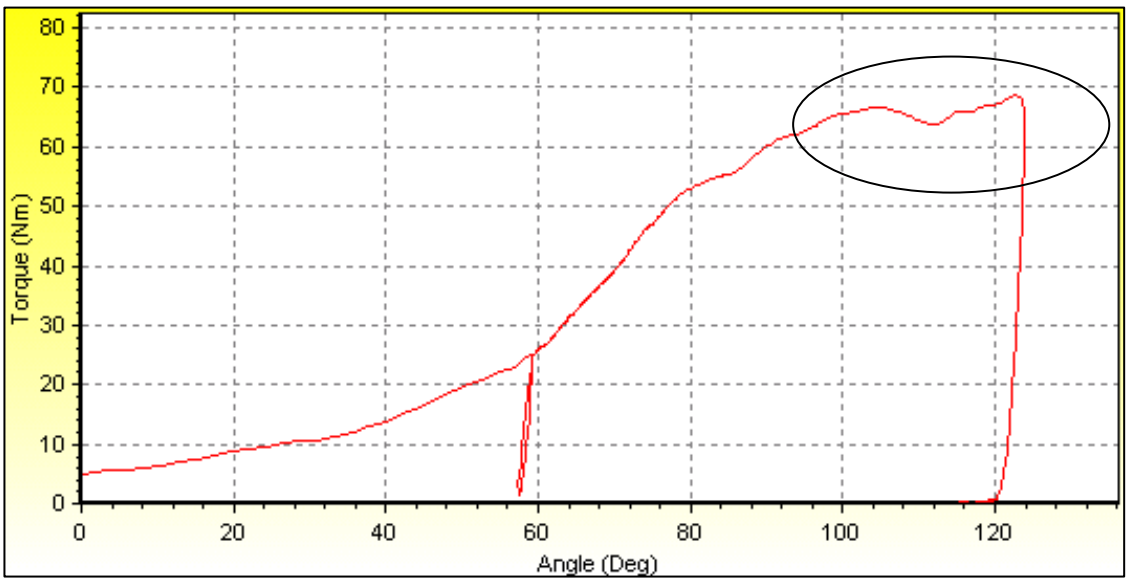

(h)

Figure 4.10 Bolt torque vs. angle results for Study 4 (continued)

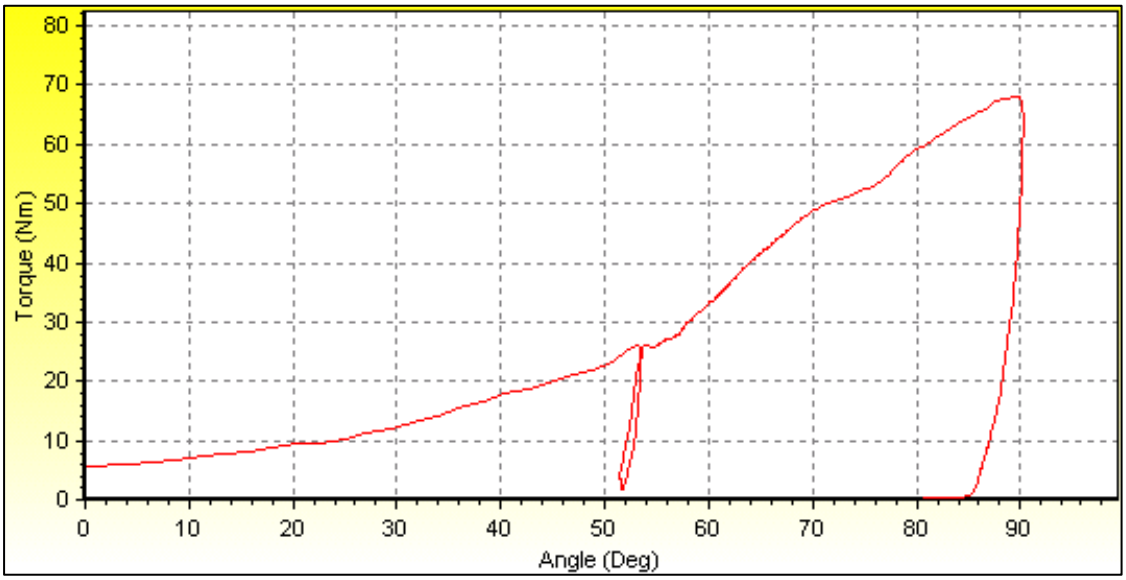

(i)

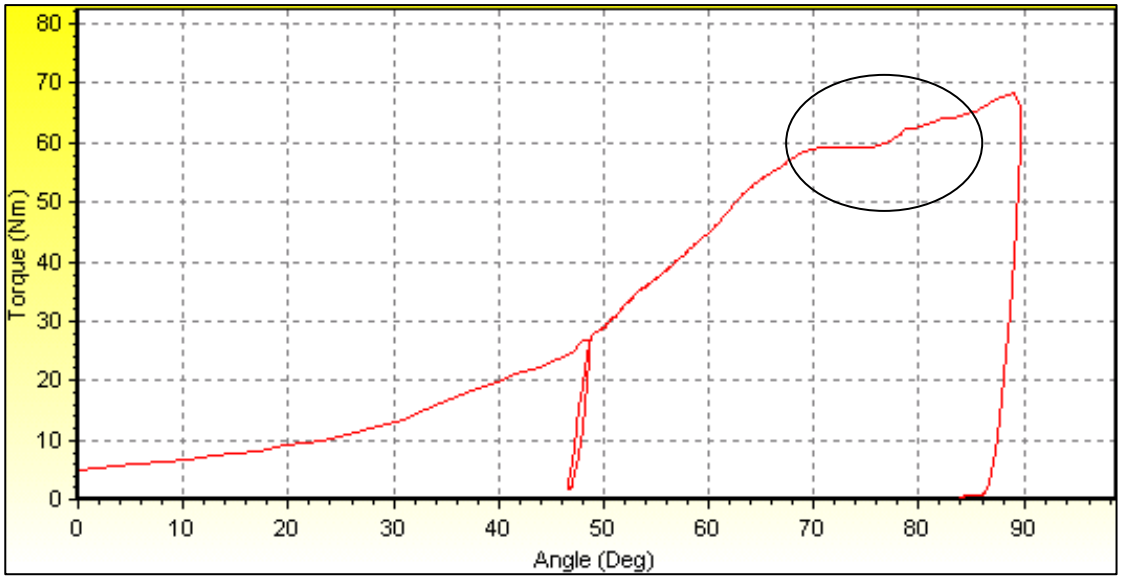

(j)

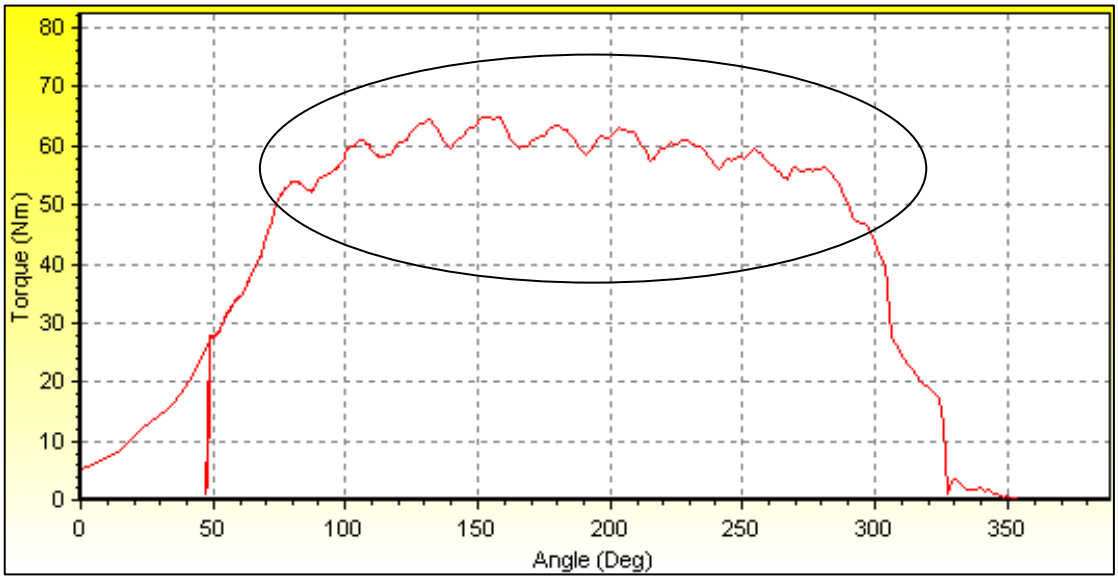

(k)

Figure 4.10 Bolt torque vs. angle results for Study 4 (continued)

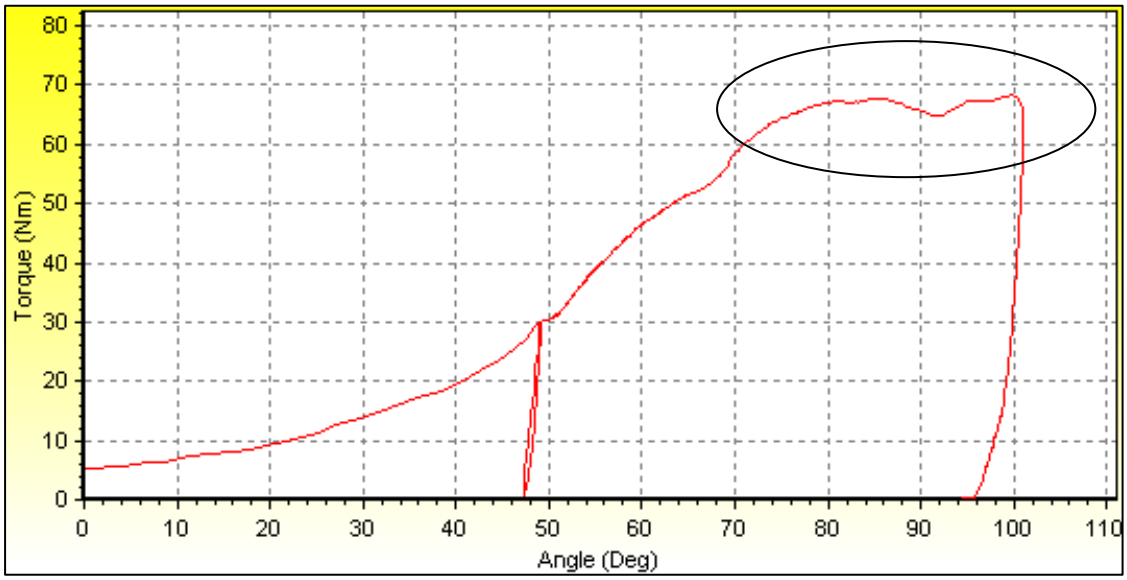

(l)

Figure 4.10 Bolt torque vs. angle results for Study 4 (continued)

It is seen that yielding occurs at 7 bolts shown in Figure 4.10 b, c, f, g, h, j and l, five above 61Nm and others at 58 and 60Nm. Moreover, one cover bolt ruptured shown in Figure 4.10 k at the end of this study.

As expected, increasing torque values at the same sealer process affects cover bolt performance poorly. 3 bolt yielded occur at 61 Nm with current sealer process and 5 yielded were seen at 68 Nm with same sealer process.

As expected, sealer process and amount of sealer also reduce the bolt performance. If there is no sealer at 68 Nm, no yielding occurs; with current sealer process 5 yielding occurs and finally with heavy sealer process 7 yielding and 1 rupture occurs. This shows the negative effect of sealer on cover bolt performance.

Although, omitting the sealer process gives better results, it is not possible to assemble cover to carrier without sealer. It is seen that after all these studies, best performance of the bolt is at the current torque value (61Nm) with improved sealer process (DANA).

5. SUMMARY AND CONCLUSIONS

A research was conducted to determine the main reasons of leakage. After taking into consideration recent studies, it was seen that the main reason was the poor sealing performance of the sealer and insufficient stiffness. New cover designs were tried like adding curvature and stamping to increase the sealer performance. Also, changing the cover hole positions was considered to improve the cover design. Moreover, thickness of the cover and flange lenght effect on the cover design was investigated during improvement studies.

During the improvement studies, to simulate the real road condition of the vehicle, vehicle durability test and comparison oriented beam fatigue tests were performed with the current rear axle cover designs – Cover 1 and 2. Then, it seems logical to take advantage of CAE analysis to improve the rear axle cover design. Because, existence of a model that correctly simulates the real conditions, saves time and money. Vehicle durability test results and vertical beam fatigue test results for both of cover 1 and cover 2 were obtained from the field and test centers. The results of the tests were compared with the model analysis results.

FE analyses were performed for all the proposed cover designs with 3g beam load and 3g beam load + forward torque. The critical load condition for these analyses is 3g beam load + forward torque load condition. Because, torsional effect which is the most important load condition for cover leakage issue is included in these analysis.

In this study, the results of the FE model were compared with the results of the test data. The locations where oil might leak were previously determined by performing several vehicle durability tests and vertical beam fatigue tests.

The results of the analyses with the current cover1, 2 and 3 correlated with the test results of cover 1 and 2 Then, it was assumed that the cover design may be improved by changing cover bolt hole locations according to Axle Cover Design Guide released by Ford Motor Company. The preliminary analyses results reveal that cover 3 had the best

performance. Accordingly cover 3 was chosen as the design to introduce modifications to improve the performance..

10 cover designs with different bolt locations were tried and no improvement was observed according to the FE model. Asymmetric current design of the cover might be its reason. Because, it is also stated in the Axle Cover Design Guide of Ford Motor Company that symmetric design of hole positions and cover should be applied to get the best performance. But, due to design limitations, it is not possible to change the asymmetric cover to symmetric design.

Two of the design features, which are the thickness of the cover and the length of the flange were also investigated. Increasing the flange length results in improvement on the maximum gap values. But, it is not very effective. Decreasing thickness results in increased gap. Because increasing thickness has a slight effect on the maximum gap, it is not likely that leakage can be prevented by changing the thickness. Besides, thicker cover has also some problems such as cost disadvantage and manufacturing difficulties.

To conclude, it can be seen that the best proposal is cover 3 design which is a hybrid cover, i.e. it is a combination of cover 1 and cover 2.

Furthermore, although it seems that increasing the flange length of the cover leads to a little bit better performance, it has nearly no effect, so there is no need to change the current design of the curvature. This change also increases manufacturing difficulty and cost. Therefore, this proposal may be also ignored.

Beside cover design studies, various tests and studies were performed to determine the paint, sealer, sealer process and torque effect on the bolt performance. It can be seen that paint on the cover bolt head decreases the friction effect then cause an additional force on cover bolt. This additional force directly causes excessive elongation and affects cover bolt clamping performance. Bolt exceeds its elastic region and plastic deformation occurs. So, load on cover bolt is decreased dramatically. To summarize, paint on cover bolt decreases friction, causes excessive elongation and results in decreasing pretension in the bolts.

Similar to paint effect, sealer on cover bolt has the same effect on bolt performance. Using excessive sealer decreases the friction then causes an additional force on cover bolt. To summarize, sealer decreases friction, causes excessive elongation and results in decreasing pretension in the bolts.

Elongation studies show the effect of sealer process. DANA sealer process and Inonu sealer process designs are compared; it is obvious from the test results that Dana sealer process is better than Inonu process. Heavy sealer (Inonu) process causes excessive bolt elongation and causes clamp load decrease.

Torque vs. angle test reveals the effect of sealer process and torque effect on bolt. When we consider all the studies, it is seen that increasing bolt torque worsens the bolt performance and excessive bolt elongation occurs. Similarly, increasing sealer quantity causes excessive elongation of the cover bolt.

To conclude, new sealer process should be implemented to prevent excessive bolt elongation and bolt loosening. Also, it is decided not to change magnitude of the applied torque value in the assembly process.

APPENDIX A: TTGD3 (TRAILER TOW GENERAL DURABILITY) TEST for LIGHT COMMERCIAL TRUCKS

Appendix A is from Ref 24 - Corporate Engineering Test Procedure - Trailer Tow General Durability Test for Light Commercial Trucks (CETP: 00.00-R-354).

A.1. Purpose of the Test

The purpose of this test is to validate the strength, durability and functionality of all components of the vehicle over 240K km or 1 life. For a good evaluation, it is mandatory that this procedure is executed as accurate as possible.

A.2. History of the Test

This is a trailer tow general durability test for European light commercial trucks. The test contains events focused on both structural and power-train durability including trailer towing. High speed cycle was improved. Also some minor changes in the descriptions of the test events are made to make the test less complex for the test drivers. On special request for quick body or chassis validation, the test can be split up in a structure (TTAD) and a driveline (TTDD) durability test, where TTDD+TTAD=TTGD.

Table A.1 Track (Event) summary of TTGD test

Code	Event
5	High Speed Road
7	Inner Durability Road
8	Gravel Road
10	Outer Durability Road
11	Comfort Road
11	Postel Road Extra
4X3	Structural input road
4Z1T	Cobbelstones
4Z1X30a	Bumps & Potholes - Alternating
4Z1X50a	Bumps & Potholes - Alternating
4Z1X50b	Bumps & Potholes - Simultaneously
4Z1X70a	Bumps & Potholes - Alternating
4Z1X70b	Bumps & Potholes - Simultaneously
4Z1X90b	Bumps & Potholes - Simultaneously
4Z1Y15a	Curb Islands - Angled
4Z1Y8a	Curb Islands - Angled
4Z1Y8b	Curb Islands - Straight
4Z3a	Resonance Road - Part 1
4Z3b	Resonance Road - Part 2
BU	Back-up Road
ST	Dust Tunnel
B/MU	Engine Off
FL	Curb Island - LH turning
FR	Curb Island - RH turning
M	Mud Bath
H	Old Hills & Gradients
ZS	Salt bath & spray
TC	Traction Assist

A.3. Coverage of the Test

TTGD3 Test for European Light Commercial Trucks consists of 120 cycles and correlates with 240,000 km (150,000 miles) or 1 life of European light truck customer Durability Vehicle Life. When the vehicle has to be tested to 1.5 lives, the first 60 cycles of the test have to be repeated at the end of the 120 cycles to accumulate 180 cycles in total.

A.4. Equipment and Facilities

A.4.1 Track Analysis

This test procedure is written for execution on the test track facilities of Lommel Proving Ground. The test consists of 120 drive cycles

A.4.2 Event Analysis

Several of passes of each event during the test are performed. Some special events driven for accelerated structural input.

A.5. Road Description

The facilities used in this test procedure are shown in the below figure A.1.

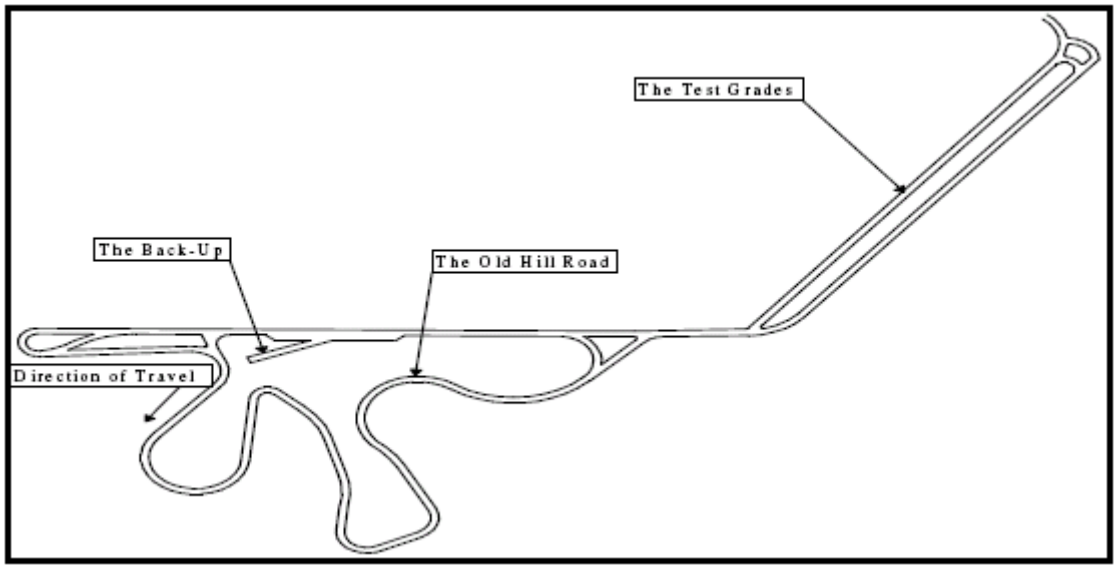

Figure A.1. TTGD test road description

A.6. Vehicle Preparation

A.6.1 Loading Conditions

The vehicle should be loaded according to CETP 00.00-R-602, Test Mass Standards. The distribution of the load can be seen in the below figure A.2. If specified by the test requester, roof load has to be added. The roof load must be evenly divided over the roof rack. The vehicle should not exceed GVM condition though. This means the roof load must be subtracted from the vehicle loading. The weights are always determined with filled up fuel tanks.

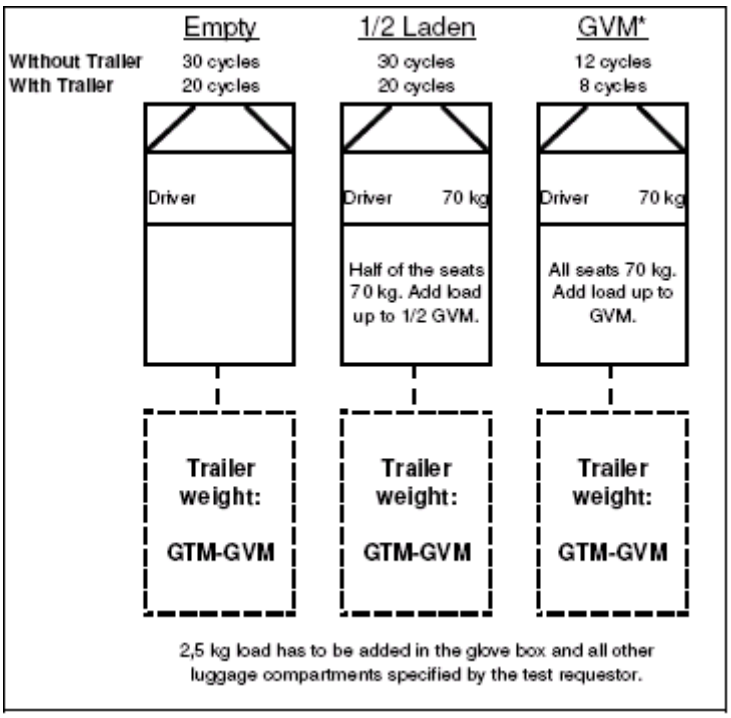

Figure A.2. TTGD test load distribution

A.6.2 Loading Schedule

The vehicle is loaded during the test according to the specifications. According to the test requester specifications, roof load has to be added in some cycles

APPENDIX B: BEAM FATIGUE TEST (RIG TEST)

Appendix B is from Ref 25 - DANA Coorporation Beam Fatigue Test Report

B.1. Introduction

To determine if the Ford Transit cover would perform adequately, a series of tests were performed on the beam fatigue rig in Dana Birmingham.

B.2. Theory

Maximum Strain is given by the following equation:

$$1g - strain = (\frac{EI}{My})$$

where:

M = Maximum tube bending moment

where M assumes the following vehicle data:-

2950kg Rear axle load

1641mm Track

1110mm Spring Centres

All load is reacted at spring centres, none at the bump stops.

y = Tube outer diameter / 2

E = Youngs Modulus

I = Second moment of area

Therefore 1G strain = 490 με

B.3. Test Procedure

Prior to the test, strain gauges are attached to the tube assemblies, inboard of the spring seats. The axle is then fitted to the beam fatigue rig. Mounting is at an angle of approximately 45 degrees to the rig bed and the hydraulic rams are fitted to the spring seat brackets as shown in Figure B.1..

The strain gauges are connected to the Spider-8 electronic measuring system. Each axle was then mounted on the beam fatigue rig and subjected to a cyclic loading of 0.5-2.5G. The axle was sealed and pressurised to allow for detection of air loss. Periodically the cover plate was checked for air loss using a leak detector spray.

Figure B.1. Rear axle beam fatigue test rig

APPENDIX C: FADSIM-TOOLBOX (GEAR-BEARING LOADS)

Appendix C is from the Ref 26 - http://www.fadsim.ford.com/etm/cae/vadsim-gear-bearing/?)

C.1. Introduction (About FADSIM TOOLBOX Gear Bearing Loads)

FADSIM Toolbox Gear-Bearing Loads is a web-based tool for the prediction of hypoid gear and bearing loads. Product applications are in front axles, rear axles and power take off units (PTU). Analysis applications are in stress and NVH analysis.

First, hypoid gear loads and mesh point location are developed in the global coordinate frame (parallel to the vehicle coordinate frame).

Results are presented for both front axles/right hand pinion and rear axles/left hand pinion for both drive and coast conditions.

The gear loads are then used to calculate bearing loads on the axle carrier/PTU at the pinion and differential case locations compression, uniaxial tension, and hydrostatic compression test results are used as input parameters in finite element simulations. Simulations of uniaxial and hydrostatic compression, uniaxial tension, simple shear

C.2. Axes of the System

Axes of the rear axle system is shown in Figure C.1.

X + Passenger to driver; Y + Front to rear; Z+ Vertically up

Drive refers to a condition when the input torque is coming from the pinion.

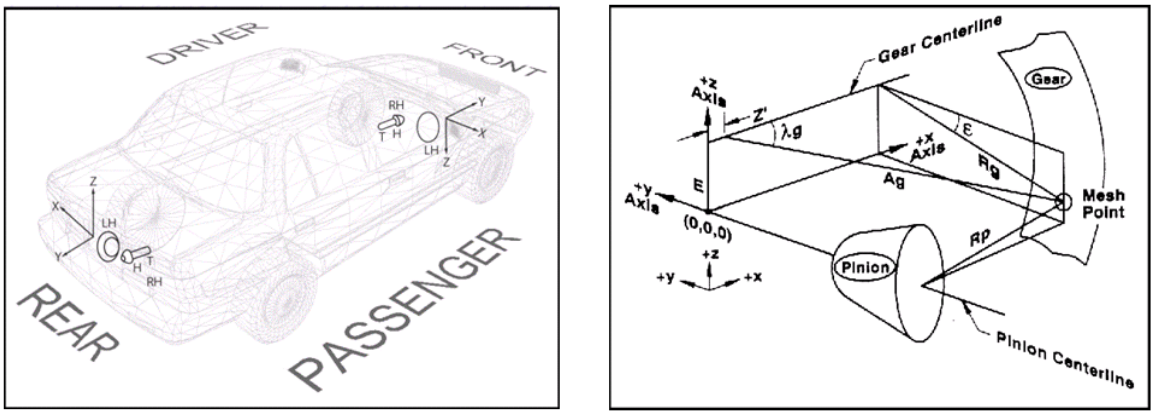

Figure C.1. Axes of the rear axle system

C.3. Inputs for FADSIM tool

C.3.1 For Gear Load Calculations

1- Pressure angle [Pinion concave (drive)]
2- Pinion offset
3- Pitch angle
4- Spiral angle
5- Mean cone distance
6- Offset angle
7- Pitch apex beyond crossing point
8- Input torque at pinion

C.3.2 For Bearing Span

1- Pinion mounting distance
2- Nominal pinion shim
3- Head pinion bearing effective load center distance
4- Head pinion cup to tail pinion cup distance
5- Head pinion bearing assy.thickness
6- Tail pinion bearing assy. thickness
7- Tail pinion bearing effective load center distance

8- Ring gear mounting distance

9- Ring gear mounting surface to LH cone seat

10- LH diff bearing effective load center distance

11- Ring gear mounting surface to RH cone seat

12- RH diff bearing effective load center distance

C.4. Outputs for FADSIM tool

All the bearing reactions to the gear loads.

APPENDIX D: ANALYSIS-GEAR LOAD EQUATIONS IN LOCAL COORDINATES

Appendix D is from the Ref 17 - Santosh Neriya, Vince Monkaba, George A. Garfinkel, "VADSIM ToolBox: Gear/Bearing Loads", *SAE Technical Paper Series*, No. 2001-01-2804, 2001, except Chapter D.4.2.

D.1. Introduction

The hypoid gear force equations are developed for rear axles in drive and coast modes .Rear axles typically have a left hand pinion and a right hand ring gear. The drive mode is when the pinion is rotating in the clockwise direction looking from the front to the rear of the vehicle and the coast mode is when the pinion is rotating in the counter-clockwise direction looking from the front to the rear of the vehicle as shown in Figure D.1. The hypoid gear pair has the mesh force composed of three components: the axial component, the separating component and the tangential component

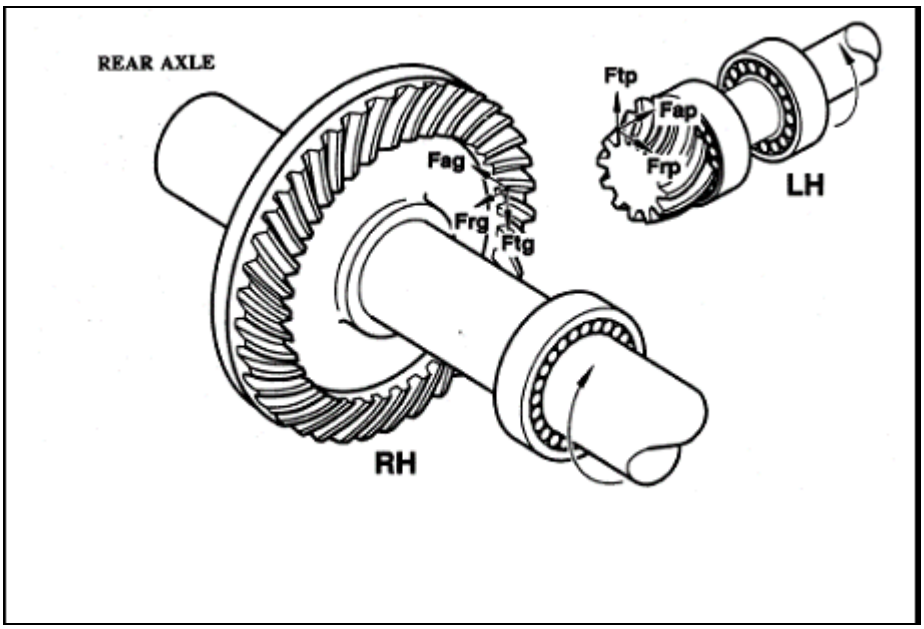

Figure D.1. Rear axle hypoid gears

D.2. Pinion & Ring Gear Axial & Separating & Tangential Force Equations

D.2.1 Pinion & Ring Gear Axial Force Equations

Axial forces of the pinion and ring gears are calculated according to the below equations D.1 and D.2

$$F_{ap} = (F_{tp} / Cos\psi_p)(\tan\phi\, Sin\gamma_p + Sin\psi_p\, Cos\gamma_p) \quad \text{(D.1)}$$

$$F_{ag} = (F_{tg} / Cos\psi_g)(\tan\phi\, Sin\gamma_g + Sin\psi_g\, Cos\gamma_g) \quad \text{(D.2)}$$

D.2.2. Pinion & Ring Gear Separating Force Equations

Seperating forces of the pinion and ring gears are calculated according to the below equations D.3 and D.4

$$F_{rp} = (F_{tp} / Cos\psi_p)(\tan\phi\, Cos\gamma_p - Sin\psi_p\, Sin\gamma_p) \quad \text{(D.3)}$$

$$F_{rg} = (F_{tg} / Cos\psi_g)(\tan\phi\, Cos\gamma_g + Sin\psi_g\, Sin\gamma_g) \quad \text{(D.4)}$$

D.2.3. Pinion & Ring Gear Tangential Force Equations

Tangential forces of the pinion and ring gears are calculated according to the below equations D.5 and D.6.

$$F_{tp} = (T / R_p) \quad \text{(D.5)}$$

$$F_{tg} = F_{tp}(Cos\psi_g / Cos\psi_p) \quad \text{(D.6)}$$

D.3. Gear Load Equations in Global Coordinates

Application engineers and CAE analysts need the gear forces in the global coordinate frame. A rear wheel drive axle global coordinate system is shown in Figure B.2. The y-axis is the pinion centerline; the x-axis is parallel to the gear centerline intersecting the y-axis.

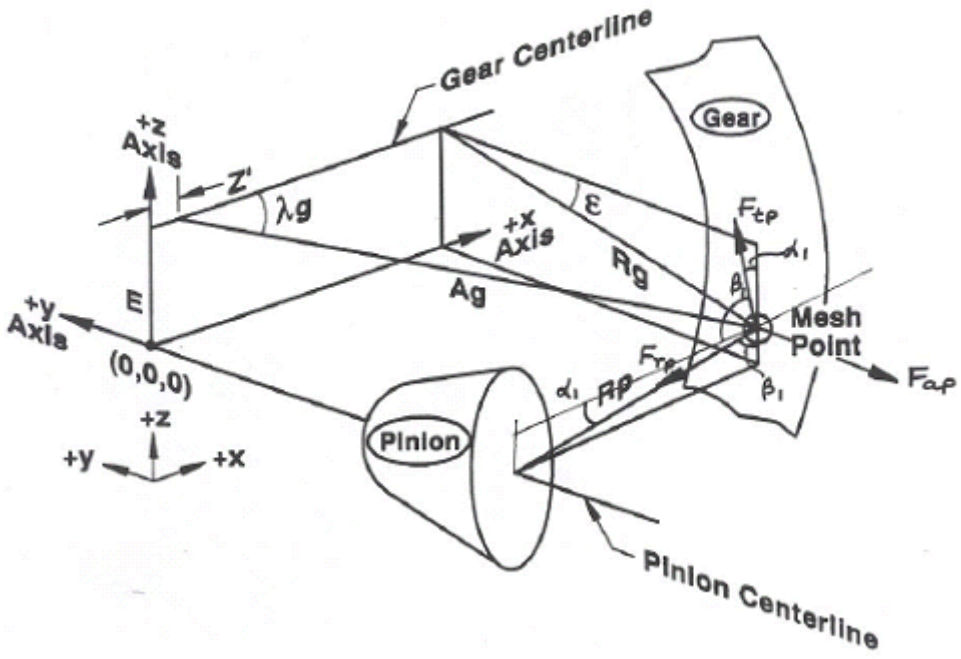

Figure D.2. Rear axle hypoid gear loads

D.3.1. The Force Equilibrium Equations For a Rear Axle Pinion in Drive Mode

The resultant forces on pinion at global coordinate system X,Y and Z are calculated according to the below equations D.7, D.8 and D.9.

$$F_{Xp} = -F_{tp}Cos\beta_1 - F_{rp}Cos\alpha_1 \quad \text{(D.7)}$$

$$F_{Yp} = - F_{ap} \quad \text{(D.8)}$$

$$F_{Zp} = F_{tp}Cos\alpha_1 - F_{rp}Cos\beta_1 \quad \text{(D.9)}$$

D.3.2. The Force Equilibrium Equations For a Rear Axle Ring Gear in Drive Mode

The resultant forces on ring gear at global coordinate system X,Y and Z are calculated according to the below equations D.10, D.11 and D.12.

$$F_{Xg} = F_{ag} \quad \text{(D.10)}$$

$$F_{Yg} = F_{tg}Cos\alpha_2 + F_{rg}Cos\beta_2 \quad \text{(D.11)}$$

$$F_{Zg} = -F_{tg}Cos\beta_2 + F_{rg}Cos\alpha_2 \quad \text{(D.12)}$$

where $Cos\alpha_1, Cos\alpha_2, Cos\beta_1, Cos\beta_2$ are direction cosines and defined as below,

$$Cos\alpha_1 = X / R_p \tag{D.13}$$

$$Cos\beta_1 = z / R_p \tag{D.14}$$

$$Cos\alpha_2 = (E - z) / R_g \tag{D.15}$$

$$Cos\beta_2 = IyI / R_g \tag{D.16}$$

D.4. Bearing Load Calculations

D.4.1. Pinion Head & Tail Bearing Load Calculations

The hypoid gear forces are applied in the global x, y and z directions at the mesh point. A hypoid pinion is shown in Figure D.3 The bearing reactions to the gear loads are at the head bearing A and the tail bearing B. These loads are dependent on the gear loads and the bearing spans and are developed using the moment equilibrium equations.

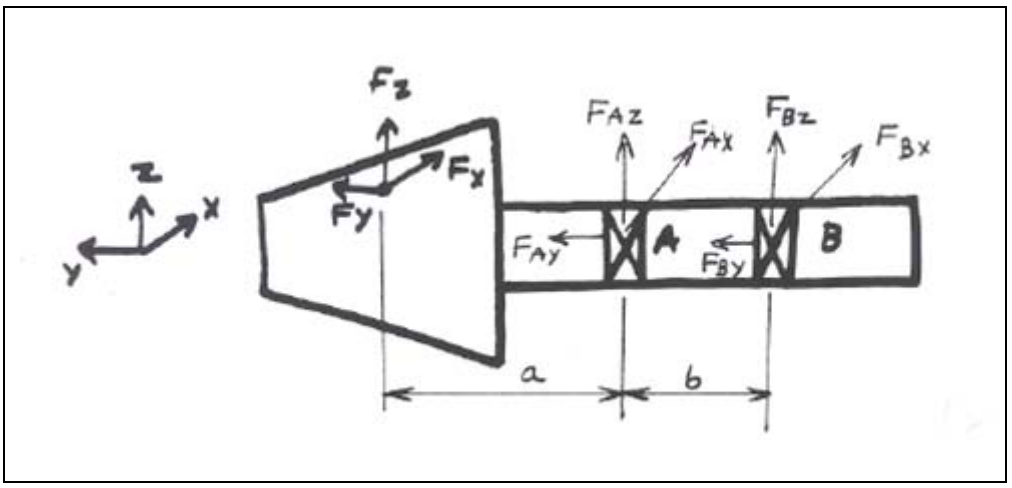

Figure D.3. Pinion head & tail bearings loads

For a rear axle pinion in DRIVE mode as shown in figure B.3, the equations are below,

Total moment at point A with respect to X direction is 0. $\sum M_{XA} = 0$. Then, Z - force on carrier at pinion tail bearing position can be calculated as shown below,

$$aF_Z - zF_Y - bF_{BZ} = 0 \tag{D.17}$$

$$F_{BZ} = (aF_Z - zF_Y)/b \tag{D.18}$$

Total moment at point B with respect to X direction is 0. $\sum M_{XB} = 0$. Then, Z - force on carrier at pinion head bearing position can be calculated as shown below,

$$(a+b)F_Z - zF_Y + bF_{AZ} = 0 \tag{D.19}$$

$$F_{AZ} = (zF_Y - (a+b)F_Z)/b \tag{D.20}$$

Total moment at point A with respect to Z direction is 0. $\sum M_{ZA} = 0$. Then, X - force on carrier at pinion tail bearing position can be calculated as shown below,

$$-xF_Y + aF_X - bF_{BX} = 0 \tag{D.21}$$

$$F_{BX} = (aF_X - xF_Y)/b \tag{D.22}$$

Total moment at point B with respect to Z direction is 0. $\sum M_{ZB} = 0$. Then, X - force on carrier at pinion head bearing position can be calculated as shown below,

$$-xF_Y + (a+b)F_X + bF_{AX} = 0 \tag{D.23}$$

$$F_{AX} = (xF_Y - (a+b)F_X)/b \tag{D.24}$$

D.4.2 Differential Bearings Load Calculations

The hypoid gear forces are applied in the global x, y and z directions at the mesh point as shown in Figure D.4 The bearing reactions to the gear loads are diff bearing C and diff bearing D. These loads are dependent on the gear loads and the bearing spans and are developed using the moment equilibrium equations.

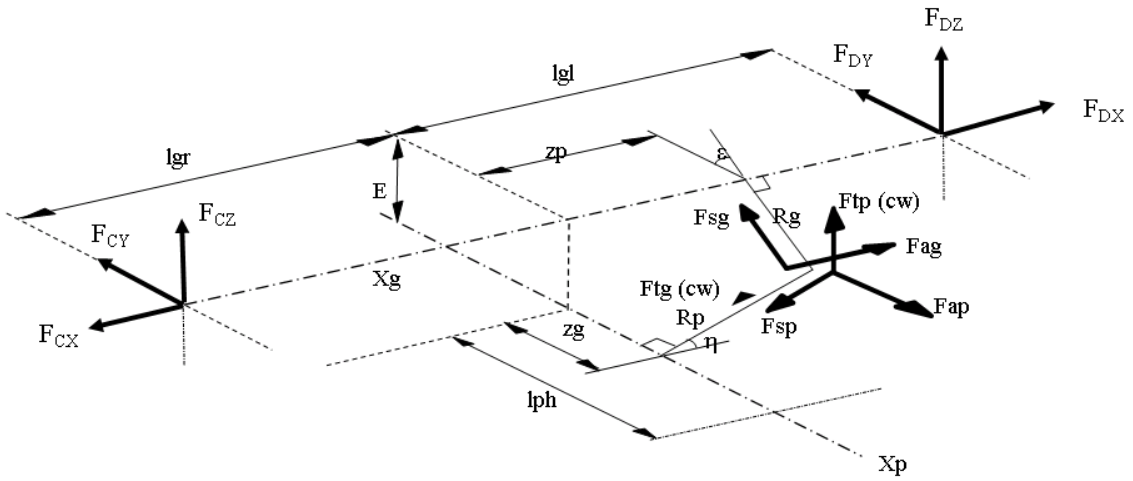

Figure D.4. Differential bearings loads

Total moment at point C with respect to Z direction is 0. $\sum M_{ZC} = 0$.Then, Y - force on carrier at diff. bearing position drive gear side can be calculated as shown below,

$$-(l_{gr} + z_p)F_Y - z_g F_X - (l_{gr} + l_{gl})F_{DY} = 0 \tag{D.25}$$

$$F_{DY} = -\frac{(l_{gr} + z_p)F_Y + z_g F_X}{(l_{gr} + l_{gl})} \tag{D.26}$$

Total moment at point D with respect to Z direction is 0. $\sum M_{ZD} = 0$ .Then, Y - force on carrier at diff. bearing position button half side can be calculated as shown below,

$$(l_{gr} + l_{gl})F_{CY} - z_g F_X + (l_{gl} - z_p)F_Y = 0 \tag{D.27}$$

$$F_{CY} = \frac{z_g F_X - (l_{gl} - z_p)F_Y}{(l_{gr} + l_{gl})} \tag{D.28}$$

Total moment at point C with respect to Y direction is 0. $\sum M_{YC} = 0$ .Then, Z - force on carrier at diff. bearing position drive gear side can be calculated as shown below,

$$-(l_{gr} + z_p)F_Z + zF_X - (l_{gr} + l_{gl})F_{DZ} = 0 \tag{D.29}$$

$$F_{DZ} = \frac{zF_X - (l_{gr} + z_p)F_Z}{(l_{gr} + l_{gl})} \tag{D.30}$$

Total moment at point D with respect to Y direction is 0. $\sum M_{YD} = 0$ .Then, Z - force on carrier at diff. bearing position button half side can be calculated as shown below,

$$(l_{gr} - z_p)F_Z + zF_X + (l_{gr} + l_{gl})F_{CZ} = 0 \tag{D.31}$$

$$F_{CZ} = -\frac{(l_{gl} - z_p)F_Z + zF_X}{(l_{gr} + l_{gl})} \tag{D.32}$$

REFERENCES

1. Bayrakçeken, H., 2006, "Failure Analysis of an Automobile Differential Pinion Shaft", Afyon Kocatepe University, Technical Education Faculty, *Engineering Failure Analysis,* Vol. 13, pp. 1422–1428.

2. Das, C. R., S. K. Albert, A. K. Bhaduri and S. K. Ray, 2005, "Failure analysis of a pinion", Materials Technology Division, Indira Gandhi Centre for Atomic Research, *Engineering Failure Analysis*, Vol. 12, pp. 287–298.

3. Stevenson, M. E., J. L. McDougall, R. D. Bowman and R. L. Herman, 2005, "Failure Analysis of a High Speed Pinion Shaft", *Journal of Failure Analysis and Prevention*, Vol. 5, pp. 48-54,.

4. Wang, M. Y., W. Zhao and R. Manoj, 2002, "Numerical Modelling and Analysis of Automotive Transmission Rattle", *Journal of Vibration and Control*, Vol. 8, pp. 921-943.

5. Asi, O., 2006, "Fatigue Failure of a Rear Axle Shaft of an Automobile", Department of Mechanical Engineering, Usak Engineering Faculty, Afyon Kocatepe University, *Engineering Failure Analysis*, Vol. 13, pp. 1293–1302.

6. Vogwell, J., 1998, "Analysis of a Vehicle Wheel Shaft Failure", *Engineering Failure Analysis*, Vol.5, No. 4, pp. 271-277.

7. Bensely, A., S. S. Jayakumara, D. M. Lala, G. Nagarajana and A. Rajadurai, 2006, "Failure Investigation of Crown Wheel and Pinion", *Engineering Failure Analysis*, Vol. 13, pp. 1285–1292.

8. Sabnavis, G., R. G. Kirk, M. Kasarda and D. Quinn, 2004, "Cracked Shaft Detection and Diagnostics", *The Shock and Vibration Digest*, Vol. 36, No. 4, pp. 287-296.

9. Clegg, R. E., 2000, “Failure of Planetary Pinions in Earth Moving Equipment - a Failure Analysis Approach”, *Engineering Failure Analysis*, Vol. 7, pp. 35-41.

10. Sinou, J. J. and A. W. Lees, 2005, “The Influence of Cracks in Rotating Shafts”, *Journal of Sound and Vibration*, Vol. 285, pp. 1015–1037.

11. Dumitru, I., L. Marsavina and N. Faur, 2007, “Experimental Study of Torsional Impact Fatigue of Shafts”, *Journal of Sound and Vibration*, Vol. 308, pp. 479–488.

12. Alvarez-Caldas, C., J. L. S. R. Garcia, B. M. Abella and A. Q. Gonzales, 2007, “Educational Software to Design Shafts and Analyze them by FEM”, *Computational Application Engineering Education*, Vol. 15, pp. 99-106.

13. Ranganath, V. R., G. Das, S. Tarafder and S. K. Das, 2004, “Failure of a Swing Pinion Shaft of a Dragline”, *Engineering Failure Analysis*, Vol. 11, pp. 599–604.

14. Law, S. S., J. Q. Bu, X. Q. Zhu and S. L. Chan, 2004, “Vehicle Axle Loads Identification Using Finite Element Method”, *Engineering Structures*, Vol. 26, pp. 1143–1153.

15. Lehr, B. C., 2000, “Applying Gasket Materials to High-Stress, Dynamic Flange Enviroments”, *SAE Technical Paper Series*, No. 2000-01-0685.

16. Lehr, B. C., 2000, “Select-a-Seal, a New Flange Sealing Technology”, *SAE Technical Paper Series*, No. 2000-01-2604.

17. Neriya, S., V. Monkaba and G. A. Garfinkel, 2001, “VADSIM ToolBox: Gear/Bearing Loads”, *SAE Technical Paper Series*, No. 2001-01-2804.

18. James, B., M. Douglas and D. Palmer, 2002, “Predicting the Contact Conditions for Hypoid Gear Sets by Analysis and a Comparison with Test Data”, *SAE Technical Paper Series*, No. 2002-01-1045.

19. Sun, Z., G. Steyer and M. Ranek, 2002, "FEA Studies on Axle System Dynamics", *SAE Technical Paper Series*, No. 2002-01-1190.

20. Beutler, K. R., 2006, "Optimized Sealing of an Axle Cover Pan Gasket Using Robust Engineering Methods", *SAE Technical Paper Series*, No. 2006-01-0739.

21. Sreedhar, S., D. Marla and D. Guo, 2006, "Fatigue Analysis for Axle Differential Cases", *SAE Technical Paper Series*, No. 2006-01-0779.

22. Hussien, A. H., A. A. Shabana, W. Tsung, M. R. Fetcho and J. Hickey, 1999, "Finite Element Dynamic Analysis of the Rear Axle System", SAE Technical Paper Series, No. 1999-01-0735.

23. Axle Design Guide, 07.5 Cover Design, FORD MOTOR COMPANY

24. Corporate Engineering Test Procedure - Trailer Tow General Durability Test for Light Commercial Trucks (CETP: 00.00-R-354)

25. DANA Coorporation Beam Fatigue Test Report

26. http://www.fadsim.ford.com/etm/cae/vadsim-gear-bearing/?